ADVANCED ENERGY MATERIALS
www.advenergymat.de

Perspectives on Improving the Safety and Sustainability of High Voltage Lithium-Ion Batteries Through the Electrolyte and Separator Region

Heather Cavers, Palanivel Molaiyan, Mozaffar Abdollahifar, Ulla Lassi, and Arno Kwade*

Lithium-ion batteries (LIBs) are promising candidates within the context of the development of novel battery concepts with high energy densities. Batteries with high operating potentials or high voltage (HV) LIBs (>4.2 V vs Li^+/Li) can provide high energy densities and are therefore attractive in high-performance LIBs. However, a variety of challenges (including solid electrolyte interface (SEI), lithium plating, etc.) and related safety issues (such as gas formation or thermal runaway effects) must be solved for the practical, widespread application of HV-LIBs. Most of these challenges arise in the region between the electrodes: the electrolyte region. This review provides an overview of recent development and progress on the electrolyte region, including liquid electrolytes, ionic liquids, gel polymer electrolytes, separators, and solid electrolytes for HV-LIBs applications. A focus on improving the safety of these systems, with some perspectives on their relative cost and environmental impact, is given. Overall, the new information is encouraging for the development of HV-LIBs, and this review serves as a guide for potential strategies to improve their safety, allowing the development of HV-LIBs, including solid-state batteries, to be accelerated to practical relevance.

1. Introduction

The global demand for the development of clean, sustainable, alternative energy technologies has increased significantly in recent years. Typical renewable energy sources, such as wind energy or solar energy, are intermittent and require intermediate energy storage systems to help integrate them with the energy grid. Replacing traditional combustion engines with mobile energy storage systems is also critical for phasing out fossil fuels. For these applications, energy storage materials with high energy densities are required. Lithium-ion batteries (LIBs), in general, offer high energy densities compared to many alternative energy storage devices. The specific energy (Wh kg^{-1}) of lithium-ion batteries is derived from the specific capacity (the amount of charge that can be stored per unit mass) and the operating potential. Batteries with high operating potentials (>4.2 V vs Li^+/Li) offer high energies, and are thus attractive for energy storage applications.[1]

Despite the benefits that high voltage LIBs (HV-LIBs) offer, there are still challenges to overcome to realize the wide usage of HV-LIBs. One of the major challenges that high operating potentials can cause, is electrolyte decomposition reactions at the negative electrode when the anode falls below the electrolyte reduction potential, which can result in the formation of a thick, insulating solid electrolyte interface (SEI).[2–4] This can result in severe capacity fading,[5,6] as well as formation of HF from $LiPF_6$ hydrolysis that can lead to further SEI growth and additional detrimental side reactions.[7] At the positive electrode, oxidation and decomposition of the electrolyte can lead to unwanted gas evolution and the formation of a solid cathode electrolyte interphase (CEI).[8–10] Detrimental interactions between the electrolyte and the conductive carbon binder system (CCB) can also challenge the lifetime and safety of HV-LIBs. This can occur when the cathode is highly polarized at high working potentials (>4.5 V vs Li/Li^+), which causes enough driving force to facilitate the intercalation of the anion into the graphitized carbon in the CCB,[11] often accompanied by solvent cointercalation. This leads to further unwanted electrolyte decomposition reactions, degradation of the CCB region and generation of gaseous byproducts.[11,12] Some HV cathode materials, such as $LiNi_{0.5}Mn_{1.5}O_4$, can undergo a dissolution of metal ions from the host structure facilitated by the electrolyte, resulting in increased capacity fading and eventual pulverization of the active material.[6] Another challenge high operating potentials pose, is creating conditions that can enable the onset of lithium plating on the surface of the negative electrode (specifically graphite anodes).[7,13] These challenges also introduce safety concerns, including gas formation and thermal

H. Cavers, M. Abdollahifar, A. Kwade
Institute for Particle Technology
Technische Universität Braunschweig
Volkmaroder Str. 5, 38104 Braunschweig, Germany
E-mail: h.cavers@tu-braunschweig.de
H. Cavers, M. Abdollahifar, A. Kwade
Battery LabFactory Braunschweig (BLB)
Technische Universität Braunschweig
Langer Kamp 19, 38103 Braunschweig, Germany
P. Molaiyan, U. Lassi
Research Unit of Sustainable Chemistry
University of Oulu
P. O. Box 4300, Oulu 90570, Finland
The ORCID identification number(s) for the author(s) of this article can be found under https://doi.org/10.1002/aenm.202200147.

DOI: 10.1002/aenm.202200147

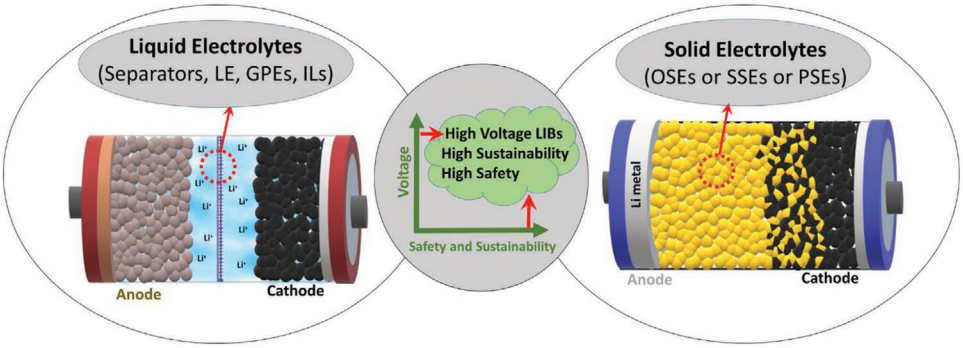

Figure 1. Schematic summarizes the strategies to improve the electrolyte region for HV-LIBs applications. The abbreviations are defined as follows: liquid electrolytes (LEs), gel polymer electrolytes (GPEs), ionic liquids (ILs), ceramic oxide solid electrolytes (OSEs), sulfide solid electrolytes (SSEs), and polymer solid electrolytes (PSEs).

runaway effects, which can ultimately lead to catastrophic cell failure.[14–16]

The challenges presented by HV-LIBs can be addressed in a variety of different ways. The problems caused by unwanted electrolyte decomposition can be addressed through electrolyte development,[17–24] electrode coatings,[25–31] or even the use of solid-state electrolytes (SEs). [32–36] Detrimental lithium plating can be mitigated through electrolyte modification,[37] tailoring the cycling procedure,[15] or choosing an anode with a higher operating potential.[14,38]

In order to further improve the stability of HV-LIBs, cell components such as the separators[39–42] or binders[43,44] must be chosen to have good thermal, chemical, and electrochemical stability. Strategies to swap out standard cell components for more sustainable materials are essential for improving the environmental impact of HV-LIBs.

For the practical, widespread application of HV-LIBs, it is crucial to address both the safety concerns and the environmental impact of the materials themselves. The challenges regarding electrode and electrolyte stability and the safety of HV-LIBs can be most effectively addressed by modifying the region separating the two electrodes (i.e., the electrolyte and separator). This region is where most safety and performance problems arise (i.e., detrimental reactions leading to catastrophic cell failure). This review will focus on improving the stability of HV-LIBs by modifying the electrolyte and separator (with commentary on strategies aiming for a lower environmental impact). It will cover novel separators, liquid electrolytes (LEs), and solid electrolytes for HV-LIBs (**Figure 1**).

2. Liquid Electrolytes for HV-LIBs

Even though many advances in solid-state batteries (SSBs) have been made in the past years, and SSBs address many of the safety concerns with LIBs, the majority of applications for LIBs require fast charging capabilities. Thus, it is still challenging to get away from LEs for commercial applications, as they are still more efficient at lithium-ion transportation than their solid-state counterparts for ambient temperature applications.[45,46] For this reason, it is still valuable to investigate alternative electrolyte compositions to improve the stability and safety of the LEs for HV-LIBs applications.

There are a variety of factors to consider when choosing electrolyte compositions. The relative environmental impact can be considered, as outlined by a study by Flamme et al., whereby the relative environmental impact of common organic solvents used in LIBs was investigated.[47] The ionic conductivity, chemical and electrochemical inertness to cell components, and suitable behavior at the electrode/electrolyte interface (EEI) are all mandatory requirements for an electrolyte in LIBs. For HV-LIBs applications, the electrochemical stability window is also a critical factor. The electrolyte must be stable in a wide electrochemical window of cell operations (0–5 V).[48,49] Additionally, one must also consider the composition of the cathode material used, as the commonly used $LiPF_6$ based carbonate electrolytes can result in loss of oxygen from the electrode lattice for certain cobalt-containing cathode materials.[21] The SEI or CEI formed on the surface of the electrode from electrolyte decomposition reactions can help to protect the electrode from structural degradation, as well as prevent continued deterioration of the EEI, caused by continued electrolyte decomposition at HV.[50]

In this section, strategies to improve the safety and voltage stability window of the electrolyte and the stability of the EEI will be investigated. These strategies include investigations of solvents with high electrochemical stabilities, as well as electrolyte additives, and a summary of the strategies covered in this section is highlighted in **Figure 2**.

2.1. Nonflammable Electrolytes

One of the major challenges of LEs for HV-LIBs applications is the inherent flammability of commonly used liquid organic electrolytes. In typical combustion processes, gaseous carbonate solvents will break down, producing hydrogen radicals and leading to chain reactions that cause increasing heat, and eventually combustion, in the battery.[51] Combustion reactions involve four main components: heat, the oxidizing agent, the fuel, and an uncontrolled chemical reaction. Removing or suppressing one of these components can inhibit the combustion reaction. There are two main mechanisms for inhibiting the combustion reaction in LEs. The first is by using gas-phase flame retardants, which scavenge the active agents of the combustion reaction (e.g., hydrogen radicals) in the gas phase and control the continuous combustion reactions (for example, with fluorinated

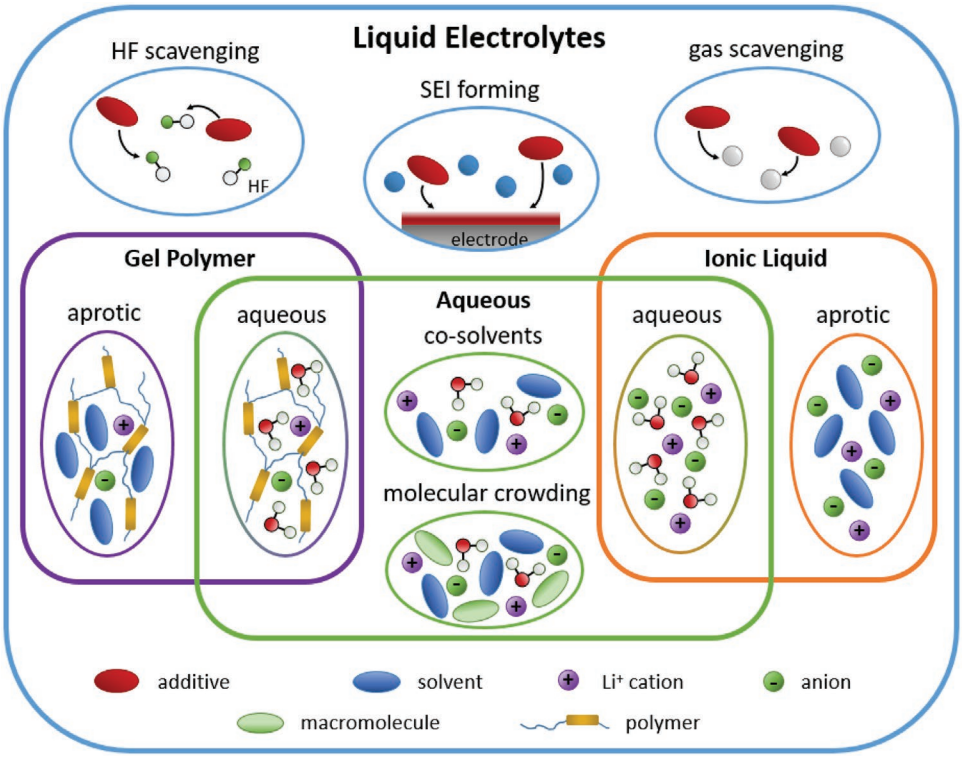

Figure 2. An overview of different LE strategies to improve the safety and sustainability of HV-LIBs, including use of additives (blue), ILs (orange), aqueous LEs (green), and GPEs (purple).

or phosphorus-containing species[52,53]). The second is by using condensed-phase flame retardants (such as alkyl phosphorus-containing species),[54–56] which promote the formation of a carbonaceous layer on the substrate surface to slow heat and mass transfer with the gas phase.[51,57] These mechanisms can be achieved through the use of alternative electrolyte chemistries. For example, phosphorous or halogen-containing compounds can suppress the hydrogen radical formation and, thus, the combustion reactions.[51] Three main strategies for enabling alternative LEs chemistries for suppressing the flammability are: by using 1) additional solvents, 2) highly concentrated electrolytes or 3) alternative solvents. Other electrolytes, such as ionic liquids (ILs), solid-state electrolytes or gel polymer electrolytes (GPEs), can have nonflammable properties, but these electrolytes will be discussed in more detail in later sections.

In earlier work on nonflammable LIB electrolytes, solvents with flame retardant capabilities such as phosphorous-based solvents[58–60] or fluorinated alkyl phosphates,[61] were used in addition to conventional LE solvents as cosolvents. However, although these compounds demonstrated the ability to inhibit the flammability of conventional LEs, they are unable to form a stable SEI layer and can thus impact the electrochemical performance.[57] Recent methods to balance the flame retardant capability of the cosolvent with the electrochemical cell performance involve the use of compounds with increased alkyl chain length, fluorinated organophosphorus compounds, replacement of the alkyl groups with aryl(phenyl) groups or the use of cyclic phosphates. Xia et al. used a triallyl phosphate to decrease the gas formation in $Li(Ni_{0.42}Mn_{0.42}Co_{0.16})O_2$|graphite pouch cells and lead to better capacity retention during cycling (**Figure 3**a).[62] Other bifunctional additives have been demonstrated to improve the cell performance through reducing the electrolyte flammability, as well as other functions, such as improving the electrochemical stability,[63] H_2O or HF scavenging[64,65] or SEI-formation.[66,67] One example of this is shown in Figure 3b from Feng et al., where the addition of 12% pentafluoro(phenoxy)cyclotriphosphazene, FPPN, reduced the electrolyte flammability, as well as improving the overcharge behavior of the electrolyte, stabilizing it at 5.05 V versus Li/Li^+ and preventing electrolyte decomposition reactions from occurring.[63] However, despite these promising results, there are still some limitations to simply adding a flame retardant solvent to the LE to suppress the flammability, such as the poor anode passivation,[52,68,69] or that these flame retardant electrolytes still contain volatile and flammable solvents[68] and may be subject to combustion at high temperatures during abuse cases.

An alternative strategy for suppressing LE flammability is by using highly concentrated LEs. With this strategy, the reduction in flammability is accomplished in two ways: the first being the increase in salt to solvent interactions, leading to reduced vapor pressure and lower volatility of the flammable solvents. The second being that the highly concentrated LE is composed of significant amount of nonflammable salt.[52] Highly concentrated LEs also show improved SEI formation, compared to the dilute LEs with flame retardant cosolvents. Zeng et al. demonstrated the formation of a stable SEI on graphite with a lithium bis(fluorosulfonyl)imide, LiTFSI, electrolyte in tris(trifluoroethyl) phosphate (TFEP) (with a molar ratio of 1:2).[70] Liang et al. demonstrated the electrochemical performance for a nonflammable, 2.2 M LiTFSI electrolyte, in

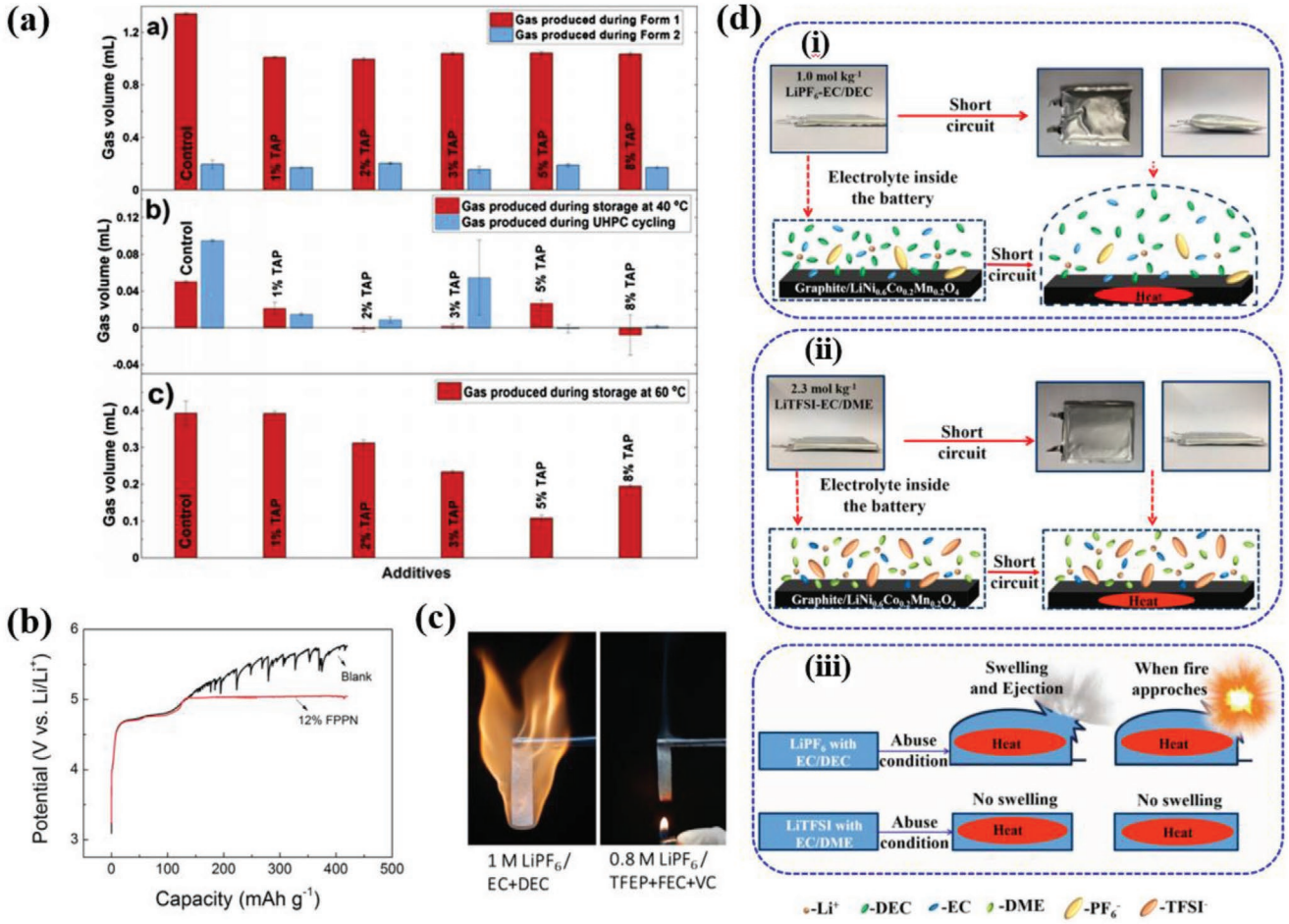

Figure 3. a) Volume of gas evolution during formation, cycling, and storage in coated NMC442|graphite pouch cells with different amounts of TAP additive in a 1 M $LiPF_6$ EC:DMC (3:7, v/v) electrolyte. Reproduced with permission.[62] Copyright 2015, Elsevier. b) Overcharge behavior of a 1 M $LiPF_6$ EC/DMC/DEC (1:1:1 v/v) electrolyte containing no additive (black solid line) and containing 12% FPPN (red solid line), respectively, in $LiNi_{0.5}Mn_{1.5}O_4$/Li cells. Reproduced with permission.[63] Copyright 2016, RSC Publishing. c) Flame tests of 0.8 M $LiPF_6$ TFEP/FEC/VC and 1 M $LiPF_6$ EC/DMC electrolyte. Reproduced with permission.[78] Copyright 2020, John Wiley and Sons. d) Photographs and schematics of batteries before and after short circuit test and situation inside of the battery under those short circuit conditions for i) 1.2 M $LiPF_6$ in EC:DEC (1:3, v/v), ii) 2.2 M LiTFSI in EC:DME (molar ratio 1:2), and iii) illustrations of those batteries under abuse conditions. Reproduced with permission.[71] Copyright 2015, The Electrochemical Society.

ether-based solvents, which showed highly reversible reactions at the graphite and NMC electrodes,[71] as well as high thermal stability under abuse conditions (as illustrated in Figure 3d). In a study by Wang et al.,[72] a high concentration $LiN(SO_2F)_2$ LE in dimethyl carbonate (up to a molar ratio of 1:1.1) was demonstrated to not only have lower flammability, but also better rate capability and cell performance, compared to commercial LEs when used in a $LiNi_{0.5}Mn_{1.5}O_4$/graphite HV-LIB. However, the viscosity of LEs with high salt concentrations can be high, and these LEs are often subject to poorer wettability and ionic conductivity,[52,73] which can impede cell performance. One solution to this is localized high concentration LEs, which preserve the solvation structure of the ions by using a solvent with a low donor number, high miscibility, and high oxidative stability to dilute the highly concentrated LE.[52] This has been demonstrated by Doi et al., whereby a highly concentrated $LiBF_4$/PC electrolyte was diluted with 1,1,2,2-tetrafluoroethyl 2,2,3,3-tetrafluoropropyl ether, enabling improved performance and an extended lifetime of $LiNi_{0.5}Mn_{1.5}O_4$ and $LiNi_{0.5}Co_{0.2}Mn_{0.3}O_2$ cathodes.[74] One of the major challenges of HV-LIBs, the detrimental interaction between the electrolyte and the CCB,[11,12] can be addressed using highly concentrated electrolytes. In a recent study by Ko et al., the nonflammable solvent sulfolane,[75] was combined with $LiBF_4$ (5.8 M) in order to minimize the parasitic interaction between the anion and CCB, due to the formation of a sulfurous-based CEI. They showed the electrochemical performance could be further enhanced with 6.6 M $LiPF_4$ electrolyte where fluoroethylene carbonate (FEC) was used as a cosolvent, which resulted in high coulombic efficiencies and long lifetime for a Li_2CoPO_4F/graphite full cell with a 5.2 V cut-off voltage.[76]

However, the use of high salt concentrations can be expensive. Another strategy for suppressing LE flammability is by using alternative solvents that have higher thermal and oxidative stabilities. This strategy enables the use of lower salt concentrations, without using volatile or flammable solvents. In a study by Zheng et al., a cyclic phosphate-based solvent was used to trap hydrogen radicals and led to an improved long

term cycling stability in a $LiNi_{0.5}Mn_{1.5}O_4$|graphite system.[77] Zeng et al. used a fluorinated phosphate-containing solvent (tris(2,2,2-trifluoroethyl)phosphate, TFEP) combined with FEC and vinylene carbonate (VC) additives to prepare a nonflammable electrolyte (Figure 3c) that demonstrated good reductive stability, no gas decomposition, and stable cycling for 100 cycles with a coulombic efficiency of up to 98.1%, and a 93 % capacity retention in Si–SiC–C|$0.35Li_2MnO_3 \cdot 0.65LiNi_{0.5}Mn_{0.5}O_2$ cells.[78] Fan et al. demonstrated a non-flammable fluorinated electrolyte with 1 M $LiPF_6$, which improved the electrochemical performance of a 5 V $LiCoPO_4$ cathode and a Ni-rich $LiNi_{0.8}Mn_{0.1}Co_{0.1}O_4$ cathode due to the formation of highly stable, fluorine rich interphases at the electrode surface.[79] In order to improve both the temperature and the voltage window, Fan et al. dissolved fluorinated carbonate electrolytes in highly fluorinated nonpolar solvents. This approach led to LEs with a wide voltage window of 0.0 to 5.6 V and high ionic conductivities over a large temperature range of –125 to 70 °C. These nonflammable LEs were shown to enable good cell performance of a variety of different electrode materials (including high-voltage (5.4 V) $LiCoMnO_4$ cathodes) at extreme temperatures.[80]

Controlling the flammability of the electrolyte is critical to enable safer LEs in HV-LIBs for long-term, large-scale applications. As shown, there are many options to do so, either through the use of flame retardant cosolvents, high concentration LEs or through new, nonflammable electrolyte solvents. However, many of these options involve the use of problematic or hazardous solvents, which can have negative health or environmental impact.[81–85]

2.2. Liquid Electrolyte Additives for Electrode Interface

LEs undergo decomposition on the surface of the electrode during the first cycling processes of the LIBs, forming a passivation layer, the SEI (anode) or CEI (cathode), consisting of both inorganic and organic products, which reflect the composition of the electrolyte. A good SEI, or CEI, is electrically insulating (to prevent continuous electrolyte degradation) and ionically conductive (to preserve the transfer of Li^+ to and from the electrode surface). The presence of a stable SEI, or CEI, passivating the electrode surface will protect the active material from degradation and prevent unwanted decomposition reactions in the electrolyte that can lead to overpotentials, gas production, and potential explosive failure of the battery.[4,86,87]

An additive is a compound added to the electrolyte with a volume or weight percent of <5%. Typically, this compound is dominant in the SEI, or CEI, formed on the target electrode, although additives for other applications can also exist, as described in the previous section. Additives designed to improve SEI/CEI composition, or SEI- and CEI-forming additives, should have the following qualities: 1) compatibility with the electrolyte and electrode materials, 2) ability to achieve significant improvement in the LIBs performance with a small amount, 3) nontoxic, and 4) low-cost.[17] The choice to use electrolyte additives is made to find the easiest, most cost-effective strategy to improve the function of the LIBs without having to change any part of the production process. The important role that the CEI plays is demonstrated (**Figure 4**) for Ni-rich cathode materials.

Additives for LEs in LIBs are some of the most widely studied battery components, especially considering their minor percent contribution to the weight of the overall battery, as they play a critical role in improving the performance. Commonly studied additives such as VC[22,88–91] and FEC[89,90,92–96] have primarily focused on promoting SEI formation on the anode, although their role on the cathode has been subjected to increasingly more interest. For HV-LIBs, the CEI on the cathode surface can be vital to promote long cycle lifetimes, as HV cathode materials are particularly susceptible to loss of active material to the electrolyte, through dissolution of the transition metal ions.[17] This ultimately leads to cracking and pulverization of the active material. The presence of HF or PF_5 species (produced from the decomposition of the standard $LiPF_6$ salt) can cause damage to the CEI, which further supports unwanted active material degradation. In recent years, multifunctional additives have been increasingly more popular. These CEI-forming additives typically contain functional groups such as isocyanate (N=C=O),[97–100] silane derivatives (Si—O),[101–106] sultones (S—O),[88,107–111] borates (B—O),[112–115] or phosphorous-containing groups,[116–120] which are capable of scavenging HF. Many of these CEI-forming additives can also promote SEI formation on the anode, serving multiple important functions in the cell. A list of relevant solvent additives and the roles they play in HV-LIBs can be found in **Table 1** and a list of relevant salt additive can be found in **Table 2**.

In a study by Wang et al.,[97] it was shown that an isocyanate-containing additive (p-toluenesulfonyl isocyanate, PTSI) could allow for long-term stable cycling for over 680 cycles at an operating potential of 4.8 V versus Li/Li^+ for $LiNi_{0.5}Co_{0.2}Mn_{0.3}O_2$ batteries. In this context, the PTSI additive lowers HF production and prevents electrolyte decomposition reactions by forming a thin, stable CEI layer on the cathode. Aupperle et al. employed an additive with a nitrile (—CN) functionalized silane that enabled long term cycling of a $LiNi_{0.6}Mn_{0.2}Co_{0.2}O_2$|Si–graphite pouch cell, and significantly reduced the gas formation.[106] Combining multifunctional additives with the more widely studied additives can also serve to further improve the cell performance, as Xu et al. showed by combining VC with 1,3-propane sultone (PS), whereby VC serves to repress electrolyte decomposition and PS serves to protect the surface of the electrodes.[108] Liu et al. took dual-additive electrolytes a step further by utilizing trimethyl borate to improve the performance of other additives, i.e., by promoting the oxidation of tetramethylene sulfone (TMS) to improve the CEI stability or through interaction with FEC to lower the onset oxidation potential.[115] Zhu et al. reported a novel phosphate-containing additive (diethyl(thiophen-2-ylmethyl)phosphate) that dramatically improved the capacity retention of an HV $LiNi_{0.5}Mn_{1.5}O_4$ battery.[120] This additive not only stabilized the CEI, but it also served to improve the thermal stability of the electrolyte and improve the resistance to combustion. Multifunctional salt-based additives, although often more expensive than solvent additives, have also been used to improve the performance and safety of HV-LIBs. Some of the most effective of these are borate-containing[132–138] or phosphate-containing[139–143] lithium salt additives, for similar reasons as the borate or phosphorous-based solvent additives. Phosphate- or borate-containing anions typically participate in the formation of a

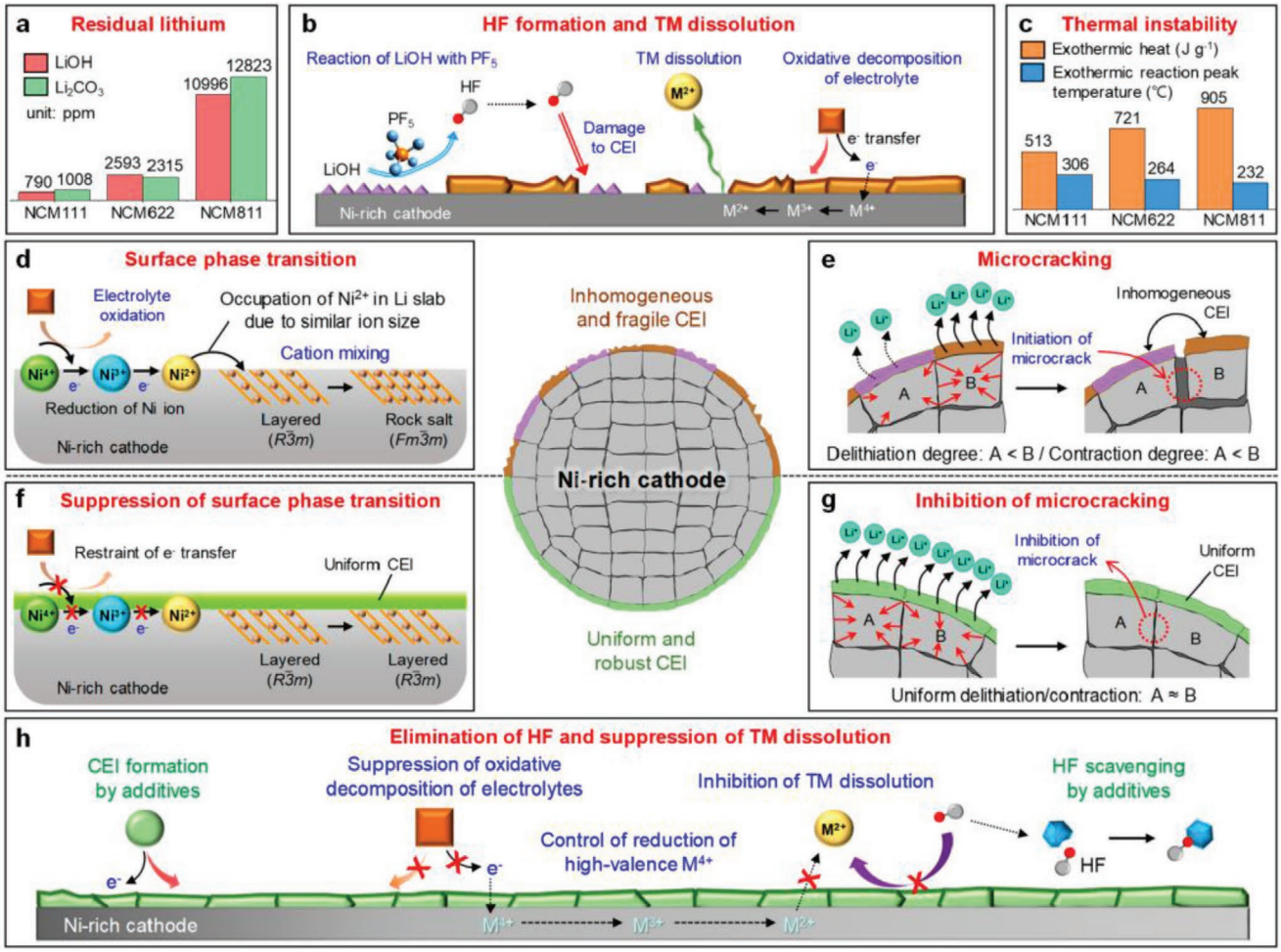

Figure 4. Summary of critical issues of Ni-rich cathodes with regards to the CEI. Reproduced with permission.[17] Copyright 2020, American Chemical Society.

CEI and SEI on both the cathode and anode surfaces, respectively, leading to a more inorganic, more stable, thinner layer on the electrode surface, which is capable of promoting Li^+ transfer. Suppressing the electrolyte decomposition in this way serves to preserve the active material in both electrodes, as well as improve the safety of the battery by suppressing unwanted decomposition that can lead to gas formation. This mechanism was demonstrated by Dong et al.,[134] where the cycling of a Ni-rich $LiNi_{0.83}Mn_{0.05}Co_{0.12}O_2$|graphite cell could be significantly improved after 200 cycles with the addition of a lithium difluoro(oxalate)borate (LiDFOB) additive. Chen et al. demonstrated that the addition of this lithium salt additive to an electrolyte composed of fluorocarbon solvents led to superior electrochemical stability up to 5.5 V versus Li^+/Li.[133] Lithium salt additives are also capable of dual-functions, as Kim et al. demonstrated with a lithium bis(trimethylsilyl)phosphate (LiTMSP) salt in a $LiNi_{1.5}Mn_{0.5}O_4$|graphite cell, where LiTMSP contributed to the formation of a stable SEI, as well as acted as an HF-scavenger.[142] Another salt additive that has been shown to positively influence the SEI is $LiPO_2F_2$, which promotes a stable, compact, ionically conductive SEI or CEI, due to the presence of decomposition products such as $Li_xPO_yF_z$.[144–146] This was demonstrated by Jiang et al. for a lithium rich $Li_{1.14}Ni_{0.133}Co_{0.133}Mn_{0.544}O_2$ cycled between 2.0 and 4.8 V versus Li/Li^+, where the capacity retention was improved from 53.6% to 85% at 3 C for 500 cycles with just 0.5 wt% $LiPO_2F_2$ in a 1 M $LiPF_6$ electrolyte in ethylene carbonate (EC):dimethyl carbonate (DMC) (1:1, v/v).[147]

As described, electrolyte additives can provide critical functions to enable LEs in HV-LIBs and improve the safety and long-term cycling capability. Electrolyte additives can provide a simple solution to improve the safety of HV-LIBs, especially for large-scale production applications, where the processes are already well-established. However, despite the improvements in the chemical, electrochemical and thermal stability of industry-standard LEs through the addition of additives, there are still many drawbacks, including the fact that these electrolytes are still inflammable.

2.3. Ionic Liquid Electrolytes for HV-LIBs

Many of the safety challenges with LEs can be addressed by use of IL electrolytes. ILs are liquid at room temperature (RT)

Table 1. Summarizes select solvent LEs additives from literature and the role they play for improving HV-LIBs.

Name	Amount	Electrolyte	Anode	Cathode	Max. voltage (V vs Li^+/Li)	Operating window (V vs Li^+/Li)	Role	Ref.
Vinylene carbonate (VC)	5%	1.2 M $LiPF_6$ in EC/DMC (3:7)	$Li_4Ti_5O_{12}$	$LiNi_{0.5}Co_{0.2}Mn_{0.3}O_2$	4.3	3.5–4.4	Lower oxidative current, passivation layer (higher impedance)	[22]
1,1,2,2-Tetrafluoro-ethyl-2,2,3,3-tetrafluoro-propyl ether (TTE)	10%							
Triallyl phosphate (TAP)	1–3%	1 M $LiPF_6$ in EC/DMC (3:7)	Graphite	$Li(Ni_{0.42}Mn_{0.42}Co_{0.16})O_2$	4.5	2.8–4.5	SEI on cathode + anode, less gas evolution	[62]
Tris(pentafluorophenyl) phosphine (TPFPP)	0.5–1 %	1 M $LiPF_6$ in EC/DMC/DEC (1:1:1)	Li-metal	$LiNi_{0.5}Mn_{1.5}O_4$	4.9	3.5–4.9	SEI on cathode, better cycling	[66]
Prop-1-ene-1,3-sultone (PES)	2%	1 M $LiPF_6$ in EC/DMC (3:7)	Graphite	$Li(Ni_{0.3}Mn_{0.3}Co_{0.3})O_2$	4.2	2.8–4.2	SEI on Ni-rich cathodes	[88]
p-Toluenesulfonyl isocyanate (PTSI)	0.5 wt%	1 M $LiPF_6$ in EC/EMC (3:7)	Li-metal	$LiNi_{0.5}Co_{0.2}Mn_{0.3}O_2$	4.5	3.0–4.5	Higher initial capacity, better thermal stability, HF scavenging	[97]
Diphenyldimethoxysilane (DPDMS)	1 wt%	1 M $LiPF_6$ in EC/EMC/DMC (1:1:1)	Li-metal	$LiNi_{0.6}Co_{0.2}Mn_{0.2}O_2$	4.3	2.8–4.3	HF scavenger, SEI cathode, better thermal stability	[101]
Triethyl borate (TEB)	2, 4, 10 wt%	2 M $LiPF_6$ in EC/DEC/DMC (3:5:2)	Li-metal	$LiNi_{0.3}Co_{0.3}Mn_{0.3}O_3$	4.5	3.0–4.5	SEI cathode, improved cycling, and rate capability with 10 wt%	[112]
Trimethyl boroxine (TMB)	2, 3, 4 wt%	1 M $LiPF_6$ in EC/DEC/DMC (3:5:2)	Li-metal	$LiNi_{0.3}Co_{0.3}Mn_{0.3}O_2$	4.5	3.0–4.5	SEI cathode	[113]
Triisopropyl borate (TIB)	1 wt%	2 M $LiPF_6$ in EC/EMC/DMC (1:1:1)	Li-metal	$LiNi_{0.6}Co_{0.2}Mn_{0.2}O_3$	4.5	3.0–4.5	SEI on cathode, betting cycling stability	[114]
Fluoroethylene carbonate (FEC)	Cosolvent	1 M $LiPF_6$ in DMC/FEC	G/Si	$LiFePO_4/LiNi_{0.5}Mn_{1.5}O_4$	5	3.5–5.2	SEI formation for Si + G anodes	[121]
Tri(hexafluoro-iso-propyl) phosphate (HFiP)	1%	1 M $LiPF_6$ in EC/DMC (3:7)	Graphite	$LiNi_{0.5}Mn_{1.5}O_4$	5	3.5–4.95	SEI on cathode + anode	[122]
	1%	1 M $LiPF_6$ in EC/DMC (1:1)	Li-metal	$Li[Li_{0.2}Mn_{0.56}Ni_{0.16}Co_{0.08}]O_2$	4.2	2.0–4.6	SEI on cathode	[123]
Triphenylphosphine oxide (TPPO)	0.50%	1 M $LiPF_6$ in EC/DMC (3:7)	Graphite	$LiNi_{0.8}Mn_{0.1}Co_{0.1}O_2$	4.3	2.8–4.3	SEI on cathode + anode	[124]
3-Methyl-1,4,2-dioxazol-5-one (MDO)	2%	1 M $LiPF_6$ in PC	Graphite	$LiNi_{0.5}Mn_{0.3}Co_{0.2}O_2$	5.3	2.8–4.2	High oxidative stability, suppress G exfoliation	[20]
Succinate anhydride (SA)	1, 2, 4, 6, 8%	1 M $LiPF_6$ in EC/DMC (1:1)	Li-metal	$LiNi_{0.5}Mn_{1.5}O_4$	5	3.5–4.95	Improve LMNO self-discharge	[125]
Triphenylamine (Ph3N)	0.25 wt%	1.2 M $LiPF_6$ in EC/DMC (3:7)	Graphite	$Li_{1.2}Ni_{0.15}Mn_{0.55}Co_{0.1}O_2$	4.5	2.2–4.6	Reduce LE oxidation, SEI cathode and improve capacity retention and lower impedance	[126]
1,4-Benzodiozane-6,7-diol (BDOD)	0.3 wt%							
[4,4′-bi(1,3,2-Dioxathio-lane)]2,2′-dioxide (BDTD)	2 wt%	2 M $LiPF_6$ in EC/EMC (3:7)	Li-metal	$LiNi_{0.5}Co_{0.2}Mn_{0.3}O_3$	4.6	3.0–4.6	SEI cathode, better capacity retention, and rate capability	[127]
Dimethoxydimethylsilane (DODSi)	2 wt%	1 M $LiPF_6$ in EC/EMC (1:2)	Li-metal	$LiNi_{0.8}Mn_{0.1}Co_{0.1}O_2$	4.3	3.0–4.5	SEI on cathode, HF scavenging	[102]
Tris(trimethylsilyl) phosphite (TMSPi)	1 wt%	1.2 M $LiPF_6$ in EC/EMC (3:7)	Graphite	$LiNi_{0.5}Mn_{0.3}Co_{0.2}O_2$	4.4	3.0–4.4	SEI on cathode, HF scavenging	[128]
Diethyl phenylphosphonite (DEPP)	0.5–5 wt%	1 M $LiPF_6$ in EC/EMC/DEC (3:5:2)	Li-metal	$LiNi_{0.8}Co_{0.15}Al_{0.05}O_2$	4.5	3.0–4.35	HF scavenger, SEI on cathode	[129]
Ethylene sulfite (ES)	5 wt%	1 M $LiClO_4$ in PC	Graphite	$LiMn_2O_4$	4.5	3.5–4.5	Film-forming additive for anode (≈1.8–2.1 V)	[130]

Table 1. Continued.

Name	Amount	Electrolyte	Anode	Cathode	Max. voltage (V vs Li^+/Li)	Operating window (V vs Li^+/Li)	Role	Ref.
1,3,2-Dioxathiolane2,2-dioxide (DTD)	1 wt%	1 M $LiPF_6$ in EC:DEC	Graphite	LFP	3.8	2.6–3.8	Improve oxidative stability electrolyte (≈6 V), anode SEI additive	[131]
Propane-1,3-sultone (PS)							Stablize SEI layer	
Sulfopropionic acid anhydride (SPA)							Stabilize SEI, improve interfacial resistance	

and are composed entirely of ions. Typical ILs exhibit favorable properties such as low volatility, low flammability, high thermal stability, and wide liquid range.[153] ILs demonstrating further favorable properties such as high ionic conductivities and a wide electrochemical, and thermal stability window have led to the use of ILs as a safer alternative for LEs in LIBs.[154,155]

Brutti et al. studied imidazolium based ILs with tetra-alkyl ammonium cations, coupled with bis(perfluoroalkyl sulfonylimide) for HV-LIBs up to 5 V versus Li^+/Li.[155] Zhao et al. also used imidazolium based ILs with phosphate functionalization to improve the rate capability of $LiFePO_4$/Li cells, however, the potential was limited to 4.6 V versus Li^+/Li.[156] Chatterjee et al. improved the performance of an industry-standard 1 M $LiPF_6$, EC:DMC, electrolyte in an NMC-111|graphite cell with the addition of a dicationic ILs.[157] In a similar study, Chatterjee et al. could also achieve very similar ionic conductivities with a thiourea-based ILs-additive to a conventional organic electrolyte (11.91 mS cm^{-1} compared to 12.2 mS cm^{-1}).[158] For LIBs with $LiNi_{0.5}Mn_{1.5}O_4$ cathodes (4.7 V vs Li^+/Li), Rath et al. demonstrated *N*-butyl-*N*-methylpyrrolidinium–TFSI-based ILs.[159] Wu et al. also used TFSI-based ILs with $LiNi_{0.5}Mn_{1.5}O_4$ cathodes to improve the performance through a series of 1 M $LiPF_6$/*N*-propyl-*N*-methylpyrrolidinium(PYR_{13})-TFSI hybrid ILs, which were demonstrated to suppress the corrosion of the Al current collector and enable stable cycling at 1 C for up to 300 cycles with ionic conductivities of up to 7.2 mS cm^{-1}.[160] ILs can demonstrate improved thermal, chemical, and electrochemical stability compared to commercial LEs in LIBs,

Table 2. Summarizes select salt LEs additives from literature and the role they play for improving HV-LIBs.

Name	Amount	Electrolyte	Anode	Cathode	Max voltage (V vs Li^+/Li)	Operating window (V vs Li^+/Li)	Role	Ref.
Magnesium bis(trifluoromethanesulfonyl) imide ($Mg(TFSI)_2$)	1 wt%	1 M $LiPF_6$ in EC/EMC (1:1)	Li-metal/G	$LiNi_{0.3}Mn_{0.3}Co_{0.3}O_2$	4.6	3.0–4.6	CEI	[18]
Lithium difluoro(oxolato)borate (LiDFOB)	1 wt%	1.3 M $LiPF_6$ in EC/EMC/DMC (3:4:3)	Graphite	$Li_{1.17}Ni_{0.17}Mn_{0.5}Co_{0.17}O_2$/0.4$Li_2MnO_3$·0.6$LiNi_{0.3}Co_{0.3}Mn_{0.3}O_2$	4.5	2.0–4.8	Improves rate capability, SEI and CEI	[137]
Lithium difluoro(bisoxolato) phosphate (LiDFBP)	1 wt%	1.3 M $LiPF_6$ in EC/EMC/DMC (3:4:3)	Li-metal	$Li_{1.17}Ni_{0.17}Mn_{0.5}Co_{0.17}O_2$/0.4$Li_2MnO_3$·0.6$LiNi_{0.3}Co_{0.3}Mn_{0.3}O_2$	4.6	2.0–4.6	CEI, improved cycling at high rates (20 C)	[141]
Lithium Bis(oxolato)borate (LiBOB)	3 wt%	1 M $LiPF_6$ in EC/DEC (1:1)	Li-metal	$LiCoPO_4$	5	3.5–5.2	CEI	[148]
	1 wt%	1.2 M $LiPF_6$ in EC/DMC (3:7)	Graphite	$Li_{1.2}Ni_{0.15}Mn_{0.55}Co_{0.1}O_2$	4.5	2.2–4.6	Good capacity retention, even better impedance when combined with Ph3N or BDOD (see above)	[126]
Lithium tetrafluoro(oxolato) phosphate (LiTFOP)	1 mol L^{-1}	EC/DEC/DMC (1:1:1)	MCMB	$LiNi_{0.8}Co_{0.2}O_2$	4.1	3.0–4.1	SEI and CEI	[149]
	1–3 wt%	1.2 M $LiPF_6$ in EC/DMC (3:7)	MCMB	$Li_{1.1}(Ni_{0.3}Co_{0.3}Mn_{0.3})_{0.9}O_2$	4.1	3.0–4.0	SEI and CEI, significate capacity retention	[150]
Lithium oxalyldifluoroborate (LiODFB)	5 wt%	1 M $LiPF_6$ in EC/EMC/PC (1:3:1)	Li-metal	$LiCoPO_4$	5.3	2.5–4.2	Higher rev. charge/discharge, better cycling	[151]
Lithium 4,5-dicyano-2-(trifluoromethyl)-imidazole (LiTDI)	1 mol L^{-1}	EC/DMC	Li-metal	$LiNMn_2O_4$	4.6	3.5–4.3	Noncorrosive, replace $LiPF_6$	[152]
Lithium difluorophosphate ($LiPO_2F_2$)	0.5 wt%	1 M $LiPF_6$ in EC:DMC (1:1)	Li-metal	$Li_{1.14}Ni_{0.133}Co_{0.133}Mn_{0.544}O_2$	4.8	2.0–4.8	SEI and CEI, improved rate capability	[147]

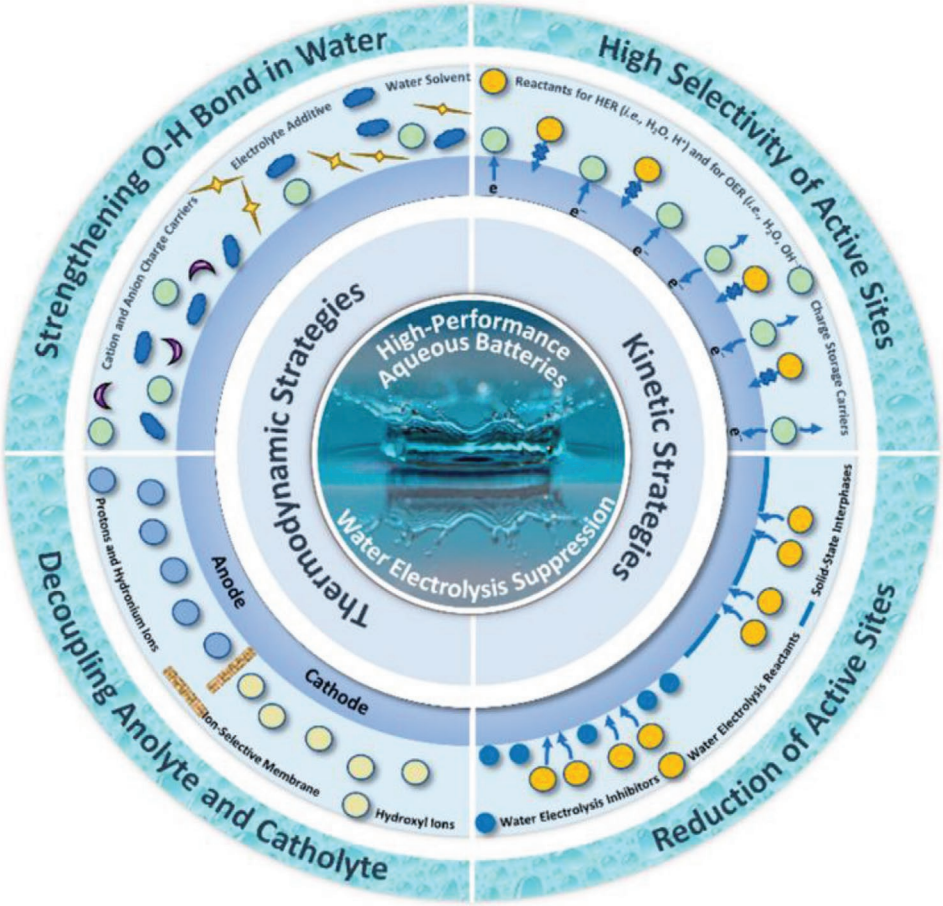

Figure 5. Summary of strategies to suppress the water electrolysis reactions in batteries. Reproduced with permission.[164] Copyright 2021, American Chemical Society.

and are even capable of achieving comparable ionic conductivities. Despite the promising results of ILs, they are still inherently more expensive and less sustainable than alternative electrolyte solutions, due to the high concentrations of lithium salts required. Additionally, ILs have limited biodegradability and can be relatively toxic, depending on the composition.[161]

2.4. Aqueous Electrolytes for HV-LIBs

Despite the fact that nonaqueous LEs are widely used commercially, there are growing concerns about the safety of these electrolytes, which use flammable organic solvents. Therefore, it is important to consider the replacement of these organic electrolytes with nonflammable, low-toxic aqueous electrolytes (AEs) in order to address these safety concerns. For large-scale battery production, AEs also offer a low-cost alternative, and allow more accessible, cheaper cell production, as the atmosphere requirements are not as strict as for traditional LEs.[162]

One of the major drawbacks of AEs is the low electrochemical stability window (ESW) of water. Typically, water has a narrow ESW (1.23 V)[163] and will undergo electrolysis, resulting in hydrogen evolution reactions (HERs) and oxygen evolution reactions (OERs), which are detrimental to the lifetime and function of the battery. There are strategies, however, to widen the ESW and prevent water electrolysis, and potentially allow AEs to be used in HV-LIBs contexts. The three main strategies to improve the ESW for water-based electrolytes are 1) "water-in-salt" electrolytes, 2) molecular crowding, and 3) gel polymer aqueous electrolytes. The idea behind all of these strategies is to suppress the electrolysis reaction of water and improve the thermodynamic stability. The electrolysis of water is a surface-controlled reaction (i.e., occurs at the electrode surface), and causes the lithium transfer reactions to be in competition with parasitic HER and OER at the surface.[164] The main approaches to suppress these parasitic water electrolysis reactions: strengthening of the O—H bonds, decoupling alkaline analyte and acidic/neutral catholyte[164] and physically inhibiting water molecules from reaching the electrode surface (summarized in **Figure 5**).[165]

2.4.1. Highly Concentrated Aqueous Electrolytes

For highly concentrated aqueous electrolytes, extremely high concentrations of lithium salt(s) (>20 M) are dissolved in the solvent. This is often referred to as a "water-in-salt" electrolyte, or "water-in-bisalt" (in the case of a second salt).[166] The

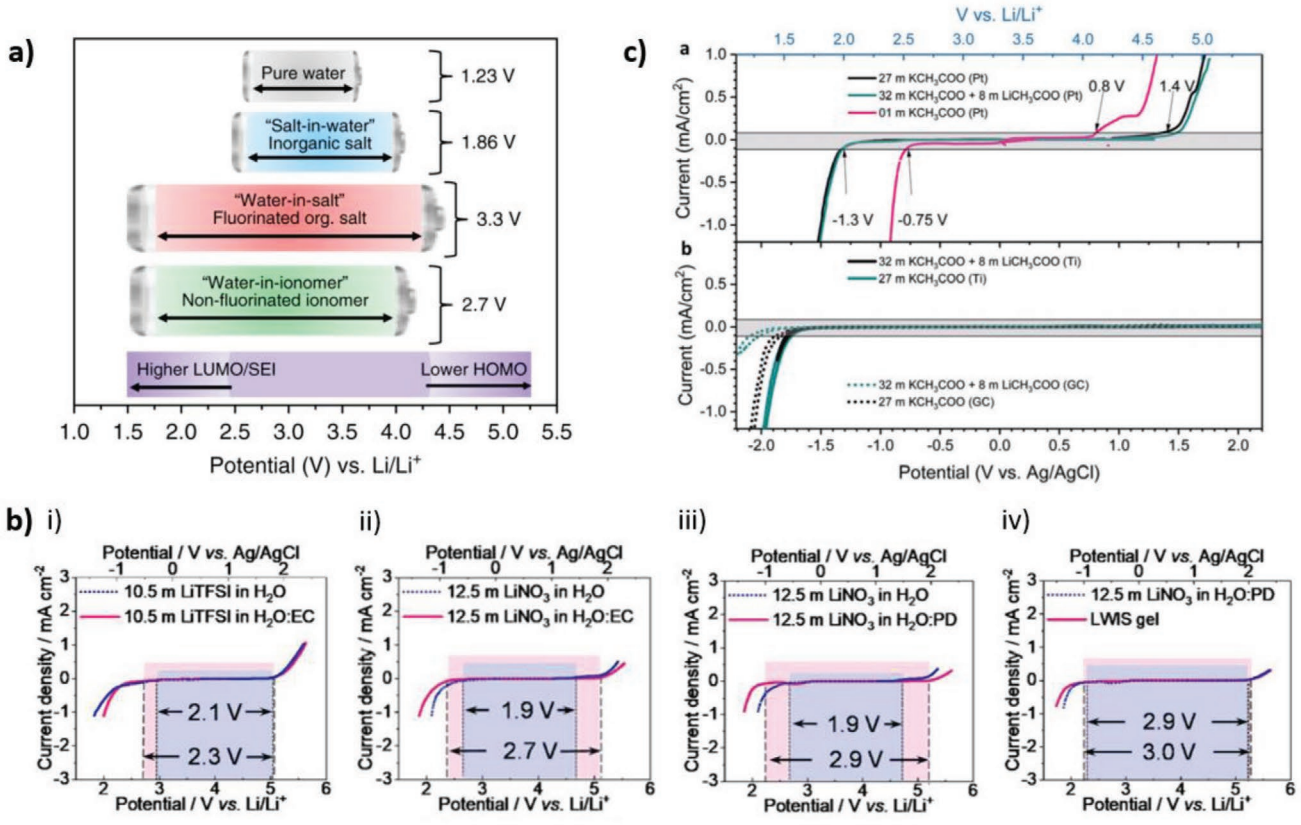

Figure 6. a) Comparison of aqueous lithium-ion battery end-of-charge voltages with various salts. The "salt-in-water" electrolyte correspond to 1 M Li_2SO_4 in a $LiTi_2(PO_4)_3|LiMn_2O_4$ cell, the "water-in-salt electrolyte" corresponds to $Li(TFSI)_{0.7}(BETI)_{0.3}\cdot 2H_2O$ in a $Li_4Ti_5O_{12}|LiNi_{0.5}Mn_{1.5}O_4$ cell, and the "water-in-ionomer" corresponds to the 50 wt% LiPAA gel electrolyte in a $TiO_2/LiMn_2O_4$ cell. Reproduced with permission.[178] Copyright 2018, Springer Nature. b) Cyclic voltammetry profiles of select "water-in-salt" electrolytes with and without cosolvents (i–iii), as well as for a liquid water in salt gel (iv). Reproduced with permission.[176] Copyright 2021, John Wiley and Sons. c) Cyclic voltammetry profiles of acetate-based electrolyte solutions using Pt foil (a) and Ti foil (b) demonstrating voltage stability windows. Reproduced with permission.[177] Copyright 2018, RSC Publishing.

solvation structure resulting from such highly concentrated AEs is an anion-containing Li^+ shell, where the number of water molecules available to solvate each ion is low and interionic interactions are promoted.[167] This solvation structure restricts the movement of water, therefore it cannot easily reach the electrode surface, as well as lowers the HOMO of water, improving its the oxidative stability to the cathode.[165] A "hydrate melt" electrolyte is similar to the "water-in-salt" electrolyte, wherein there are no free water molecules, with all water molecules participating in the Li^+ solvation.[168] This type of solvation structure also leads to a shift of the LUMO to the anion, resulting in anion derived SEI layers on the electrode surface. These anion derived SEI layers also tend to be more stable in concentrated electrolytes solutions, which prevent side reactions at the surface of the electrode and hydrogen evolution. The widening of the electrochemical stability window in this way, is demonstrated in **Figure 6**a.

Suo et al. demonstrated this principle with a 21 M LiTFSI water-in-salt electrolyte with a voltage window of 3 V and an upper voltage limit of 4.9 V versus Li/Li^+ and successfully applied it in full cells using Mo_6S_8 and $LiMn_2O_4$ as the anode and cathode, respectively.[167] There have been a variety of other "water-in-salt" studies using Li-salts demonstrating wider voltage windows from 2 V to >3 V.[169–174] Binary Li-salt mixtures, or "water-in-bisalt", have also been studied. A study by Ko et al. achieved a voltage window of 4.85 V with an upper voltage window of 5.05 V using 22.2 M LiTFSI combined with 33.3 M LiPTFSI (which could be classified as a hydrate melt, given the lack of free water molecules), although the ionic conductivity was limited to 0.1 mS cm^{-1}.[175] Jaumaux et al. demonstrated that the addition of a cosolvent, 1,5-pentanediol (PD) could allow a decrease in the required concentration of Li-salt (12.5 M, rather than 25 M), using a much cheaper salt (i.e., $LiNO_3$) (Figure 6b).[176] The high cost and relative toxicity of Li-salts have led to studies regarding mixed-cation "water-in-salt" electrolytes, allowing the use of cheaper, greener salts, while still maintaining the benefits for limitation of water hydrolysis and Li transfer capability. For example, Lukatskaya et al. prepared a mixed-cation acetate salt electrolyte with 32 M KOAc and 8 M LiOAc and demonstrated its performance with a c-TiO_2 anode and $LiMn_2O_4$ cathodes (Figure 6c).[177] While pure Li-salt in water electrolyte solutions still come with some challenges, choice of a cosolvent or alternative salt can improve not only the electrochemical and thermal stability, but also the cost and relative safety of the electrolyte.

2.4.2. Molecular Crowding

Despite the promising performances, the "water-in-salt" approach is intrinsically more expensive, and unattractive for large-scale applications. For this reason, the molecular crowding approach, whereby the properties of the solution can be modified using macromolecules (e.g., proteins, polysaccharides or complex sugars) is more attractive.[179] The presence of these macromolecules can reduce the activity of the water molecules because of changes in the water's H-bonding structure through interactions with the macromolecules. The macromolecules must be water soluble with good Li^+ interaction, such as poly(ethylene oxide) (PEO),[180] or other alternatives. Xie et al. demonstrated the success of this approach with PEO, causing a widening of the voltage window to 1.3–4.5 V versus Li/Li^+ and demonstrating stable cycling of this 2 M aqueous electrolyte in a lithium titanium oxide, $Li_4Ti_5O_{12}$ (LTO)|$LiMn_2O_4$ (LMO) full cell for 300 cycles.[179] Shang et al. proposed an electrolyte system whereby tetraethylene glycol dimethyl ether (TEGDME) is introduced as a new component, for an electrolyte composition of $Li_4(TEGDME)(H_2O)_7$, to help suppress the water electrolysis reaction and improve both the SEI and CEI formation.[181] This electrolyte was demonstrated with LTO|LMO full cells, where it was shown that there was a preferential distribution of TEGDME and the anion at the cathode surface, expelling water and reducing the possibility of an OER taking place.

Despite the promising work being done to improve the electrochemical stability window of aqueous electrolytes, it should be mentioned that the potential window is generally estimated using linear sweep voltammetry, which can lead to an overestimation of the stability. The results for this method depend heavily on the amount of electrolyte, cut-off current density, and chosen scan rate.[182] There is still much more work to be done in this direction, but using the molecular crowding approach may offer an ideal solution to enable low Li-salt concentration, AEs using biodegradable, low-cost macromolecules for HV-LIBs applications.

2.4.3. Aqueous Gel Polymer Electrolytes

The third option, using aqueous GPEs, uses a similar concept to the other two, wherein movement of water molecules within the electrolyte is restricted, but in this case the water molecules are confined within the polymer chains, due to the strong interactions between water and the polymer backbone. This concept will be discussed in more detail in the following section on GPEs. Using GPEs to suppress the water electrolysis reaction can allow much lower needed salt concentrations (lowering the cost) and do away with the need for a separator (increasing the energy density).

3. Gel Polymer Electrolytes for HV-LIBs

As both options to improve the safety and relative toxicity of the LEs discussed previously (i.e., ILs or AEs) still have a variety of inherent problems, such as low ionic conductivities or high cost, an alternative is still required. GPEs represent a balanced approach between LEs and solid-state electrolytes. With GPEs the LE is confined within a highly porous polymer matrix, which allows the thermal, chemical, electrochemical, and mechanical stability of the LEs to be improved.[183] The GPEs are capable of immobilizing the solvent molecules, decreasing their volatility and increasing their electrochemical stability and the safety of the battery.[184,185] In addition, GPEs have much higher ionic conductivities than solid state electrolytes (in some cases comparable to those of the current industry standard LEs) and offer better interfacial interactions, due to the inclusion of LEs.[186] GPEs have also been shown to suppress dendrite formation and improve the SEI composition, due to the dense structure, which hampers dendrite growth and promotes lithium salt distribution within the amorphous regions.[187–190]

The polymers required to form the host framework in GPEs typically must be capable of fast segmental chain movement, possess functional groups that promote salt dissolution, have a low glass transition temperature and high molecular weight, and of course a high thermal and electrochemical stability window.[191] For practical applications in LIBs, GPEs must also have good mechanical and chemical stability, high ionic conductivity, high Li^+ transference numbers, and promote good interfacial contact with the electrode surfaces.[192] In recent years, there has been a great deal of research into the topic of GPEs, with studies demonstrating the application of GPEs in HV batteries with more common polymers (such as PEO,[193–197] PVDF,[198–202] and acrylate-based polymers such as polyacrylonitrile, PAN,[203–207] or poly(methyl methacrylate), PMMA),[208,209] as well as with more sustainable, biodegradable polymers such as cellulose[185,210–217] or starch.[218,219] Some of these GPEs have even been capable of ionic conductivities comparable to commercial LEs (≈11.07 mS cm^{-1} for a 1 M $LiPF_6$ electrolyte in EC:DMC (1:1, v/v)).[220] Generally, GPEs can be split into two categories: physical and chemical GPEs. Physical GPEs are when the LE is contained within an inert polymer matrix. Chemical GPEs are when cross-linkers exist to facilitate chemical bonding with the functional groups of the polymer matrix.[221–223]

Physical GPEs, based on commonly used polymers, have been able to demonstrate performances similar to those of LEs, in large part due to their ability to uptake LE. An example of the extreme LE uptake of a chitosan–PEGGE GPEs is demonstrated in **Figure 7**a. Huang et al. demonstrated a blended poly(vinylidenefluoride-*co*-hexafluoropropylene–poly(butyl methacrylate–acrylonitrile–styrene), P(VdF-HFP)P/BMA-AN-St)-based GPEs, which possessed ionic conductivities of 1.4 mS cm^{-1} and enabled stable cycling of $LiNi_{0.5}Mn_{1.5}O_4$|Li cells for 150 cycles at 1 C, with a 98% capacity retention and a voltage window of 3–5 V versus Li^+/Li.[200] Liang et al. prepared GPEs with poly(vinylidene fluoride-cohexafluoropropylene) (PVDF-HFP), as well as PVDF-HFP-poly(propylene carbonate (PPC) polymers and a 1 M $LiPF_6$, EC:DMC electrolyte that demonstrated ionic conductivities of up to 1.18 mA cm^{-1}, and lithium transference numbers of 0.47.[199] These GPEs enable stable cycling of $LiFe_{0.2}Mn_{0.8}PO_4$|Li cells for 100 cycles at 0.2 C, with a voltage window of 2.5–4.4 V versus Li^+/Li. Song et al. used core–shell nanocomposite polymer fibers with a PPC shell and a PVDF-HFP/SiO_2 composite core.[201] These

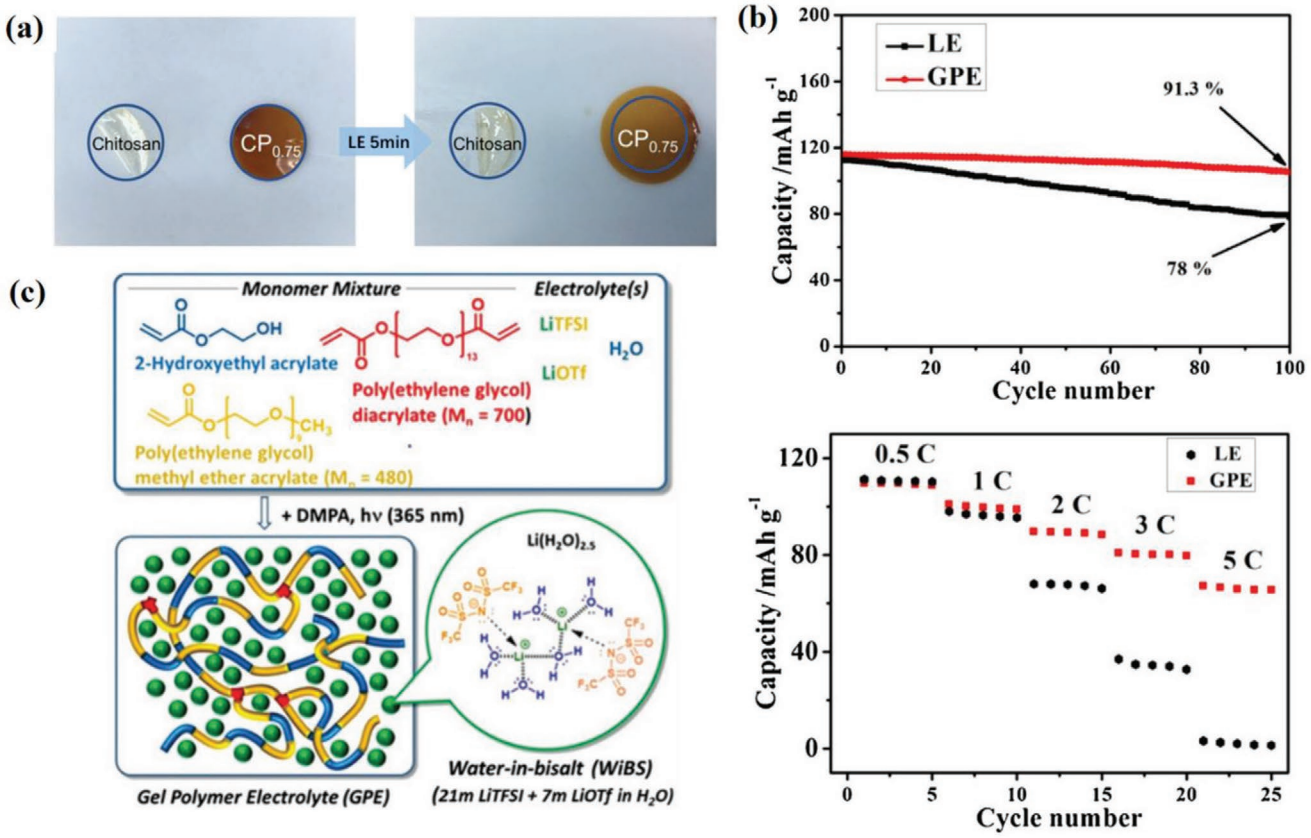

Figure 7. a) Demonstrates the extreme LE uptake of a cross-linked chitosan-PEGGE-based GPEs compared to pure chitosan. Reproduced with permission.[193] Copyright 2018, American Chemical Society. b) The cycling performance of LMNO|Li batteries based on a LE (1 M LiODFB-PC (1:1 in volume)) and on a cellulose-supported poly(propylene carbonate), infused with LE, GPE. Reproduced with permission.[210] Copyright 2016, Elsevier. c) A schematic of the UV-cured, acrylic GPE with incorporated water-in-bisalt electrolyte. Reproduced with permission.[225] Copyright 2019, RSC Publishing.

GPEs could achieve stable cycling of $LiFeO_4$|Li cells for 100 cycles at 1 C, with an ionic conductivity of 1.05 mS cm^{-1}. The ceramic particles enabled better Li^+ transfer, with transference numbers of 0.77.

For physical GPEs, discussed above, the polymer matrix is typically prepared first and then the electrolyte is incorporated into the matrix later, during cell assembly. This can lead to some downsides, such as poor electrolyte/electrode compatibility or more complex cell-assembly. Recent studies have investigated alternatives, such as the study by Hosseinioun et al., which demonstrated the performance of an in situ, cross-linked PMAA-based GPE (IC of 3.9 mS cm^{-1}) in an NMC-111/G full-cell with relatively stable cycling for 400 cycles at 0.1 C in a voltage range of 2.8–4.3 V versus Li/Li^+.[209]

However, despite the relative success of GPEs based on common polymers, in order to improve the sustainability of LIBs, it is important to explore materials based on more biodegradable materials. For example, a study by Zhao et al. demonstrated GPEs based on a cellulose-supported poly(propylene carbonate) network with an ionic conductivity of 1.14 mS cm^{-1} that enabled good coulombic efficiency and rate performance of a $LiNi_{0.5}Mn_{1.5}O_4$|Li battery, cycled from 3.5 to 5 V versus Li^+/Li (shown in Figure 7b).[210] Li et al. used glutamic acid derivatives as gelators for a commercial 1 M $LiPF_6$, EC:DMC, electrolyte, where conductivities of up to 9.20 mS cm^{-1} were obtained. The ESW of these glutamic acid-derived GPEs was up to 5.85 V versus Li^+/Li (higher than that of commercial electrolytes at 5.05 V).[218] However, undesirable solvents, such as THF and CH_2Cl_2, were still used in the preparation of these GPEs. Luo et al. used aqueous methods to prepare a lignocellulose-based GPEs with a hydroxyl propyl methyl cellulose polymer additive that demonstrated ionic conductivities of 6.14 mS cm^{-1} and a lithium transference number of 0.75 with an ESW of up to 5.32 V versus Li^+/Li.[213] These were cycled in $LiFeO_4$|Li cells and demonstrated stable cycling for 50 cycles at 0.2 C and better rate capability (1.5 C) than cells with LE and a Celgard 2400 separator. Han et al. used chitosan–lignocellulose composites to prepare GPEs that could enable stable cycling of $LiFePO_4$|Li cells for 100 cycles at 0.2 C, in a window of 2.0–4.5 V versus Li^+/Li, with an ESW of up to 4.8 V versus Li^+/Li, and a higher lithium transference number of 0.9.[215] The ionic conductivity was a bit lower, at 2.89 mS cm^{-1}, although still comparable to LEs. Ren et al. could achieve similar performances of $LiFePO_4$|Li with a PAN–lignocellulose composite GPEs with improved ionic conductivities (2.94–4.23 mS cm^{-1}) and stability window (up to 5.68 V vs Li^+/Li), as well as a high lithium transference of 0.84.[206] Environmentally friendly chemical GPEs have also been investigated. Xu et al. showed improved interfacial contact

Table 3. Summary of selected GPEs from literature along with their respective ionic conductivity (mS cm^{-1}), temperature T (°C), Li transference no., and maximum voltage (V vs Li$^+$/Li), RT refers room temperature.

Composition	Abbreviation	Li salt	Ionic conduct. [mS cm^{-1}]	T [°C]	Li transference no.	Max. voltage (V vs Li$^+$/Li)	Ref.
Chitosan–poly(ethylene glycol) diglycidyl ether	Chitosan–PEGGE	$LiPF_6$	0.2	20	0.869	5	[191]
Ceramic silica–poly(ethylene oxide)	SiO_2–PEO	$LiPF_6$	0.8–2	30	0.31–0.5	5	[192]
Ethoxylated trimethylolpropane triacrylate	ETPTA	$LiPF_6$	0.11–0.19	RT	–	4.2	[193]
Poly(vinylidene difluoride) with silica	PVDF/SiO_2, PVDF-HFP/SiO_2	$LiPF_6$	4.01–9.9	RT	≈0.28	≈4.5	[196]
Poly(vinylidene fluoridehexafluoropropylene)-poly(propylene carbonate)	PVDF-HFP-PPC	$LiPF_6$	1.8	RT	0.47	4.8	[197]
P(VdF-HFP))-poly(butyl methacrylate-acrylonitrile styrene)	P(VDF-HHFP)-P(BMA-AN-St)	$LiPF_6$	1.4	RT	–	5	[198]
P(VDF-HFP)-poly(propylene carbonate) silica composite	P(VdF-HFP)-SiO_2/PPC	LiTFSI	1.05	25	0.77	4.1	[199]
Polyhedral oligomeric silsesquioxane composite poly(acrylonitrile-maleic anhydride)	POSS-P(AN-MAH))	$LiPF_6$	2.51	RT	0.53	5.6	[201]
Poly(acrylonitrile-polyhedral oligomeric silesquioxane)	P(AN-POSS)	$LiPF_6$	6.06	RT	0.59	5.7	[201]
Poly(propylene carbonate)-based composite with silica	G-PPC-CPE	LiTFSI	0.164	RT	0.83	4.66	[202]
Polyacrylonitrile/cellulose composite	PAN/cellulose	$LiPF_6$	1.99	RT	–	5	[203]
Polyacrylonitrile and lignocellulose (60%)	PAN-LC	$LiPF_6$	2.94–4.23	25–50	0.84	5.68	[204]
Polyacrylonitrile with *N*-vinylpyrrolidone	P(AN-NVP)	$LiPF_6$	4.54	RT	0.55	5.11	[205]
Polymethyl methacrylate	PMMA	LiTFSI LiBOB	3.9	20	–		[207]
Cellulose-supported poly(propylene carbonate)	PPC-GPE	LiODFB	1.14	RT	0.68	5	[208]
Cellulose aerogel membrane	CAM	$LiPF_6$	5.76	25	–	4.6	[209]
Cyanoethyl cellulose-cellulose nanofibres-poly-L-lactic acid	CEC-CNF-PLLA	$LiPF_6$	1.07	–	0.48	5	[210]
Cyanoethyl cellulose-poly-L-lactic acid	CEC-PLLA		1.12	–	0.82		
Lignocellulose-based with hydroxy propyl methyl cellulose additive	LC/HPMC	$LiPF_6$	6.14	25	0.75	5.32	[213]
chitosan (15%)–lignocellulose	CSLC-15	$LiPF_6$	2.89	RT	0.9	4.8	[213]
Polyvinyl alcohol composite lignocellulose	PVA-LC	$LiPF_6$	2.5–4.17	30	0.59–0.73	5.2	[214]
Cellulose		LiTFSI	6.34	RT	0.82	4.5	[215]
Potato starch and lignocellulose		$LiPF_6$	1.2	RT	0.79	5.5	[185]
Polyethylene glycol methyl ether acrylate	MPEGA		1.2	40			[218]
Glutamic acid derivatives	G-16, G-18, and G-22		7.09–9.20	20	–	5.85	[218]
Poly(diallyldimethylammonium) bis(trifluoromethane) sulfonimide	PDADMATFSI	LiTFSI	3.35	22	0.41	4.9	[227]
2-Hydroxyethyl acrylate	HEA	LiTFSI	0.4	20	0.27–0.36	≈4.6	[228]

with the electrode in $LiFePO_4$|Li cells with a cross-linked chitosan–PEGGE-based GPEs (ionic conductivity of 0.274 mS cm^{-1} and lithium transference of 0.869) and relatively stable cycling at 0.2 C for 360 cycles.[193]

Some of the most promising GPEs for HV-LIBs have been aqueous GPEs, as the non-cross-linked portions of the polymer chains can interact with water molecules through hydrogen bonding, decreasing the amount of "free" water, and helping to expand the ESW.[183,224] Recent work by Langevin et al. where they incorporated a water-in-bisalt electrolyte into a UV-cured acrylic polymer matrix, increasing the ESW to 4.1 V,[225] due to the reduction of free water and increase in the retention of free water through polymer coordination. This GPE is demonstrated in Figure 7c. Cresce et al. developed an aqueous GPE based on cross-linked PEG acrylate polymers with LiTFSI in water and trimethylphosphate (37:40:2 molar ratio) for 4 V LIBs.[226]

GPEs offer a solution going forward to improve the safety and sustainability of LEs, without sacrificing the performance of LIBs (**Table 3**). In recent years, GPEs have demonstrated performances comparable to those of LEs with similar

electrode/electrolyte interface compatibility.[193,194,204,229] With further research and development, GPEs could be upscaled to enable large-scale, green production for cheaper, safer, and more sustainable HV-LIBs.

4. Separators

The separator in an electrochemical battery, typically with liquid-electrolytes, provides physical separation between the cathode and the anode electrodes. It also serves as the medium for the transfer of lithium ions during the charge and the discharge processes (**Figure 8**a). The separator plays an important role in the electrochemical performance and safety of LIBs. In separators, ionic conductivity degree, porosity, pore size, low internal resistance, and high electrolyte wettability, as well as chemical, mechanical, and thermal stability are the main parameters that greatly influence the performance of LIBs, with respect to internal resistance, long cycle performance, high capacity, and safety.[230–233] Separators are made of different kinds of porous polymer membrane materials (PPM) with pore sizes in the range of hundreds of nanometers.[234] PPM made by polyolefin (POS), including polyethylene (PE) and polypropylene (PP) have been developed and widely used in commercial LIBs, due to the excellent mechanical properties, high chemical stability, and low cost.[230,231,235–237] Nevertheless, the POS suffer from lower wettability with the LEs, which results in poor performance, particularly high-rate capability. [238,239] Additionally, the POS display serious thermal shrinkage at high temperature, which may lead to internal short-circuiting or even fires and explosions.[231,238] Therefore, the POS separators have usage limitation at high-temperature[231] as well as in HV-LIBs.[240] Herein, the alternatives and modifications for POS for HV-LIBs are discussed.

As an alternative for POSs, poly(vinyl alcohol) (PVA) is water-soluble and has hydroxyl groups to increase the interfacial bonding in the membranes, and also provide a good chemical, thermal, and mechanical stability.[241–244] Therefore, PVA-based membranes as separators can be a good choice for HV-LIBs. Karuppiah et al.[242] prepared PVA/melamine/LAP (PVAM) nanocrystals composite nanofiber membranes (Figure 8b) using the electrospinning method, and demonstrated its performance as a superior separator in HV anode LIBs, with three times larger electrolyte uptake than the commercial PE. The ionic conductivity of the PVAM membrane was higher (1.77 mS cm^{-1}) than that for the commercial PE membrane (0.636 mS cm^{-1}) at room temperature. Some chemical and electrochemical characterizations of PVAM and PE membranes are shown in Figure 8c–f.

Recently, the Zaghib group[245] has developed alumina-flame retardant separators through grafting halogen- and phosphorus-based molecules on the alumina surface (Figure 8g), and then integrating the modified powders into the pore structure of the cellulose separators, for safe NMC/graphite cells. This modified separator can compete with commercial (e.g., Celgard 3501, generally the Celgard separators made by PP[246,247] and in some cases combined with polyethylene resins[248]) separators in terms of electrochemical performance. For instance, the first discharge capacities for the NMC/graphite cells made with different separators were about 180 mAh g^{-1}. The cellulose/alumina-phosphate separators (with a thickness of Al_2O_3 layer in nm range) showed higher safe operation, and more thermal stability, when it was soaked with the combustible electrolyte. Combustion required three attempts to start burning, compared to the industry standard separator, and therefore resisted combustion for longer, and remained stable up to 300 °C. Additionally, the cellulose/alumina-phosphate separator operates at HV as another main advantage, in comparison to the pristine cellulose, and commercial (Celgard 3501) separators (Figure 8h–j).

The Zhang group has studied HV cathode materials, such as Li_2CoPO_4F, with operating potentials between 2.0 and 5.5 V versus Li/Li^+,[249] and they found that the positive covers of coin cells and separators can affect the performances of HV cathode materials. This group[240] has reported the effects of different separators and positive cell covers on the performance of a HV spinel, a $LiCr_{0.05}Ni_{0.45}Mn_{1.5}O_4$ cathode (LCrNMO), with cells that were cycled between 3.0 and 4.9 V versus Li/Li^+. The cyclic voltammetry (CV) curves of the Li|LCrNMO half cells, using Al-clad SS-316 positive covers and different separators, are shown in **Figure 9**a. The CV curves from the first and second cycles are almost identical for all the separators used, except for the cells with the Celgard 3501 separator, which showed a significant difference in performance. These cells have also demonstrated significant differences in the columbic efficiencies (CE), depending on the separator, with the CE of the first charge/discharge cycles on the order of 66% for Celgard 3501, and about 90% for Celgard K1640. Additionally, the rate capability and long-term cycling stability show that the cell with Celgard 3501 separator had poor stability, while the cell with the Celgard K1640 separator demonstrated much better performance under the same conditions (Figure 9b,c).

The main reason for the rapid capacity fading of $LiNi_{0.5}Mn_{1.5}O_4$ could be Mn^{2+} release from this cathode, however, besides this, significant capacity fading can also arise from the electrolyte (e.g., carbonates) decompositions at high electrochemical potential (for the $LiNi_{0.5}Mn_{1.5}O_4$ cathode), resulting in the formation of gases and other compounds. With a view to prevent and neutralize the decomposition products, as well as prevent the dissolution of soluble transition metal ions, Leitner et. al.[250] have proposed an electrochemically active separator containing $Li_{4+x}Ti_5O_{12}$ between two PO separator sheets (Celgard 2340), for application in graphite|$LiNi_{0.5}Mn_{1.5}O_4$ cells. These pouch full cells, with the improved separator, were cycled for hundreds of cycles with commercial electrolyte without any major capacity fading. However, when the commercial PO separator is used, a poor cycling stability results, as shown in Figure 9b,c.

As a modification on POS separators, Zua et al.[251] have reported a poly(vinylidene fluoride)/ethyl cellulose and amino-functionalized nano-SiO_2 (PVDF–EC–(A-SiO_2)) composite coated on PE as a high performance separator for 5 V HV-LIBs. Compared to the commercial PE membrane separator, the PVDF–EC–(A-SiO_2) displayed higher melting temperature, better wetting behavior, and a higher ESW, 5.3 V (vs Li/Li^+), as well as improved ionic conductivity from 0.34 to 0.79 mS cm^{-1}. Additionally, the HV-LIB based on $LiNi_{0.5}Mn_{1.5}O_4$|Li, using the PVDF–EC–(A-SiO_2) membrane have exhibited superior rate capability performance (Figure 9f–i).

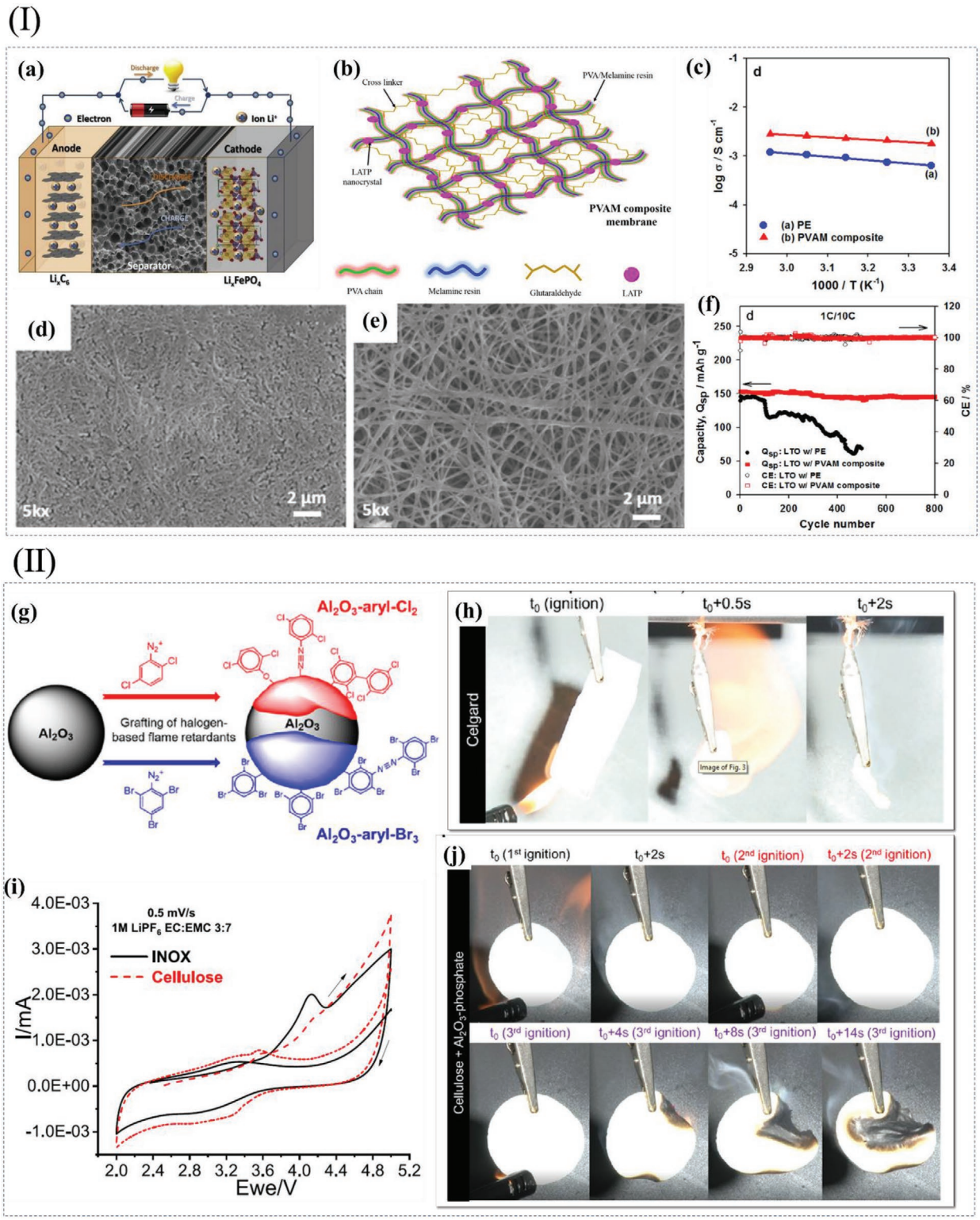

Figure 8. (I): a) Schematic illustration of main component of a LIBs. Reproduced with permission.[230] Copyright 2019, Elsevier. b) Schematic representation of PVAM composite membranes, c) Arrhenius plot of the PVAM and PE separator at various temperatures, The E_a of the PE separator the PVAM composite membrane are about 13.54 and 9.73 kJ mol^{-1}. SEM images of d) the PE and e) PVAM membranes. f) The cycling stability of $Li_4Ti_5O_{12}$ (LTO) anode materials with different separators at high C rate, with voltage range of 1.0–2.5 V (vs Li/Li^+), electrolyte: 1 M $LiPF_6$ in a mixture of ethylene carbonate (EC) and diethyl carbonate (DEC) (1:1 v/v,). Reproduced with permission.[242] Copyright 2020, American Chemical Society. (II): g) Schematic of grafting halogen- and phosphorus-based molecules on alumina surface. h) CV tests at a scan rate of 0.5 mV s^{-1} for coin-cells assembled with a stainless-steel spacer (bare electrode) and a cellulose separator working electrode. Vertical flame test for i) Celgard and j) cellulose + alumina-phosphate separators. Reproduced with permission.[245] Copyright 2021, Elsevier.

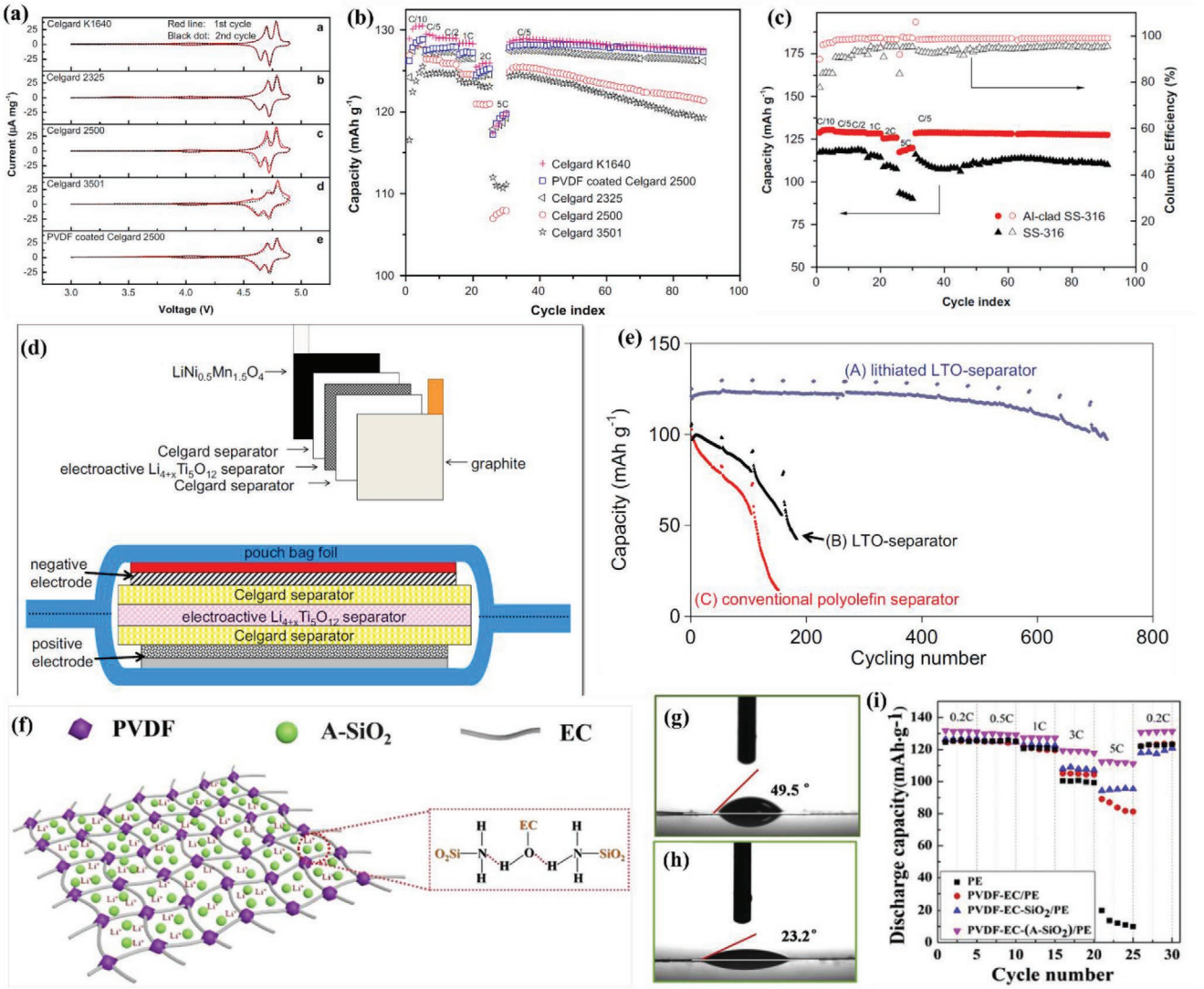

Figure 9. The Li|$LiCr_{0.05}Ni_{0.45}Mn_{1.5}O_4$ half cells using Al-clad SS-316-coin cell cans and various separators: a) CV curves at 0.01 mV s^{-1}. b) Rate performance and long-term cycling stability. Li|$LiCr_{0.05}Ni_{0.45}Mn_{1.5}O_4$ half cells using an SS–316 and an Al-clad SS-316 cans with a PE Celgard K1640 separator. c) Rate capability, long-term cycling stability, and Coulombic efficiency. Electrolyte: 1 M $LiPF_6$ in EC/EMC (3:7 ratios in volume), and voltage range 3–4.9 V versus Li/Li^+. The electrode composition $LiCr_{0.05}Ni_{0.45}Mn_{1.5}O_4$/Super P/PVDF = 80/10/10. Reproduced with permission.[240] Copyright 2012, Elsevier. d) Schematic illustration of set-up of pouch cell including electroactive separator, $Li_{4+x}Ti_5O_{12}$ (LTO), two polyolefin separator sheet (Celgard 2340), graphite as anode and $LiNi_{0.5}Mn_{1.5}O_4$ as cathode. e) Discharge capacity over cycle number of graphite|HV-spinel cells containing different separators. Cathode electrode composition: $LiNi_{0.5}Mn_{1.5}O_4$/carbon black/graphite/PVDF-HFP: 88/3/3/6 wt%. Anode electrode composition graphite/PVDF-HFP: 94/6 wt%. Electrolyte (1 M $LiPF_6$ in 1:1 mixture of EC:EMC. Current: 3 cycles at 0.2 C and then 1 C every 50 cycles. cut-off voltage: 4.8 V. Reproduced with permission.[250] Copyright 2013, Elsevier. f) The schematic representation of the surface of PVDF–EC–(A-SiO_2) composite membranes and hydrogen-bonding between EC and A-SiO_2. Contact angle pictures of composite membranes for g) PE, and h) PVDF–EC–(A-SiO_2)/PE. i) C-rate capability of the $LiNi_{0.5}Mn_{1.5}O_4$ cathode using various separators under 0.5 C rate between 3.5 and 5.0 V. the electrode composition: $LiNi_{0.5}Mn_{1.5}O_4$:PVDF:carbon black, 8:1:1, wt%. Electrolyte: 1 M $LiPF_6$/EC:EMC (1:3, v/v). Reproduced with permission.[251] Copyright 2018, Elsevier.

Reports have shown[252–255] that the performance of polymer-based separators were effectively improved by doping inorganic nanoparticles. For instance, the Lee group[256] has established evaporation-induced, close-packed SiO_2 nanoparticle-embedded PET nonwoven composite separators (NW-separator), with an excellent improvement in the thermal shrinkage for HV-LIBs applications. Luo et al.[257] have reported that 10 wt% nano-CeO_2 in PE separator, coated with a poly(methyl methacrylate-butyl acrylate-acrylonitrile-styrene) (P(MMA-BA-AN-St)) copolymer, showed high conductivity (2.5 mS cm^{-1}) at room temperature, and a separator with 100 wt% nano-CeO_2 exhibited better mechanical strength. These separators were utilized in HV-LIBs, with $Li/LiNi_{0.5}Mn_{1.5}O_4$ between 3 and 5 V versus Li/Li^+. Some of the results for this investigation are shown in **Figure 10**a–g. According to comprehensive evaluation of the separators illustrated in Figure 10h, the separator with 100 wt% nano-CeO_2 content in the separator could be selected as the most suitable

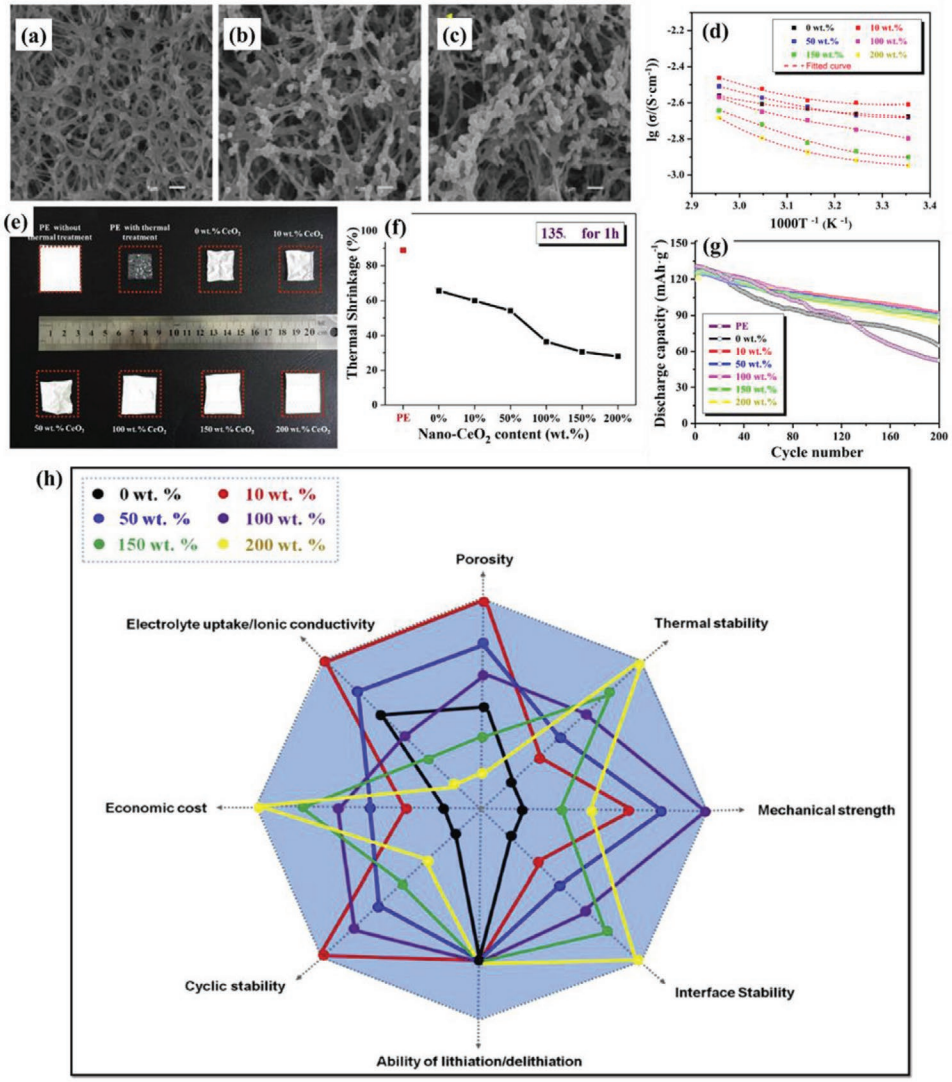

Figure 10. The P(MMA-BA-AN-St)/PE separators with different contents of nano-CeO_2:SEM images of a) 0 wt%, b) 10 wt%, and c) 100 wt%. d) Temperature dependence of ionic conductivity of the separators. e) Pictures of the separators before and after heating treatment at 135 °C for 1 h. f) Corresponding thermal shrinkage percentage based on the area for the separators. g) Cyclic stability of Li|$LiNi_{0.5}Mn_{1.5}O_4$ cells using different separators at 0.2 C rate, electrolyte: 1 M $LiPF_6$ in solvent (EMC/EC/DEC:5/3/2, wt%). h) The effect of nano-CeO_2 contents on the performance of the separators Reproduced with permission.[257] Copyright 2017, Elsevier.

separator overall, when taking into consideration both the comprehensive performances and economic cost.

PVDF-HFP has been used as a separator in LIBs.[258–260] Bui et al.[261] have developed a multilayer PVDF-HFP membrane with thicknesses of about 13, 15, and 24 µm for the two-, three-, and four-layer PVDF-HFP membrane separators, with highly porous, lamellar structures for application in HVBs, specifically with $LiNi_{0.5}Mn_{1.5}O_4$ as a cathode, and an operating potential of 3.5–4.9 V versus Li/Li^+. Due to the superior electrolyte wettability and highly porous structure of the PVDF-HFP separators, an improved electrolyte uptake volume and outstanding electrolyte retention was obtained, thus, demonstrating higher electrochemical performances compared to that of a commercial separator (Celgard).

Ko et al.[262] developed a reversible 4.8 V HV-LIB, Li_2CoPO_4F|Gr, in concentrated electrolytes. Different separators, binders, and electrolytes have been used and optimized in the full-cell designs. For the optimization of separators, by employing a quartz fiber separator instead of a PP separator (PP3501, Celgard, named as PP) in Li_2CoPO_4F|Li half-cells, the cell could be further improved, as demonstrated by the CV results of the cells in commercial electrolytes presented in **Figure 11**a,b. As can be seen, the optimized cell design with a quartz fiber separator showed four sharp redox pairs for the first time, while only two oxidation peaks and one broad reduction peak have been reported in the literatures before this study, indicating the new design decreases cell impedance. The full cell investigation can also be seen in Figure 11c, where a highly reversible HV-LIB battery, cycled in high concentrated electrolyte, is demonstrated, due to the optimized electrolyte, separator, and binder. The optimized full cell, employing 5.9 M $LiBF_4$/PC:FEC, showed a capacity retention of 70% after 700 cycles

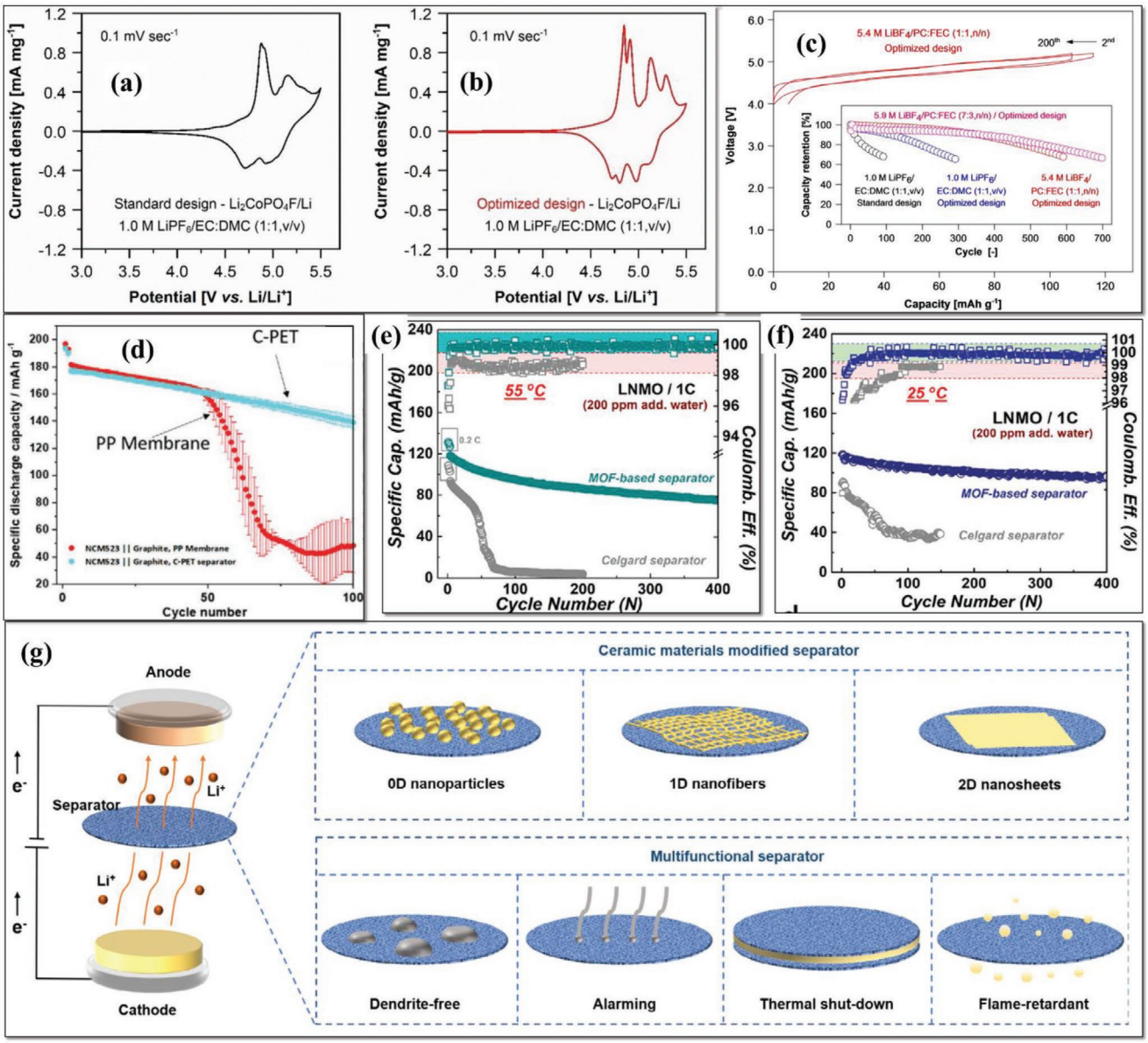

Figure 11. CV of Li_2CoPO_4F/Li half-cells with a) standard design: PP separator, cathode composition: Li_2CoPO_4F/pristine AB composite:pristine AB:PVDF (85:10:5 wt%) and b) optimized design: heated quartz fiber separator, cathode composition: Li_2CoPO_4F/annealed AB composite:annealed AB:LiPAA (85:10:5 wt%), and finally the electrode coated with 5 wt% SiO_2. The standard and the optimized electrodes dried at 120 °C for 12 h, and 200 °C for 1 h under vacuum, respectively. The commercial electrolyte 1 M $LiPF_6$/EC:DMC (1:1, v/v) was used for both testes, and the scan rate was 0.1 mV s^{-1}. c) Li_2CoPO_4F|Gr full-cell with different concentrated electrolytes, cathode loading was about 1.3–2.2 mg cm^{-2}, the N/P ratio was between 1.3 and 1.4. Reproduced with permission.[262] Copyright 2020, John Wiley and Sons. d) cycling stability of NCM523|Gr cells at voltage range of 2.8–4.5 V, N/P ratio: 1.35/1.00, with C-PET (γ-AlOOH-coated PE terephthalate) and PP membrane (polypropylene, Celgard 2500) separators. Reproduced with permission.[275] Copyright 2020, John Wiley and Sons. e,f) Cycling stability of Celgard and MOF-based ($Cu_3(BTC)_2$, HKUST-1) separators for Li|$LiNi_{0.5}Mn_{1.5}O_4$ (LNMO) cells at 25 and 55 °C at a 1 C current rate (1 C = 200 mAh g^{-1}). Reproduced with permission.[280] Copyright 2020, RSC Publishing. g) A schematic illustration of separator construction for high-safety LIBs. Reproduced with permission.[263] Copyright 2020, John Wiley and Sons.

and an average CE of about 99.6% for the entire cycle lifetime. These authors further developed the Li_2CoPO_4F|Gr full cell with graphitized acetylene black as a novel anode material,[76] a heat-treated quartz fiber separator, and a 6.6 M $LiBF_4$/SL:FEC (9:1 n/n) electrolyte. This full-cell exhibited an impressive capacity retention of 93% after 1000 cycles with CE of about 99.9%.

Commercial separators, particularly the PE types, have a tendency to shrink at high temperature over 100 °C, due to poorer thermal stability, resulting in internal short circuits, and creating a safety hazard.[263] After shutdown, the cell temperature may continue to increase, due to temperature hysteresis and slow heat dissipation,[264] resulting in worsening mechanical properties of the separator. Hence, besides robust thermal and mechanical stability, separators are required to shut down and block the pores when overheating or short circuit occurs. Therefore, it is vital to develop a separator that possesses a

meltdown temperature much higher than its shutdown temperature, to prevent loss of mechanical integrity and direct contact of electrodes and to prevent thermal runaway. Thus, robust mechanical properties are expected of the separator, even above the shutdown temperature. Many strategies have been investigated to maintain robust mechanical properties of separators after shutdown, such as trilayer separators, for instance, where a PE layer is sandwiched between two porous polymer layers such as polypropylene (PP), PP|PE|PP[265] or polybenzimidazole (PBI), PBI|PE|PBI,[266] and other trilayer separators.[267,268] Other strategies include coating separators with thermal-resistant polymers,[269–271] and with numerous high thermal resistant, and flame retardant materials, such as metal oxides and hydroxides.[263,272–274] Recently, Ding et al.[264] developed a trilayer separator with β-crystal polypropylene (β-iPP), with the middle layer composed of nano-Al_2O_3-PE (β-iPP-Al_2O_3|Al_2O_3-PP-PE|β-iPP-Al_2O_3). The Al_2O_3 nanoparticles lower lithium-ion migration impedance and stabilize SEI film formation. This trilayer separator showed better mechanical and thermal stability at high voltages, as well as a better electrochemical performance, compared to a commercial PP|PE|PP separator, although with costlier materials and processes.

Klein et al.[275] studied NCM523|graphite full cells at 4.5 V with different separators: PP membrane (Celgard 2500), PP fiber (FS2190; Freudenberg), C-PET (γ-AlOOH-coated PE terephthalate), and C-PE (α-Al_2O_3-coated PE membrane). Although the PP membranes demonstrated excellent cycling at 4.3 V (97% after 100 cycles), at 4.5 V, a capacity roll-over started after 50 cycles, indicating formation of Li metal dendrite.[276] By using a PP fiber separator, the early capacity roll-over at 4.5 V was prevented, however, Li metal dendrites were still formed, due to the electrode cross-talk phenomena, whereby transition metals, M^{n+} (here, Mn, Co, and Ni), dissolve into the electrolyte and are transported through the separator and deposited at the anode material (graphite). Interestingly, when a C-PET separator coated with γ-AlOOH was used, it leads to in situ formation of difluorophosphate additive in high amounts, resulting in an improving cycling performance (Figure 11d).

The dissolution of M^{n+} from cathodes into the electrolyte is often unavoidable during charge/discharge cycling, mostly under high temperature and cell voltage conditions.[277,278] This electrode cross-talk, as a result, could seriously affect the battery performance. Even in the case of $LiFePO_4$ as the cathode, which possesses a stable crystal structure and low working voltage, iron deposition is still detected on the graphite anode after a long cycle life.[279] As a main result of the electrode cross-talk, lithium dendrite growth could easily be initiated on the transition metals deposited on the anode particles, which is a safety issue for LIBs. Also, H_2O and subsequently hydrofluoric acid (HF) electrolyte decomposition products, which can be produced during cycling, are another issue, and can cause fast capacity fading and cell failure.[280] Modifying/coating separators can be a solution for addressing these issues, for instance, Xu et al.[281] developed a multifunctional polymeric separator, which is a PP separator (Celgard 2320) coated by lithium-ion-exchange enabling zeolite, which acted as an HF scavenger. This zeolite enhanced thermal stability, and, importantly, traps transition metal ions and absorbs trace water to decrease cross-talk and the formation of HF. In full cell batteries, NMC532 + LMO|Gr, with this modified separator, delivered a CE up to 99.89%, and achieved a capacity retention of 78% after 500 cycles. However, as they used a thick coated Li-zeolite, the rate capability and energy density of cells was limited, and it could not be applied in practical applications. Chang et. al.[280] introduced a metal–organic framework, MOF, and separator ($Cu_3(BTC)_2$, HKUST-1) for enhancing the electrochemical performance of the HV cathode materials LNMO (Figure 11e,f), and NCM-family materials in half-cell tests. MOF has good water scavenging ability, and suppressed transition metal diffusion, as well as a robust chemical and mechanical stability. Recently, Son et al.[282] fabricated a powerful H_2O and HF scavenging PE separator, coated by porous silica and (3-isocynatopropyl)triethoxysilane. The NCM811|Gr cell fabricated with this coated separator exhibited a high capacity retention of about 80% at temperatures of 55 °C. Additionally, the coated separator improved the cycling stability of cells even with an electrolyte containing 1000 ppm of H_2O.

In summary, many studies have been done to develop safe separators for high-performance LIBs, which are illustrated in Figure 11g.[263] Altering traditional separators with ceramic and/or polymer materials is one of the most efficient methodologies to improve the thermal and mechanical stability of separators, as well as improve the electrochemical performance of cells through H_2O and HF scavenging or metal ion diffusion suppression. Overall, the separators, despite being inactive components in conventional LIBs systems, must be optimized, modified, and retested when HV cathodes, such as $LiNi_{0.5}Mn_{1.5}O_4$, are considered in the full cell, in order to improve the overall energy density, performance, and safety.

5. SEs

SSBs are an emerging trend for next-generation batteries and use fully all solid electrodes and electrolytes. Tremendous interest in developing SEs and SSBs to provide safe and durable batteries can play a significant role in future mobility. SEs determine the main properties of SSBs. The significant difference between the two battery chemistries is that SSBs have a SE; LIBs have a liquid electrolyte. SSBs offer potentially low flammability, higher electrochemical stability, cathodes with higher potentials (>4.2 V), good performance, safety at low cost, and higher energy density than conventional batteries.[283] Still, they have their issues: there is a lack of suitable SEs,[284] the interface between the electrodes and the SE can hamper performance, and SEs are a crucial component of SSBs.[285–288] Much effort has gone into finding new SEs with high ionic conductivities, and many practical hurdles are still needed to overcome. So far, there are more than 30 types of SEs, such as oxides, sulfides, halides, polymers, hydrides, are demonstrated and reported, such as with oxide-based $Li_{3x}La_{2/3-x}TiO_3$ [LLTO, 10^{-4} S cm^{-1}),[289,290] $Li_7La_3Zr_2O_{12}$ (LLZO, 10^{-4} S cm^{-1}),[291,292] sulfides based Li_2S–P_2S_5 (LPS, 10^{-3} S cm^{-1}),[293,294] $Li_{10}GeP_2S_{12}$ (LGPS, 10^{-2} S cm^{-1}),[285,295] halide-based Li_3MCl_6 (M = In, Y, Er, 10^{-3} S cm^{-1}),[296] and hydride-based $Li_2B_{12}H_{12}$ (LBH, 10^{-3} S cm^{-1})[297,298] at RT. These classified SEs possess excellent Li-ion conductivities comparable to, or even higher than, organic LEs (e.g., 1 M L^{-1} $LiPF_6$ in

EC and DMC solution, 10^{-2} S cm^{-1}).[299] Besides ionic conductivity, several problems accompany finding the best SE combination for SSBs, such as interfacial resistance, the interface between cathode/SEs, SEs/anode, and cycling life. Additionally, until now, no large-scale production process for these SEs exists. In principle, there are three main methods to produce SEs on a laboratory scale: high-temperature reaction, mechanochemical reaction(milling), and wet chemistry. Until today, most SEs have been prepared by mechanochemical milling based on feasibility, faster production, and safety concerns. The following sections summarize the development of the different classes of SEs and the HV cathode material's competence with the electrochemical performance of SSBs. This section will cover recent developments of composite SEs (polymer and oxide), sulfide, and halide SEs for high voltage SSBs applications.

5.1. Composite Solid Electrolytes (CSEs)

This section will discuss polymer and oxide SEs, their combination, CSEs, and an overview of HV-SSBs applications. Developing SE materials that match HV cathodes and Li anode is quite significant for creating SSBs. $Li_7La_3Zr_2O_{12}$(LLZO) ceramic oxide SEs (OSEs), consisting of the garnet crystal structure, have shown great attention due to the high ionic conductivity (especially Ta-doped $Li_{6.4}La_3Zr_{1.4}Ta_{0.6}O_{12}$ (LLZTO, 1 mS cm^{-1}), excellent stability against Li-metal anode, and wide electrochemical window.[300,301] NASICON structure type $Li_{1.7}Al_{0.3}Ti_{1.7}(PO_3)_4$ (LATP) SEs are also promising candidates for SSBs, due to their high ion conductivity, excellent stability toward moisture, and lower cost.[302] However, these OSEs can hinder the interfacial compatibility between SEs and electrodes, and cause severe interfacial side reactions, limiting the performance of SSBs. Another challenge for OSEs is processibility, as they require higher sintering temperature, and LATP is not stable against Li metal. Polymer SEs (PSEs) are gaining more interest, spurred by finding better safety and higher voltage applications for SSBs. Many classes of polymer electrolytes (phosphates, polyethers, polyesters, nitrile-based, polysiloxane, polyurethane) have been studied so far, most commonly PEO is often investigated and used in conventional batteries.[303] The main difference between inorganic ceramic and polymer SEs is their mechanical properties. Polymers are more accessible to processing than ceramics, which reduces fabrication costs. The SSBs performance depends on the electrolyte and their properties. Polyether and lithium phosphorus oxy-nitride-based electrolytes are commonly used in solid-state batteries. PEO-type SEs have attracted significant attention and made rapid development in lithium-ion batteries. However, their low ionic conductivity and low lithium-ion transference number at ambient temperature prevent their practical application. PEO-based solid polymer electrolytes (SPEs) have recently gained popularity in the SSBs, due to their low cost, chemical versatility, excellent lithium dendrite resistance, and good cyclability.[304]

For this reason, more often, OSEs are combined with PSEs, such as CSEs.[305] The CSE membrane is easy to integrate with the LIB and ASSB process, has good mechanical strength, excellent processability, and cycle life. Moreover, PEO/lithium bis(trifluoromethane sulfonyl)imide (PEO-LiTFSI) is relatively easy to process, and has low ionic conductivity at RT. Combining them with ceramic SEs improves the ionic conductivity and the performance of batteries. In the CSE, LLZO, with higher ionic conductivity, acts as the primary conductive phase. PEO acts as the percolating network, connecting LLZO particles and adding the benefit of ease of fabrication. Many researchers have demonstrated the enhanced ionic conductivity of PEO-based composite solid polymer electrolytes (CSPEs) by introducing inert fillers (such as Al_2O_3, TiO_2, and SiO_2) in the PEO matrix, as well as active fillers with high ionic conductivity, such as garnet-type $Li_{6.4}La_3Zr_2Al_{0.2}O_{12}$(LLZAO), NaSICON-type $Li_{1+x}Al_xTi_{2-x}(PO_4)_3$(LATP), perovskite-type $Li_{0.34}La_{0.51}TiO_3$(LLTO).[306] Gu et al. recently reported that adding $Li_7La_3Zr_{1.4}Ta_{0.6}O_{12}$ (LLZTO) ceramic SEs particles to polymer electrolytes PEO-LiTFSI and PVDF-HFP improved the ionic conductivity, mechanical strength, and electrochemical window (5 V).[307] They reported that the ASSBs with a composite cathode NMC_{622}, CSPEs, and graphite composite-based anode showed a specific capacity of 179.56 and 146.73 mAh g^{-1} (charge and discharge cycle, current rate at 0.05 C, respectively). This demonstrates how promising CSPE are for SSBs, because of a good cyclability, rate performance, and better interface stability. Wang et al. introduced a new composite GPE, consisting of LATP, poly(propylene carbonate, PPC), and PVDF-HFP, designed and constructed through a solution-casting method.[308] They reported that composite GPEs have a higher ionic conductivity of 0.94 mS cm^{-1} at 30 °C, and a wider electrochemical window of 5.2 V. Using this SE membrane, LFP-based SSBs ($LiFePO_4$–Li) delivered excellent cycling stability.

Chen et al. reported that HV ASSBs, with higher Ni-rich $LiNi_{1-x}Co_{0.2}Mn_xO_2$ (NMC622) cathode, Li anode, and SPE (PEO_{10}-LiTFSI-$PYR_{14}TFSI_2$) solid polymer electrolyte, provided better cycling performance and C-rate capability high voltage compatibility (**Figure 12** I).[309] The NCM622 cells first discharge capacity was (159.2 mAh g^{-1}), with a columbic efficiency of 88.2% at 0.1 C. Incorporation and combination of two polymer networks with PEO-contained PSE (Figure 12 II), along with a linear PAN, are reported by Li et al.[310] This concept provided better oxidative stability, and a voltage window of 4.1 V to over 5.1 V versus Li/Li^+, by introducing 2 wt% of PAN. Using these SEs delivered excellent cyclability of lithium metal for $LiNi_{0.6}Mn_{0.2}Co_{0.2}O_2$ cathodes, and a capacity of over 150 mAh g^{-1} was achieved at 90 °C. Wen et al. reported that introducing graphene oxide (GO–PEO) enabled flexible solid polymer electrolytes for SSBs.[311] Adding 1 wt% GO allowed the conductivity to reach 0.0154 mS cm^{-1} at 24 °C, far better than without GO, improving the electrochemical performance, and enabling wide electrochemical stability (≈5 V), and mechanical strength. They demonstrated SSBs ($LiFePO_4$/GO–PEO/Li) with excellent cyclability and rate capability, possessing a discharge capacity of 142 mAh g^{-1} at 0.5 C with 91% capacity retention after 100 cycles.[311]

5.2. Halide Solid Electrolytes (HSEs)

So far, there has been many developments of OSEs, PSEs, sulfide solid electrolytes (SSEs), and continuing search for

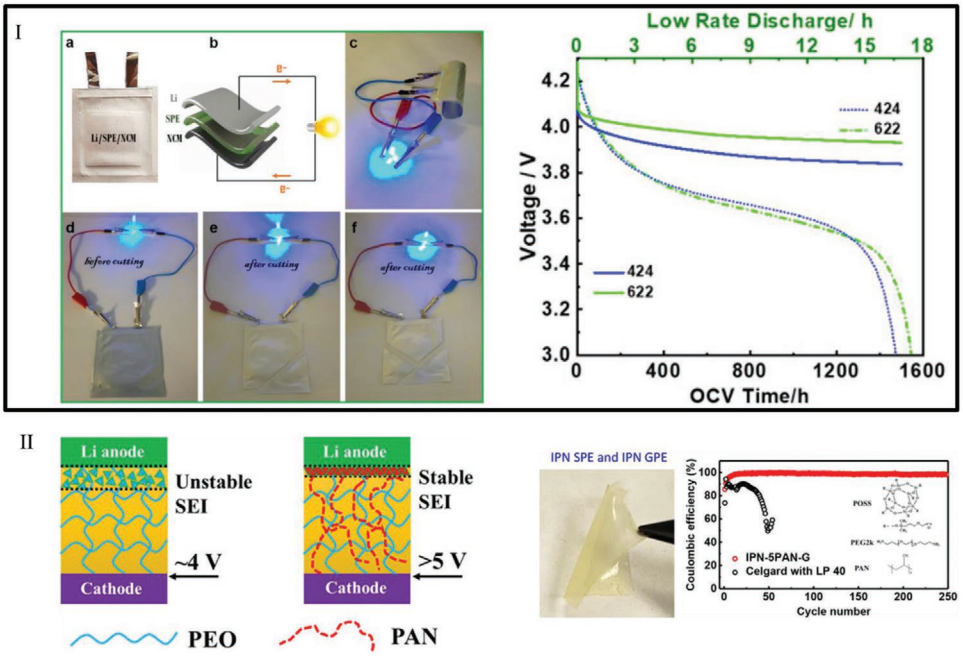

Figure 12. I) Demonstrations of SSBs flexible and prototype pouch cell configurations with solid polymer electrolytes before cutting, after cutting, and multiple cutting with working conditions. The self-discharge and OCV time of two different NMC cathodes (NMC_{622} and NMC_{424}). Reproduced with permission.[309] Copyright 2019, Elsevier. II) A scheme of high anodic voltage and stable SEI with the addition of PAN into the PEO Network. A microscope image of IPN SPEs polymer SEs. Coulombic efficiency measurement of the Li/Cu a symmetrical cell using IPN-5PAN-G and a control electrolyte, the capacity at 0.5 mAh cm^{-2} and current density of 0.5 mA cm^{-2} reported at RT. Reproduced with permission.[310] Copyright 2021, American Chemical Society.

better SEs for HV-SSBs applications. However, many challenges remain to be overcome for an optimized performance, processibility, and stability. The HSEs are recently emerging and finding new materials to improve SSBs. HSEs have high ionic conductivity and soft mechanical properties, and can be used with 4 V-class cathode materials, and a superior oxidative stability and electrochemical window. The general formula of HSEs is Li_3MX_6 (M = Y, In, Er, Sc, etc. X = Cl, Br, I, F) and depends on doping level of different metals with halogen compounds.[312–314] Many HSEs are recently reported, such as monoclinic Li_3InCl_6 (≈2 mS cm^{-1}),[315,316] orthorhombic $Li_{3-x}M_{1-x}Zr_xCl_6$ (M = Y, Er, ≈1.4 mS cm^{-1}),[312,317] spinel $Li_2Sc_{2/3}Cl_4$ (1.5 mS cm^{-1}),[318] monoclinic Li_xScCl_{3+x} (3 mS cm^{-1}),[319] and trigonal Fe^{3+}-substituted Li_2ZrCl_6 (1 mS cm^{-1}).[320] Most commonly, two different HSEs were widely reported Li_3ICl_6 (LIC) and Li_3YCl_6 (LYC), which have a monoclinic structure ($C2/m$, 0.71 mS cm^{-1} LIC) and the trigonal structure ($P\bar{3}m1$, 0.65 mS cm^{-1} LYC), respectively.[315] Both HSEs structures show relatively high ionic conductivity with those reported from the ball milled powders.[321,322] Asano et al. reported two different HSEs LYC and Li_3YBr_6 (LYB), synthesized via ball-milling followed by annealing.[312] Many superionic SEs have been widely investigated, but their limited electrochemical stability windows leads to an unwanted protective coating for HV cathode materials. On the other hand, thermodynamic calculations of HSEs for stable HV materials suggest the electronegativity difference between M and X (Li_3MX_6) affect the structural properties and stability of these materials.[323] This study[324] also found that chlorides have the highest oxidation potential (≈4.3 V vs Li/Li^+), larger bandgap, and higher elastic moduli, making them suitable HSEs for HV cathodes. Along with high ionic conductivity, the excellent electrochemical stability of HSEs in a 2.8–4.3 V window suggests the feasibility of 4 V-class cathode materials, without any additional coatings for SSBs. Zhang et al.[325] reported and designed the incorporation of F for HSEs of $Li_3InCl_{4.8}F_{1.2}$ and LIC, to form a dual-halogen SE. $Li_3InCl_{4.8}F_{1.2}$ reported ionic conductivity over 10^{-4} S cm^{-1} at RT, and exhibits a practical anodic limit at 6 V. The incorporation of a $Li_3InCl_{4.8}F_{1.2}$ cathode SE with LCO (In//Li_6PS_5Cl//LIC HSEs//$Li_3InCl_{4.8}F_{1.2}$/LCO, voltage range of 2.6–4.47 V (vs Li/Li^+)) enabled HV SSBs with better electrochemical performance (**Figure 13**a,b). The charge and discharge profiles of the SSBs for three cycles, at a low current density of 0.063 mA cm^{-2}, demonstrate a specific capacity of 160.6 mAh g^{-1}, with a high Coulombic efficiency of 92%. These are more promising HSEs, in terms of electrochemical stability, chemical stability, and deformability. The Nazar group has reported a new and advanced material design of the metastable trigonal phase of Li_3YbCl_6, with an ionic conductivity of 0.1 mS cm^{-1}, and Zr mixed $Li_{3-x}Yb_{1-x}Zr_xCl_6$ HSEs, with conductivities of 1.1 mS cm^{-1} at RT, which is higher than LYC.[324] They also demonstrated SSBs with the uncoated 4V-class cathode materials of NMC622 and $Li_{2.7}Yb_{0.7}Zr_{0.3}Cl_6$, with good electrochemical performance, as shown in Figure 13c,d. HSEs are promising, with remarkable electrochemical performance and material stability for SSBs, in comparison to other SEs, such as sulfides or oxides.[323]

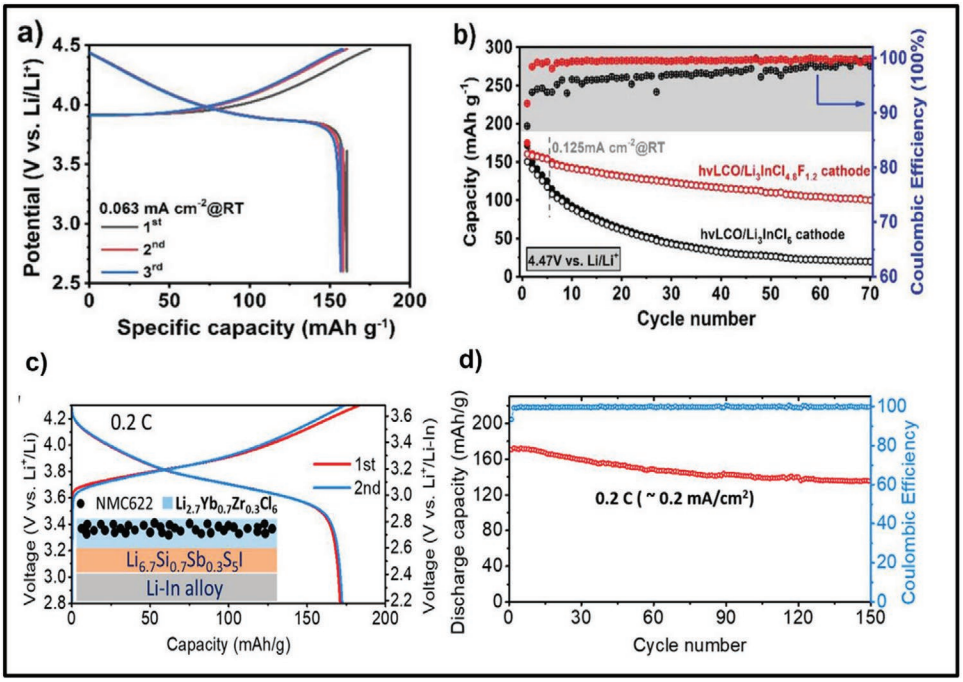

Figure 13. a,b) Discharge/charge curves of $Li_3InCl_{4.8}F_{1.2}$ high cathode SE cell for first three cycles at 0.063 mA cm^{-2}. The electrochemical performance of high voltage LCO full cells using $Li_3InCl_{4.8}F_{1.2}$ and Li_3InCl_6 cathode SE. Reproduced with permission.[325] Copyright 2021, John Wiley and Sons. c,d) Charge/discharge profiles for SSBs consist of cathode materials NMC_{622} and $Li_{6.7}Si_{0.7}Sb_{0.3}I_5S$ separator, Li–In alloy as an anode, the initial two cycles at 0.2 C rate and Coulombic efficiency, discharge capacity, and the number of cycles. Reproduced with permission.[324] Copyright 2021, American Chemical Society.

5.3. SSEs

Among inorganic SEs, sulfide-based SEs have exceptionally high ionic conductivities, in the range of 10^{-4} to 10^{-2} S cm^{-1} at ambient temperature. SSEs are promising candidates for SSBs, due to their high ionic conductivity, electrochemical operating window, excellent mechanical properties, and is easily reproducible.[285,326] SSEs have attracted much attention due to their isotropic ion conduction, zero grain boundary resistance, and relatively low-cost starting materials, based on earth-abundant elements. There are still significant challenges for the application of SSEs: a) SSEs are extremely sensitive to moisture and quickly react with water in the air to produce toxic H_2S gas and affect the structure of the electrolyte; b) problems of the interface between electrode and electrolyte still need to be understood. SSEs can be processed in several forms (glass, glass–ceramic, and crystalline) and have a wide range of available chemistries.[327,328] Several SSEs have been discovered with an ionic conductivity of more than 10 mS cm^{-1}, comparable to the organic electrolytes used in LIBs. However, the main challenges associated with the commercialization and processing of SSEs are their instability toward air/moisture, as well as Li metal, which leads to complex processing requirements.[329,330] In the following section, we discuss the most recent SSEs and considerations regarding development of high voltage applications.

Kato and Kanno, researchers from Toyota and the Tokyo Institute of Technology, have claimed to discover sulfide-based materials.[285] Tetragonal $Li_{10}GeP_2S_{12}$ (LGPS) is an ultrafast lithium SSEs, which shows conductivity values on par with those of LEs, sparking enthusiasm for the development of SSBs.[285] Due to the low-cost price and earth abundance of silicon, the replacement of germanium by silicon is highly desired. The first silicon-containing tetragonal LSiPS ($Li_{11}Si_2PS_{12}$) was synthesized under high-pressure conditions.[331] Besides, Kanno et al. added $Li_{9.54}Si_{1.74}P_{1.44}S_{11.7}Cl_{0.3}$ to the LSiPS family, a sulfide that shows the highest specific conductivity (25 mS cm^{-1}) reported for LGPS-type materials.[327] Recently, Ham et al. reported on the facile solid-state synthesis and characterization of tetragonal Li_7SiPS_8, a new member of the tetragonal LGPS-type family.[332] Li_7SiPS_8 exhibits a total ionic conductivity of 2 mS cm^{-1} at RT, thus rendering it an attractive candidate as an SE in SSBs. Notably, various SSEs have been synthesized and registered with much-improved moisture stability, e.g., As-substituted Li_4SnS_4,[333] Sb-doped $Li_{10}GeP_2S_{12}$,[334] $Li_{6.6}Ge_{0.6}Sb_{0.4}S_5I$.[335] The argyrodite family is among the superionic Li-ion conductors, and key SEs for SSBs.[336,337] The Zeier group continuously investigates the new mechanism, synthesis process, site order and disorder for argyrodite type SSEs for HV-SSBs applications.[287,294,328,338,339] Wang et al. recently reported the structure and lithium-ion mechanism of argyrodite type $Li_{6-x}PS_{5-x}Br_{1+x}$ with increasing Br^-/S^{2-} sites.[340] Increasing the bromide content ($Li_{5.3}PS_{4.3}Br_{1.7}$ $x = 0.7$) boosts the ionic conductivity to 11 mS cm^{-1} at 25 °C, with the activation energy of 0.18 eV. Introducing argyrodite doped aliovant cation (Ca^{2+} or Al^{3+}) substitute could also improve the ionic conductivities ($Li_{5.35}Ca_{0.1}PS_{4.5}Cl_{1.55}$) with 10.2 mS cm^{-1} at RT reported by Adeli et al.[341] The aliovalent doping of the Li^+ site generated the vacancies population, which improves the Li^+ diffusion and conductivity. Moreover, a PFG-NMR study investigated the influence of mechanical modification on the ion transport of SE particles.[341] The same

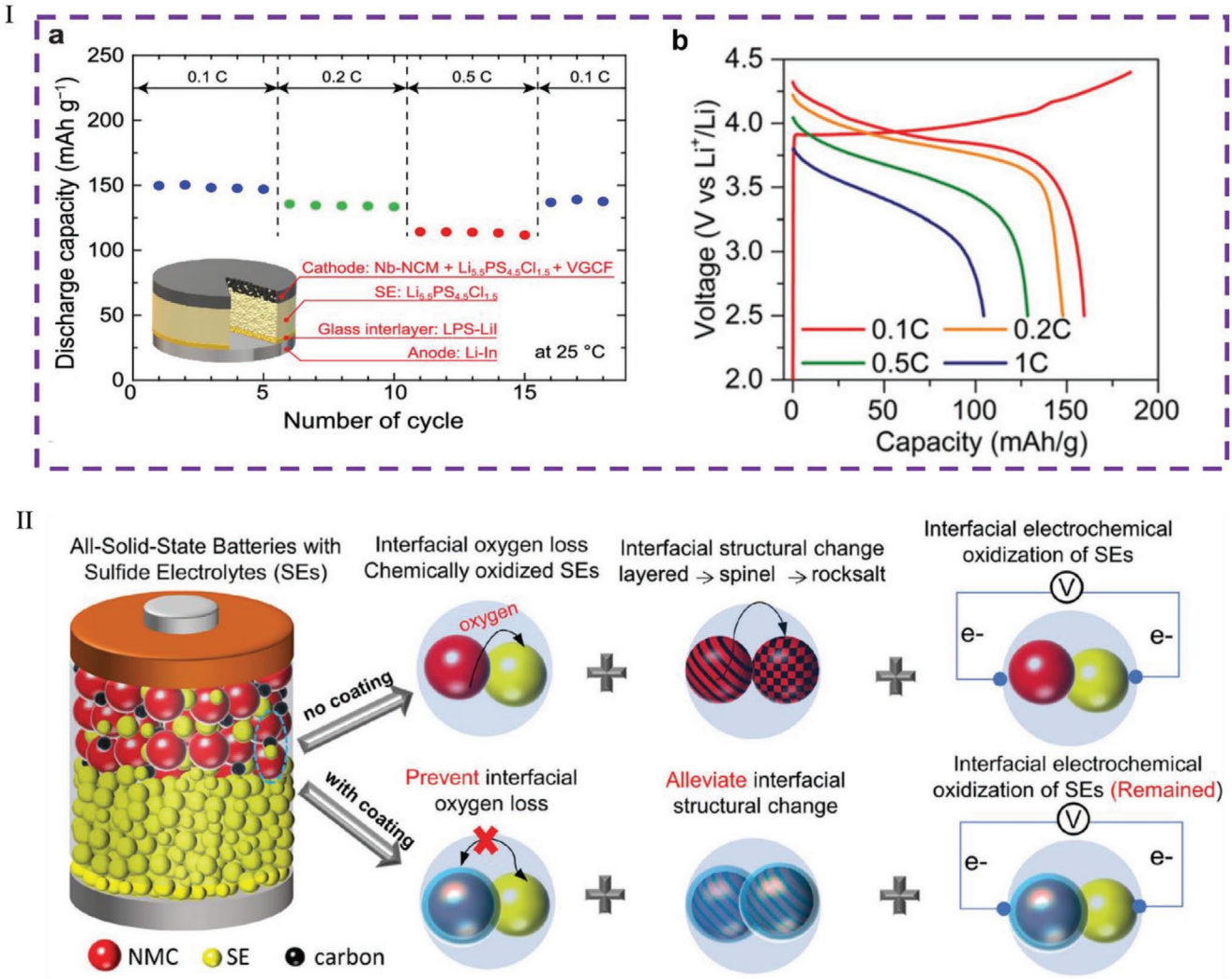

Figure 14. I a) The electrochemical performance of Nb-coated NMC, LPSCl, an additional interlayer of LPS, with different C-rate capability (1 C = 3.1 mA cm^{-1}, i.e., 180 mA g^{-1}) and different C-rate with the charge and discharge profiles of 20 cycle. Reproduced with permission.[344] Copyright 2020, American Chemical Society. b) The HV-SSBs electrochemical performance of LNTO-coated single crystal NMC532 with different current densities. II) Understanding the interfacial mechanism and coating strategy effects of SSBs. Reproduced with permission.[345] Copyright 2021, John Wiley and Sons.

group reported adding more Cl-rich argyrodite to $Li_{6-x}PS_{5-x}Cl_{1+x}$, to show that increasing the Cl^-/S^{2-} ratio has a systematic and remarkable impact on the Li-ion diffusivity in the lattice.[342]

The most promising Cl argyrodite, $Li_{5.5}PS_{4.5}Cl_{1.5}$, exhibits a cold-pressed conductivity of 9.4 mS cm^{-1} at RT (12 mS cm^{-1} on sintering), which is more applicable for HV cathodes for SSEs to SSBs (**Figure 14** I).[343,344] Unfortunately, $Li_{10\pm x}M_{1\pm y}P_{2\pm p}S_{12\pm q}$ (M = Ge, Si) SSEs are not stable with lithium metal. For this reason, these kinds of SSEs need protection layers, such as graphite or indium metal, to insulate the contact between SEs and anode. The protection layer helps the battery performance when the LGPS electrolyte is used with Li metal.

Moreover, except for the argyrodite Li_6PS_5X (X = Cl, Br, I)-type SSEs, which undergo relatively slow reactions at the interface, most SSEs decompose rapidly in contact with lithium metal, which poses additional challenges during the SSE preparation. Interestingly, the most promising Li-argyrodites LPSCl could be more stable (over 150 h) with lithium metal than LGPS.[346] Although, after 150 h a short circuit was reported from this SSE, which could indicate there are more significant challenge for application in SSBs. On the other hand, the Janek group has been investigating and demonstrating the benefit of cathode active material coatings, to improve the cycling performance for application in HV-SSBs.[45,294,347–350] To achieve high energy density SSBs, thin lithium metal or anode free concepts are introduced by Lee et al. from the Samsung group. They reported composite anode (Ag–C), high nickel content NMC (with high-energy-density (900 Wh L^{-1})) all-solid-state pouch cells, which demonstrated 1000 cycles and a coulombic efficiency >99.8%.[351] Using an anode-free concept, or thin Li metal, could be helpful to solve the problem of lithium dendrite growth through the SE separator, and SE reduction by Li metal. Ye and Li recently introduced the multilayer design concept SSEs for SSBs, which helps prevent lithium dendrite growth during the process.[346] Interestingly, the performance has been improved for a Li-metal anode, paired with a single

Table 4. High voltage cathodes, solid-state electrolytes for SSBs with configurations and electrochemical performance. RT refers to room temperature.

SSBs configuration (cathode//electrolyte//anode)	Solid electrolyte (ionic conduct.)	Voltage range (Li^+/Li vs V)	Temp. [°C]	Capacity [mAh g^{-1}]	Cycle performance	Ref.
$LiNi_{0.6}Mn_{0.2}Co_{0.2}O_2$ (NMC622) + PVDF-HFP + CNTs + Super P + LLZTO + LiTFSI + NMP//CSPE//Gr + PVDF-HFP + Super P + LLZTO + LiTFSI + NMP	15% LLZTO/PVDF-HFP in Li salt (CSPE) 0.1 mS cm^{-1}	2.5–4.4	RT	179.56 (0.05 C)	96% (0.05 C, 30 cycles)	[307]
$LiFePO_4$ (LFP) + Super-P + PVDF + 1-methyl-2-pyrrolidinone (NMP)//PPL-GPEs//Li	PPL GPEs (PVDF-HFP, PPC, LATP) 0.94 mS cm^{-1}	2.5–4.2	25	164 (0.1 C)	99% (0.5 C, 150 cycles)	[308]
$LiNi_{0.6}Mn_{0.2}Co_{0.2}O_2$ (NMC622)//IPN-5PAN//Li	IPN-5PAN (PEG + POSS + PAN) 0.195 mS cm^{-1}	2.5–4.2	60	150.7 (0.1 C)	97.8% (0.1 C, 50 cycles)	[310]
$LiFePO_4$ + PEO + carbon black (CB) + acetonitrile// GO–PEO//Li	GO–PEO SEs 1.54×10^{-5} S cm^{-1}	2.5–4.0	60	142 (0.5 C)	91% (0.5 C, 100 cycles)	[311]
$LiCoO_2$ + $Li_{2.633}Er_{0.633}Zr_{0.367}Cl_6$/$Li_3PS_4$ /$Li_{11}Sn_6$ and Li_3PS_4 (80:20 in wt%)	Li_3PS_4	3.0–4.3	RT	110 (0.1 C)	95% (0.5 C, 1000 cycles)	[314]
LZO-$LiNi_{0.90}Co_{0.05}Mn_{0.05}O_2$ (NMC) + Li_6PS_5Cl + carbon nanofibers + PTFE//Li_6PS_5Cl//Ag–C	Li_6PS_5Cl (1.81 mS cm^{-1})	2.5–4.25	60	215 (0.2 C)	99.8% (0.5 C, 1000 cycles)	[351]
$LiNi_{0.8}Mn_{0.1}Co_{0.1}O_2$ (SC-NMC811) + $Li_{5.5}PS_{4.5}Cl_{1.5}$ (LPSCl) + $Li_{9.54}Si_{1.74}(P_{0.9}Sb_{0.1})_{1.44}S_{11.7}Cl_{0.3}$ (LSPS) + PTFE/LPSCl-LSPS-LPSCl/Li/G	$Li_{9.54}Si_{1.74}(P_{0.9}Sb_{0.1})_{1.44}S_{11.7}Cl_{0.3}$ (LSPS) $Li_{5.5}PS_{4.5}Cl_{1.5}$ (LPSCl) multilayer design approach	2.5–4.3	55	178.6 (0.5 C) 81.0 (20 C)	82% (20 C, 10 000 cycles)	[346]
$LiNi_{0.6}Mn_{0.2}Co_{0.2}O_2$ (NMC622) + $Li_{2.7}Yb_{0.7}Zr_{0.3}Cl_6$//$Li_{6.7}Si_{0.7}Sb_{0.3}S_5I$//Li-In	$Li_{6.7}Si_{0.7}Sb_{0.3}S_5I$ 10 mS cm^{-1}	2.8–4.3	RT	170 (0.2C)	99.6% (0.2 C, 150 cycles)	[324]
$LiNb_{0.5}Ta_{0.5}O_3$ (LNTO)@ $LiNi_{0.5}Mn_{0.3}Co_{0.2}O_2$ (SC-NMC532)//LGPS//In-Li	$Li_{10}GeP_2S_{12}$ (LGPS) 8.4 mS cm^{-1}	2.5–4.4	RT	104.7 (1 C)	85.8% (C/3, 500 cycles)	[345]
$LiFePO_4$ (LFP) + Super-P + CSPE + 1-methyl-2-pyrrolidinone (NMP)//CSPE//Li	(CSPE) $Li_{6.4}La_3Zr_{1.4}Ta_{0.6}O_{12}$ + PVDF + LiTFSI 0.24 mS cm^{-1}	2.8–4.4	24	98 (1 C)	88% (1 C, 200 cycles)	[353]
$LiNi_{0.5}Co_{0.2}Mn_{0.3}O_2$ (NMC) + $Li_{5.4}PS_{4.4}Cl_{1.6}$ + VGCF + PTFE//$Li_{5.4}PS_{4.4}Cl_{1.6}$ + PTFE//Li or Li-coated with Al_2O_3	$Li_{5.4}PS_{4.4}Cl_{1.6}$ (8.4 mS·cm^{-1})	2.8–4.2	60	135.3 (0.05 C)	80.2% (0.05 C, 150 cycles)	[354]
$LiNi_{0.5}Co_{0.3}Mn_{0.2}O_2$ (NMC) + PVDF + Super P//PIPCE (LiTFSI-$SN_{0.05}$-10 wt% FEC)–15 wt% PEO//Li	PIPCE (LiTFSI-$SN_{0.05}$-10 wt% FEC)–15 wt% PEO) 0.1 mS cm^{-1}	2.7–4.2	RT	169 (0.1 C	80% (0.1 C, 120 cycles)	[355]
$LiNi_{0.88}Co_{0.10}Al_{0.02}O_2$ NCA88 (SC) + $Li_{2.60}Yb_{0.60}Hf_{0.40}Cl_6$ + Super P//$Li_6PS_5Cl_{0.5}Br_{0.5}$//$Li_{0.5}In$ + $Li_6PS_5Cl_{0.5}Br_{0.5}$	$Li_6PS_5Cl_{0.5}Br_{0.5}$	3.0–4.3	30	188 (0.5 C)	83.6% (0.5 C, 1000 cycles)	[356]

crystal NMC811 cathode, and multilayer designed SSEs, such as $Li_{5.5}PS_{4.5}Cl_{1.5}$ (LPSCl), $Li_{9.54}Si_{1.74}(P_{0.9}Sb_{0.1})_{1.44}S_{11.7}Cl_{0.3}$ (LSPS), at elevated temperature (55 °C), which showed stable cyclic performance and 82% capacity retention after 10000 cycles at a 20 C rate and 2000 cycles at a 1.5 C rate, respectively. It could open the window for these SSEs to be applied with HV cathode materials in SSBs. One of the main challenges in SSEs, i.e., the interface compatibility, has a crucial, but still poorly understood role, in the performance of SSBs.[352] The electrochemical reactions of SSEs cause the large interfacial resistance between the SSEs and typical layered oxide-based cathodes. Understanding the mechanism of interfacial resistance, as well as introducing coating strategies on layered oxide-based high voltage cathode materials, could be helpful. A new interfacial coating design could prevent the large interfacial resistance between SSEs and HV cathodes, as well as electrochemically oxidize SEs to form non-oxygen species (Figure 14 II).[345] The interfacial coating strategy effectively suppresses chemically oxidized, oxygen-containing species, and mitigates the coinciding interfacial structural change. Understanding coating strategies and interfacial reactions are essential for SSEs, which are more reliable for improving the stability of HV cathode materials. In addition, the energy densities of SSBs can significantly rise through using lithium metal as an anode, as the solid–solid contact between the lithium and the electrolyte prohibits critical safety issues. Also, SEs acting as a rigid physical barrier between the anode and cathode can help to prevent dendrite growth, as well as optimize energy density and utilize limited space.

In summary, the various types of SEs, such as polymers, sulfide, halide, and oxide SEs, have received global attention in many years. In HV-SSBs, there are certainly experiments with CSEs, such as polymers and oxides, or sulfide and halides, that take advantage of both types of electrolytes that have been widely considered and investigated. The core mechanisms that SEs offer for HV-SSBs applications are the voltage stability window, material composition, high ionic conductivity, and scalable and easy fabrication. Here, we discussed the most recent developments and performance of different SEs for HV-LIBs (**Table 4**), focusing on high-performance SEs with acceptable operating temperatures, higher ionic conductivities, and suitable electrochemical stability windows. Still, there are several challenges to overcome to identify the ideal SEs (**Figure 15**).

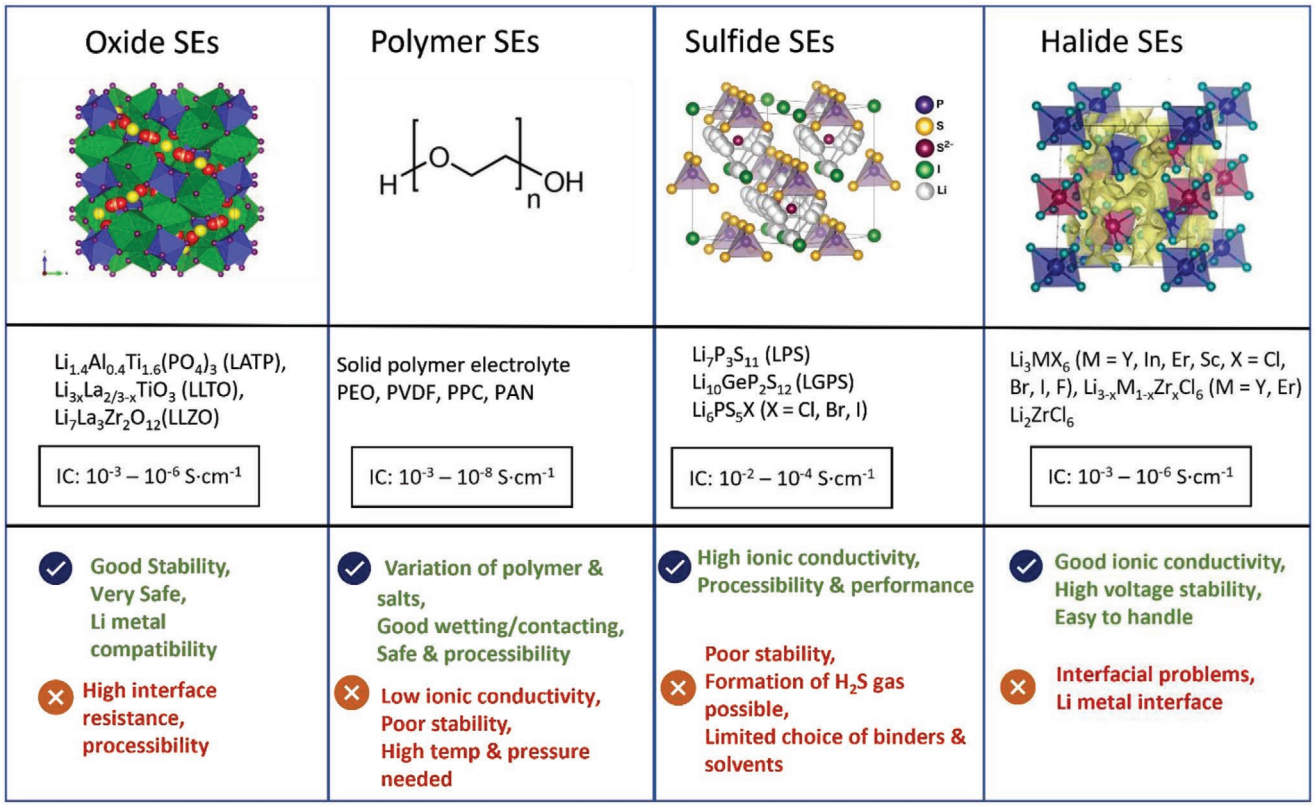

Figure 15. An overview of SEs development for HV-SSBs. The ideal SEs should have high ionic conductivity (IC), easy processing, HV compatibility, safe environmental handling, and low-cost synthesis. Additionally, sulfide and halide SEs, and polymer and oxide SEs combinations offer better stability and HV cathode compatibility for HV SSBs applications. Halide SE image reproduced with permission.[323] Copyright 2021, American Chemical Society. Sulfide SE image reproduced with permission.[338] Copyright 2018, American Chemical Society. Oxide SE image reproduced with permission.[362] Copyright 2015, Elsevier.

Additionally, SEs can still be subject to safety issues, especially in abuse cases, and quantitative safety analysis of SEs is still necessary.[330,357] That being said, advanced HV battery systems based on SEs would revitalize the battery field, due to their safety, good stability, ecological impact, long cycles, and low cost.

6. Conclusion and Outlook

Various safety challenges accompany HV-LIBs, and addressing them is critical for widespread practical applications. Undesirable reactions occurring in the electrolyte region are the primary cause of catastrophic battery failure, so this region should be the focus for improving the safety of HV-LIBs. Additionally, with the growing global challenges regarding climate change, pursuing more sustainable strategies for large-scale energy storage applications is important. Strategies to improve the safety of HV-LIBs, with commentary on sustainable options, were discussed herein (**Table 5**).

a) The use of LEs in HV-LIBs will likely continue, due to their superior rate capabilities. Electrolyte additives can improve the safety of LEs by enhancing the stability of the SEI and CEI, gas, or HF scavenging and preventing continuous electrolyte

Table 5. Summarizing of advantages and disadvantages of different approaches to improve the electrolyte region for HV batteries.

Category	Benefits	Drawbacks
Liquid electrolyte	Lower cost, good wettability, easy cell assembly, high ionic conductivity	Generally high volatility, high flammability, higher toxicity, lower thermal stability
Ionic liquids	Low volatility, low flammability, high thermal stability, good interfacial compatibility	High cost, higher toxicity, low ionic conductivity
Gel polymer electrolytes	Higher thermal, mechanical, and electrochemical stability, good wetting, higher ionic conductivity, higher interfacial compatibility, no need for a separator, more environmentally friendly	More complicated cell assembly
Separators	Improve thermal stability, limit cross-talk, and lithium dendrite growth	Not able to address solvent volatility or interfacial compatibility, making more resistance
Solid electrolytes	Good stability, safety, high voltage stability, ionic conductivity, good processability	Interfacial issues, lower ionic conductivity than LEs, short cycle life

degradation. This approach still employs the use of volatile solvents, however, which higher flammability. LEs employing additional flame retardant solvents, alternative flame retardant solvents or high concentrations can improve the thermal and electrochemical stability. However, many LEs still use volatile or hazardous solvents, making them less risky for HV-LIBs.

b) The choice of separators can also help improve the chemical and electrochemical stability of LEs. There are sustainable options available, which possess the required high thermal and electrochemical stability, that can help to improve the safety of HV-LIBs.

c) ILs can achieve superior interfacial compatibility and ionic conductivity compared to many SEs and possess similar electrochemical and thermal stabilities. However, the cost of high salt concentrations for the implementation of ILs can be daunting and limits the scalability of HV-LIBs based on ILs.

d) AEs can improve the sustainability of LEs by moving away from more toxic and flammable organic solvents and improving the ease of handling for cell building, as the atmospheric moisture content is not a concern. The poor voltage stability of aqueous electrolytes can be improved through "water-in-salt" electrolytes, molecular crowding, or GPEs. "Water-in-salt" electrolytes. While these electrolytes demonstrated that the voltage stability windows of AEs could be widened, they still have the same cost concerns as ILs. Both molecular crowding and aqueous GPEs utilize similar strategies. By employing cheap, biodegradable macromolecules or polymers, AEs with higher voltage stabilities, higher ionic conductivities, and good quality interfacial compatibilities can be feasibly used in high voltages LIBs in the future, even for large-scale applications, although more development of AEs is still required for HV applications.

e) GPEs represent a balanced alternative to LEs and SSEs. Commonly used LEs can be contained within a polymer framework, improving the safety of the LEs without restricting the ionic conductivity and interfacial stability. They can also be produced with nontoxic, biodegradable polymer materials and have promising scalability. GPEs can also be beneficial for AEs, improving the electrochemical stability and performance. The separator can also be removed, which can further boost the energy density of the LIBs.

f) SEs offer the safest alternative to LEs for HV-LIBs applications. In general, they have high chemical, electrochemical, and thermal stabilities and are not prone to unwanted side reactions that could lead to explosive battery failure. However, despite the numerous safety advantages, SEs still have more limited ionic conductivities as well as electrode and electrolyte interface compatibility. They can be more expensive and less sustainable (in the case of SEs composed of certain transition metals).

At HVs (especially in the case of fast charging), there are more likely to be detrimental side reactions that can lead to catastrophic battery failure. Pursuing electrolytes or separators that can address these problems, and still be sustainable and easily scaled up, is an essential topic for the practical application of LIBs. The cell materials, size, operating window, and application must be considered carefully when selecting an electrolyte for HV applications. This review serves as a guide for potential strategies to improve the safety and stability of HV-LIBs for practical applications. However, there are still external factors contributing to abuse cases,[358,359] and the electrolyte alone is not always capable of preventing thermal runaway.[360] This must also be considered when designing battery packs and battery management systems.[361]

Acknowledgements

H.C., P.M., and M.A. contributed equally to this work. This work was supported by the German Federal Ministry for Education and Research (BMBF) for the funding of the research project EVanBatter (Reference No. 03XP0340B) and the research project FastChargeLongLife (Reference No. 03XP0313) from GreenBatt-Cluster projects are acknowledged. This work was also supported and funded by EU/EURF (PASS, A76178) and EU/Interreg Nord (SolBat, Grant No. 20202885) projects are acknowledged.

Open access funding enabled and organized by Projekt DEAL.

Conflict of Interest

The authors declare no conflict of interest.

Keywords

gel polymer electrolytes, ionic electrolytes, Li-ion batteries, liquid electrolytes, separators, solid electrolytes, solid-state batteries

Received: January 12, 2022
Revised: March 31, 2022
Published online: May 6, 2022

[1] F. Wu, J. Maier, Y. Yu, *Chem. Soc. Rev.* **2020**, *49*, 1569.
[2] L. Wang, A. Menakath, F. Han, Y. Wang, P. Y. Zavalij, K. J. Gaskell, O. Borodin, D. Iuga, S. P. Brown, C. Wang, K. Xu, B. W. Eichhorn, *Nat. Chem.* **2019**, *11*, 789.
[3] L. von Kolzenberg, A. Latz, B. Horstmann, *ChemSusChem* **2020**, *13*, 3901.
[4] P. Verma, P. Maire, P. Novák, *Electrochim. Acta* **2010**, *55*, 6332.
[5] J. C. Fang, Y. F. Xu, G. L. Xu, S. Y. Shen, J. T. Li, L. Huang, S. G. Sun, *J. Power Sources* **2016**, *304*, 15.
[6] A. Manthiram, K. Chemelewski, E. S. Lee, *Energy Environ. Sci.* **2014**, *7*, 1339.
[7] M. R. Palacín, *Chem. Soc. Rev.* **2018**, *47*, 4924.
[8] H. Wang, X. Li, F. Li, X. Liu, S. Yang, J. Ma, *Electrochem. Commun.* **2021**, *122*, 106870.
[9] H. Maleki Kheimeh Sari, X. Li, *Adv. Energy Mater.* **2019**, *9*, 1901597.
[10] D. Huang, C. Engtrakul, S. Nanayakkara, D. W. Mulder, S. D. Han, M. Zhou, H. Luo, R. C. Tenent, *ACS Appl. Mater. Interfaces* **2021**, *13*, 11930.
[11] X. Qi, B. Blizanac, A. DuPasquier, P. Meister, T. Placke, M. Oljaca, J. Li, M. Winter, *Phys. Chem. Chem. Phys.* **2014**, *16*, 25306.
[12] S. Ko, Y. Yamada, L. Lander, A. Yamada, *Carbon* **2020**, *158*, 766.
[13] T. Waldmann, B. I. Hogg, M. Wohlfahrt-Mehrens, *J. Power Sources* **2018**, *384*, 107.
[14] W. Chang, C. Bommier, T. Fair, J. Yeung, S. Patil, D. Steingart, *J. Electrochem. Soc.* **2020**, *167*, 090503.
[15] W. Mai, A. M. Colclasure, K. Smith, *J. Electrochem. Soc.* **2020**, *167*, 080517.
[16] C. Pastor-Fernández, T. F. Yu, W. D. Widanage, J. Marco, *Renewable Sustainable Energy Rev.* **2019**, *109*, 138.

[17] K. Kim, H. Ma, S. Park, N.-S. Choi, *ACS Energy Lett.* **2020**, *5*, 1537.
[18] R. Wagner, B. Streipert, V. Kraft, A. Reyes Jiménez, S. Röser, J. Kasnatscheew, D. R. Gallus, M. Börner, C. Mayer, H. F. Arlinghaus, M. Korth, M. Amereller, I. Cekic-Laskovic, M. Winter, *Adv. Mater. Interfaces* **2016**, *3*, 1600096.
[19] N. Pereira, M. C. Ruotolo, M. Y. Lu, F. Badway, G. G. Amatucci, *J. Power Sources* **2017**, *338*, 145.
[20] S. Röser, A. Lerchen, L. Ibing, X. Cao, J. Kasnatscheew, F. Glorius, M. Winter, R. Wagner, *Chem. Mater.* **2017**, *29*, 7733.
[21] S. Tan, Y. J. Ji, Z. R. Zhang, Y. Yang, *ChemPhysChem* **2014**, *15*, 1956.
[22] A. Tornheim, M. He, C.-C. Su, Z. Zhang, *J. Electrochem. Soc.* **2017**, *164*, A6366.
[23] X. Zhang, L. Zou, Y. Xu, X. Cao, M. H. Engelhard, B. E. Matthews, L. Zhong, H. Wu, H. Jia, X. Ren, P. Gao, Z. Chen, Y. Qin, C. Kompella, B. W. Arey, J. Li, D. Wang, C. Wang, J. G. Zhang, W. Xu, *Adv. Energy Mater.* **2020**, *10*, 2000368.
[24] Y. Dong, B. T. Young, Y. Zhang, T. Yoon, D. R. Heskett, Y. Hu, B. L. Lucht, *ACS Appl. Mater. Interfaces* **2017**, *9*, 20467.
[25] J. Li, Y. Liu, W. Yao, X. Rao, S. Zhong, L. Qian, *Solid State Ionics* **2020**, *349*, 115292.
[26] X. L. Xu, S. X. Deng, H. Wang, J. B. Liu, H. Yan, *Nano-Micro Lett.* **2017**, *9*, 22.
[27] L. David, K. Dahlberg, D. Mohanty, R. E. Ruther, A. Huq, M. Chi, S. J. An, C. Mao, D. M. King, L. Stevenson, D. L. Wood, *ACS Appl. Energy Mater.* **2019**, *2*, 1308.
[28] S. Deng, B. Xiao, B. Wang, X. Li, K. Kaliyappan, Y. Zhao, A. Lushington, R. Li, T. K. Sham, H. Wang, X. Sun, *Nano Energy* **2017**, *38*, 19.
[29] L. Zhu, T.-F. Yan, D. Jia, Y. Wang, Q. Wu, H.-T. Gu, Y.-M. Wu, W.-P. Tang, *J. Electrochem. Soc.* **2019**, *166*, A5437.
[30] Y. Wu, M. Li, W. Wahyudi, G. Sheng, X. Miao, T. D. Anthopoulos, K. W. Huang, Y. Li, Z. Lai, *ACS Omega* **2019**, *4*, 13972.
[31] Y. Zhou, Y. Lee, H. Sun, J. M. Wallas, S. M. George, M. Xie, *ACS Appl. Mater. Interfaces* **2017**, *9*, 9614.
[32] J. Ma, Z. Liu, B. Chen, L. Wang, L. Yue, H. Liu, J. Zhang, Z. Liu, G. Cui, *J. Electrochem. Soc.* **2017**, *164*, A3454.
[33] J. Hu, P. He, B. Zhang, B. Wang, L. Z. Fan, *Energy Storage Mater.* **2020**, *26*, 283.
[34] H. Duan, M. Fan, W. P. Chen, J. Y. Li, P. F. Wang, W. P. Wang, J. L. Shi, Y. X. Yin, L. J. Wan, Y. G. Guo, *Adv. Mater.* **2019**, *31*, 1807789.
[35] M. A. Nowroozi, I. Mohammad, P. Molaiyan, K. Wissel, A. R. Munnangi, O. Clemens, *J. Mater. Chem. A* **2021**, *9*, 5980.
[36] P. Molaiyan, R. Witter, *Mater. Lett.* **2019**, *244*, 22.
[37] M. C. Smart, B. V. Ratnakumar, *J. Electrochem. Soc.* **2011**, *158*, A379.
[38] A. Kwade, W. Haselrieder, R. Leithoff, A. Modlinger, F. Dietrich, K. Droeder, *Nat. Energy* **2018**, *3*, 290.
[39] H. Wen, J. Zhang, J. Chai, J. Ma, L. Yue, T. Dong, X. Zang, Z. Liu, B. Zhang, G. Cui, *ACS Appl. Mater. Interfaces* **2017**, *9*, 3694.
[40] Y. Zhai, K. Xiao, J. Yu, B. Ding, *Electrochim. Acta* **2015**, *154*, 219.
[41] J. Sheng, S. Tong, Z. He, R. Yang, *Cellulose* **2017**, *24*, 4103.
[42] J. Zhang, L. Yue, Q. Kong, Z. Liu, X. Zhou, C. Zhang, Q. Xu, B. Zhang, G. Ding, B. Qin, Y. Duan, Q. Wang, J. Yao, G. Cui, L. Chen, *Sci. Rep.* **2014**, *4*, 3935.
[43] J. Li, R. Klöpsch, S. Nowak, M. Kunze, M. Winter, S. Passerini, *J. Power Sources* **2011**, *196*, 7687.
[44] T. Zhang, E. Paillard, *Front. Chem. Sci. Eng.* **2018**, *12*, 577.
[45] Y. Horowitz, C. Schmidt, D. hwan Yoon, L. M. Riegger, L. Katzenmeier, G. M. Bosch, M. Noked, Y. Ein-Eli, J. Janek, W. G. Zeier, C. E. Diesendruck, D. Golodnitsky, *Energy Technol.* **2020**, *8*, 2000580.
[46] B. V. Lotsch, J. Maier, *J. Electroceram.* **2017**, *38*, 128.
[47] B. Flamme, G. Rodriguez Garcia, M. Weil, M. Haddad, P. Phansavath, V. Ratovelomanana-Vidal, A. Chagnes, *Green Chem.* **2017**, *19*, 1828.
[48] M. Hu, X. Pang, Z. Zhou, *J. Power Sources* **2013**, *237*, 229.
[49] C. Liu, Z. G. Neale, G. Cao, *Mater. Today* **2016**, *19*, 109.
[50] S. K. Heiskanen, J. Kim, B. L. Lucht, *Joule* **2019**, *3*, 2322.
[51] K. Deng, Q. Zeng, D. Wang, Z. Liu, G. Wang, Z. Qiu, Y. Zhang, M. Xiao, Y. Meng, *Energy Storage Mater.* **2020**, *32*, 425.
[52] R. Gond, W. Van Ekeren, R. Mogensen, A. J. Naylor, R. Younesi, *Mater. Horiz.* **2021**, *8*, 2913.
[53] Y. Gu, S. Fang, L. Yang, S. I. Hirano, *J. Mater. Chem. A* **2021**, *9*, 15363.
[54] Q. Wang, J. Sun, X. Yao, C. Chen, *Electrochem. Solid-State Lett.* **2005**, *8*, A467.
[55] Y. Zhong, W. Wu, R. Wu, Q. Luo, Z. Wang, *Polym. Degrad. Stab.* **2014**, *105*, 166.
[56] X. Liu, C. Zhang, S. Gao, S. Cai, Q. Wang, J. Liu, Z. Liu, *Mater. Chem. Phys.* **2020**, *239*, 122014.
[57] J. Kalhoff, G. G. Eshetu, D. Bresser, S. Passerini, *ChemSusChem* **2015**, *8*, 2154.
[58] K. Xu, M. S. Ding, S. Zhang, J. L. Allen, T. R. Jow, *J. Electrochem. Soc.* **2002**, *149*, A622.
[59] X. Wang, E. Yasukawa, S. Kasuya, *J. Electrochem. Soc.* **2001**, *148*, A1058.
[60] Y. E. Hyung, D. R. Vissers, K. Amine, *J. Power Sources* **2003**, *119–121*, 383.
[61] K. Xu, S. Zhang, J. L. Allen, T. R. Jow, *J. Electrochem. Soc.* **2002**, *149*, A1079.
[62] J. Xia, L. Madec, L. Ma, L. D. Ellis, W. Qiu, K. J. Nelson, Z. Lu, J. R. Dahn, *J. Power Sources* **2015**, *295*, 203.
[63] J. Feng, X. Gao, L. Ci, S. Xiong, *RSC Adv.* **2016**, *6*, 7224.
[64] R. Zhou, J. Huang, S. Lai, J. Li, F. Wang, Z. Chen, W. Lin, C. Li, J. Wang, J. Zhao, *Sustainable Energy Fuels* **2018**, *2*, 1481.
[65] Y. Zhu, X. Luo, H. Zhi, X. Yang, L. Xing, Y. Liao, M. Xu, W. Li, *ACS Appl. Mater. Interfaces* **2017**, *9*, 12021.
[66] M. Xu, Y. Liu, B. Li, W. Li, X. Li, S. Hu, *Electrochem. Commun.* **2012**, *18*, 123.
[67] Z. Hu, F. Xian, Z. Guo, C. Lu, X. Du, X. Cheng, S. Zhang, S. Dong, G. Cui, L. Chen, *Chem. Mater.* **2020**, *32*, 3405.
[68] J. Wang, Y. Yamada, K. Sodeyama, E. Watanabe, K. Takada, Y. Tateyama, A. Yamada, *Nat. Energy* **2018**, *3*, 22.
[69] X. Cao, Y. Xu, L. Zhang, M. H. Engelhard, L. Zhong, X. Ren, H. Jia, B. Liu, C. Niu, B. E. Matthews, H. Wu, B. W. Arey, C. Wang, J. G. Zhang, W. Xu, *ACS Energy Lett.* **2019**, *4*, 2529.
[70] Z. Zeng, V. Murugesan, K. S. Han, X. Jiang, Y. Cao, L. Xiao, X. Ai, H. Yang, J. G. Zhang, M. L. Sushko, J. Liu, *Nat. Energy* **2018**, *3*, 674.
[71] H. Liang, X. Zuo, L. Zhang, W. Huang, Q. Chen, T. Zhu, J. Liu, J. Nan, *J. Electrochem. Soc.* **2020**, *167*, 090520.
[72] J. Wang, Y. Yamada, K. Sodeyama, C. H. Chiang, Y. Tateyama, A. Yamada, *Nat. Commun.* **2016**, *7*, 12032.
[73] X. Fan, C. Wang, *Chem. Soc. Rev.* **2021**, *50*, 10486.
[74] T. Doi, M. Hashinokuchi, M. Inaba, *Curr. Opin. Electrochem.* **2018**, *9*, 49.
[75] Q. Zheng, G. Li, X. Zheng, L. Xing, K. Xu, W. Li, *Energy Environ. Mater.* **2021**, *0*, 1.
[76] S. Ko, Y. Yamada, A. Yamada, *Joule* **2021**, *5*, 998.
[77] Q. Zheng, Y. Yamada, R. Shang, S. Ko, Y. Y. Lee, K. Kim, E. Nakamura, A. Yamada, *Nat. Energy* **2020**, *5*, 291.
[78] Z. Zeng, X. Liu, X. Jiang, Z. Liu, Z. Peng, X. Feng, W. Chen, D. Xia, X. Ai, H. Yang, Y. Cao, *InfoMat* **2020**, *2*, 984.
[79] X. Fan, L. Chen, O. Borodin, X. Ji, J. Chen, S. Hou, T. Deng, J. Zheng, C. Yang, S. C. Liou, K. Amine, K. Xu, C. Wang, *Nat. Nanotechnol.* **2018**, *13*, 715.
[80] X. Fan, X. Ji, L. Chen, J. Chen, T. Deng, F. Han, J. Yue, N. Piao, R. Wang, X. Zhou, X. Xiao, L. Chen, C. Wang, *Nat. Energy* **2019**, *4*, 882.
[81] F. Pena-Pereira, A. Kloskowski, J. Namieśnik, *Green Chem.* **2015**, *17*, 3687.

[82] W. T. Tsai, *J. Hazard. Mater.* **2005**, *119*, 69.
[83] A. Rodríguez, I. Bravo, D. Rodríguez, M. Tajuelo, Y. Diaz-De-Mera, A. Aranda, *RSC Adv.* **2016**, *6*, 21833.
[84] J. Han, L. Kiss, H. Mei, A. M. Remete, M. Ponikvar-Svet, D. M. Sedgwick, R. Roman, S. Fustero, H. Moriwaki, V. A. Soloshonok, *Chem. Rev.* **2021**, *121*, 4678.
[85] V. B. Silva, Y. H. Santos, R. Hellinger, S. Mansour, A. Delaune, J. Legros, S. Zinoviev, E. S. Nogueira, E. S. Orth, *Green Chem.* **2022**, *24*, 585.
[86] M. Gauthier, T. J. Carney, A. Grimaud, L. Giordano, N. Pour, H. H. Chang, D. P. Fenning, S. F. Lux, O. Paschos, C. Bauer, F. Maglia, S. Lupart, P. Lamp, Y. Shao-Horn, *J. Phys. Chem. Lett.* **2015**, *6*, 4653.
[87] E. Peled, S. Menkin, *J. Electrochem. Soc.* **2017**, *164*, A1703.
[88] J. Xia, L. Ma, C. P. Aiken, K. J. Nelson, L. P. Chen, J. R. Dahn, *J. Electrochem. Soc.* **2014**, *161*, A1634.
[89] C. C. Nguyen, B. L. Lucht, *J. Electrochem. Soc.* **2014**, *161*, A1933.
[90] A. L. Michan, B. S. Parimalam, M. Leskes, R. N. Kerber, T. Yoon, C. P. Grey, B. L. Lucht, *Chem. Mater.* **2016**, *28*, 8149.
[91] J. Li, H. Liu, J. Xia, A. R. Cameron, M. Nie, G. A. Botton, J. R. Dahn, *J. Electrochem. Soc.* **2017**, *164*, A655.
[92] Y. Jin, N. J. H. Kneusels, P. C. M. M. Magusin, G. Kim, E. Castillo-Martínez, L. E. Marbella, R. N. Kerber, D. J. Howe, S. Paul, T. Liu, C. P. Grey, *J. Am. Chem. Soc.* **2017**, *139*, 14992.
[93] G. Yang, R. L. Sacci, I. N. Ivanov, R. E. Ruther, K. A. Hays, Y. Zhang, P.-F. Cao, G. M. Veith, N. J. Dudney, T. Saito, D. T. Hallinan, J. Nanda, *J. Electrochem. Soc.* **2019**, *166*, A178.
[94] L. Hu, Z. Zhang, K. Amine, *Electrochem. Commun.* **2013**, *35*, 76.
[95] M. He, C. C. Su, Z. Feng, L. Zeng, T. Wu, M. J. Bedzyk, P. Fenter, Y. Wang, Z. Zhang, *Adv. Energy Mater.* **2017**, *7*, 1700109.
[96] J. Im, J. Lee, M.-H. Ryou, Y. M. Lee, K. Y. Cho, *J. Electrochem. Soc.* **2017**, *164*, A6381.
[97] P. Dong, D. Wang, Y. Yao, X. Li, Y. Zhang, J. Ru, T. Ren, *J. Power Sources* **2017**, *344*, 111.
[98] G. Liu, N. Xu, Y. Zou, K. Zhou, X. Yang, T. Jiao, W. Yang, Y. Yang, J. Zheng, *ACS Appl. Mater. Interfaces* **2021**, *13*, 12069.
[99] R. Wang, X. Dai, Z. Qian, Y. Sun, S. Fan, K. Xiong, H. Zhang, F. Wu, *ACS Mater. Lett.* **2020**, *2*, 280.
[100] W. Wang, T. Yang, S. Li, J. Lu, X. Zhao, W. Fan, C. Fan, X. Zuo, S. Tie, J. Nan, *J. Power Sources* **2021**, *483*, 229172.
[101] B. Deng, H. Wang, W. Ge, X. Li, X. Yan, T. Chen, M. Qu, G. Peng, *Electrochim. Acta* **2017**, *236*, 61.
[102] S. H. Jang, K. Jung, T. Yim, *Curr. Appl. Phys.* **2018**, *18*, 1345.
[103] H. Wang, D. Sun, X. Li, W. Ge, B. Deng, M. Qu, G. Peng, *Electrochim. Acta* **2017**, *254*, 112.
[104] X. Yan, C. Chen, X. Zhu, L. Pan, X. Zhao, L. Zhang, *J. Power Sources* **2020**, *461*, 228099.
[105] H. Wang, S. Chen, Y. Li, Y. Liu, Q. Jing, X. Liu, Z. Liu, X. Zhang, *Adv. Energy Mater.* **2021**, *11*, 2101057.
[106] F. Aupperle, G. G. Eshetu, K. W. Eberman, A. Xioa, J. S. Bridel, E. Figgemeier, *J. Mater. Chem. A* **2020**, *8*, 19573.
[107] J. Self, D. S. Hall, L. Madec, J. R. Dahn, *J. Power Sources* **2015**, *298*, 369.
[108] D. Xu, Y. Kang, J. Wang, S. Hu, Q. Shi, Z. Lu, D. He, Y. Zhao, Y. Qian, H. Lou, Y. Deng, *J. Power Sources* **2019**, *437*, 226929.
[109] R. Petibon, L. Madec, L. M. Rotermund, J. R. Dahn, *J. Power Sources* **2016**, *313*, 152.
[110] Y. K. Han, J. Yoo, J. Jung, *J. Phys. Chem. C* **2016**, *120*, 28390.
[111] W. Song, B. Hong, S. Hong, Y. Lai, J. Li, Y. Liu, *Int. J. Electrochem. Sci.* **2017**, *12*, 10749.
[112] Z. Wang, L. Xing, J. H. Li, M. Xu, W. Li, *J. Power Sources* **2016**, *307*, 587.
[113] Q. Yu, Z. Chen, L. Xing, D. Chen, H. Rong, Q. Liu, W. Li, *Electrochim. Acta* **2015**, *176*, 919.
[114] Z. Qin, S. Hong, B. Hong, B. Duan, Y. Lai, J. Feng, *J. Electroanal. Chem.* **2019**, *854*, 113506.
[115] Q. Liu, G. Yang, S. Li, S. Zhang, R. Chen, Z. Wang, L. Chen, *ACS Appl. Mater. Interfaces* **2021**, *13*, 21459.
[116] Q. Ma, X. Zhang, A. Wang, Y. Xia, X. Liu, J. Luo, *Adv. Funct. Mater.* **2020**, *30*, 2002824.
[117] Y. Qian, Y. Kang, S. Hu, Q. Shi, Q. Chen, X. Tang, Y. Xiao, H. Zhao, G. Luo, K. Xu, Y. Deng, *ACS Appl. Mater. Interfaces* **2020**, *12*, 10443.
[118] N. von Aspern, S. Röser, B. Rezaei Rad, P. Murmann, B. Streipert, X. Mönnighoff, S. D. Tillmann, M. Shevchuk, O. Stubbmann-Kazakova, G. V. Röschenthaler, S. Nowak, M. Winter, I. Cekic-Laskovic, *J. Fluorine Chem.* **2017**, *198*, 24.
[119] S. Bolloju, C. Y. Chiou, T. Vikramaditya, J. T. Lee, *Electrochim. Acta* **2019**, *299*, 663.
[120] Y. Zhu, X. Luo, H. Zhi, Y. Liao, L. Xing, M. Xu, X. Liu, K. Xu, W. Li, *J. Mater. Chem. A* **2018**, *6*, 10990.
[121] E. Markevich, G. Salitra, K. Fridman, R. Sharabi, G. Gershinsky, A. Garsuch, G. Semrau, M. A. Schmidt, D. Aurbach, *Langmuir* **2014**, *30*, 7414.
[122] A. von Cresce, K. Xu, *J. Electrochem. Soc.* **2011**, *158*, A337.
[123] S. Tan, Z. Zhang, Y. Li, Y. Li, J. Zheng, Z. Zhou, Y. Yang, *J. Electrochem. Soc.* **2013**, *160*, A285.
[124] K. Beltrop, S. Klein, R. Nölle, A. Wilken, J. J. Lee, T. K. J. Köster, J. Reiter, L. Tao, C. Liang, M. Winter, X. Qi, T. Placke, *Chem. Mater.* **2018**, *30*, 2726.
[125] V. Tarnopolskiy, J. Kalhoff, M. Nádherná, D. Bresser, L. Picard, F. Fabre, M. Rey, S. Passerini, *J. Power Sources* **2013**, *236*, 39.
[126] Y. Zhu, Y. Li, M. Bettge, D. P. Abraham, *Electrochim. Acta* **2013**, *110*, 191.
[127] S. H. Lee, S. Yoon, E. H. Hwang, Y. G. Kwon, Y. G. Lee, K. Y. Cho, *J. Power Sources* **2018**, *378*, 112.
[128] C. Peebles, R. Sahore, J. A. Gilbert, J. C. Garcia, A. Tornheim, J. Bareño, H. Iddir, C. Liao, D. P. Abraham, *J. Electrochem. Soc.* **2017**, *164*, A1579.
[129] X. Yang, J. Chen, Q. Zheng, W. Tu, L. Xing, Y. Liao, M. Xu, Q. Huang, G. Cao, W. Li, *J. Mater. Chem. A* **2018**, *6*, 16149.
[130] G. H. Wrodnigg, J. O. Besenhard, M. Winter, *J. Electrochem. Soc.* **1999**, *146*, 470.
[131] P. Jankowski, N. Lindahl, J. Weidow, W. Wieczorek, P. Johansson, *ACS Appl. Energy Mater.* **2018**, *1*, 2582.
[132] Z. Xiao, J. Liu, G. Fan, M. Yu, J. Liu, X. Gou, M. Yuan, F. Cheng, *Mater. Chem. Front.* **2020**, *4*, 1689.
[133] L. Chen, X. Fan, E. Hu, X. Ji, J. Chen, S. Hou, T. Deng, J. Li, D. Su, X. Yang, C. Wang, *Chem* **2019**, *5*, 896.
[134] Q. Dong, F. Guo, Z. Cheng, Y. Mao, R. Huang, F. Li, H. Dong, Q. Zhang, W. Li, H. Chen, Z. Luo, Y. Shen, X. Wu, L. Chen, *ACS Appl. Energy Mater.* **2020**, *3*, 695.
[135] S. Li, Y. Liang, J. Xie, L. Ai, Y. Xie, C. Li, C. Wang, X. Cui, *J. Electroanal. Chem.* **2018**, *823*, 688.
[136] J. G. Han, J. Bin Lee, A. Cha, T. K. Lee, W. Cho, S. Chae, S. J. Kang, S. K. Kwak, J. Cho, S. Y. Hong, N. S. Choi, *Energy Environ. Sci.* **2018**, *11*, 1552.
[137] J. Cha, J. G. Han, J. Hwang, J. Cho, N. S. Choi, *J. Power Sources* **2017**, *357*, 97.
[138] Y. Li, G. M. Veith, K. L. Browning, J. Chen, D. K. Hensley, M. P. Paranthaman, S. Dai, X. G. Sun, *Nano Energy* **2017**, *40*, 9.
[139] C. Wang, L. Yu, W. Fan, J. Liu, L. Ouyang, L. Yang, M. Zhu, *ACS Appl. Energy Mater.* **2018**, *1*, 2647.
[140] M. S. Milien, U. Tottempudi, M. Son, M. Ue, B. L. Lucht, *J. Electrochem. Soc.* **2016**, *163*, A1369.
[141] J. G. Han, I. Park, J. Cha, S. Park, S. Park, S. Myeong, W. Cho, S. S. Kim, S. Y. Hong, J. Cho, N. S. Choi, *ChemElectroChem* **2017**, *4*, 56.
[142] J. Kim, V. A. K. Adiraju, N. Rodrigo, J. Hoffmann, M. Payne, B. L. Lucht, *ACS Appl. Mater. Interfaces* **2021**, *13*, 22351.
[143] S. Jeong, K. C. Kim, S. R. Lee, J. Mun, *Electrochim. Acta* **2019**, *300*, 156.

[144] L. Ma, L. Ellis, S. L. Glazier, X. Ma, J. R. Dahn, *J. Electrochem. Soc.* **2018**, *165*, A1718.
[145] G. Yang, J. Shi, C. Shen, S. Wang, L. Xia, H. Hu, H. Luo, Y. Xia, Z. Liu, *RSC Adv.* **2017**, *7*, 26052.
[146] W. Zhao, G. Zheng, M. Lin, W. Zhao, D. Li, X. Guan, Y. Ji, G. F. Ortiz, Y. Yang, *J. Power Sources* **2018**, *380*, 149.
[147] B. Jiang, J. Li, B. Luo, Q. Yan, H. Li, L. Liu, L. Chu, Y. Li, Q. Zhang, M. Li, *J. Energy Chem.* **2021**, *60*, 564.
[148] V. Aravindan, Y. L. Cheah, W. C. Ling, S. Madhavi, *J. Electrochem. Soc.* **2012**, *159*, A1435.
[149] M. Xu, A. Xiao, W. Li, B. L. Lucht, *J. Electrochem. Soc.* **2010**, *157*, A115.
[150] Y. Qin, Z. Chen, J. Liu, K. Amine, *Electrochem. Solid-State Lett.* **2010**, *13*, A11.
[151] S. Shui Zhang, *Electrochem. Commun.* **2006**, *8*, 1423.
[152] L. Niedzicki, S. Grugeon, S. Laruelle, P. Judeinstein, M. Bukowska, J. Prejzner, P. Szczeciński, W. Wieczorek, M. Armand, *J. Power Sources* **2011**, *196*, 8696.
[153] J. W. Park, K. Ueno, N. Tachikawa, K. Dokko, M. Watanabe, *J. Phys. Chem. C* **2013**, *117*, 20531.
[154] S. Menne, J. Pires, M. Anouti, A. Balducci, *Electrochem. Commun.* **2013**, *31*, 39.
[155] S. Brutti, E. Simonetti, M. De Francesco, A. Sarra, A. Paolone, O. Palumbo, S. Fantini, R. Lin, A. Falgayrat, H. Choi, M. Kuenzel, S. Passerini, G. B. Appetecchi, *J. Power Sources* **2020**, *479*, 228791.
[156] K. Zhao, H. Liang, M. Zhou, G. Zhang, C. Zhao, J. Ge, Y. Xia, Z. Gao, *ChemistrySelect* **2018**, *3*, 4421.
[157] K. Chatterjee, A. D. Pathak, A. Lakma, C. S. Sharma, K. K. Sahu, A. K. Singh, *Sci. Rep.* **2020**, *10*, 9606.
[158] K. Chatterjee, A. D. Pathak, K. K. Sahu, A. K. Singh, *ACS Omega* **2020**, *5*, 16681.
[159] P. Chandra Rath, C. J. Wu, J. Patra, J. Li, T. C. Lee, T. J. Yeh, J. K. Chang, *J. Mater. Chem. A* **2019**, *7*, 16516.
[160] C. J. Wu, P. C. Rath, J. Patra, D. Bresser, S. Passerini, B. Umesh, Q. F. Dong, T. C. Lee, J. K. Chang, *ACS Appl. Mater. Interfaces* **2019**, *11*, 42049.
[161] S. P. F. Costa, A. M. O. Azevedo, P. C. A. G. Pinto, M. L. M. F. S. Saraiva, *ChemSusChem* **2017**, *10*, 2321.
[162] Y. Wang, J. Yi, Y. Xia, *Adv. Energy Mater.* **2012**, *2*, 830.
[163] M. Zhang, S. Makino, D. Mochizuki, W. Sugimoto, *J. Power Sources* **2018**, *396*, 498.
[164] Y. Sui, X. Ji, *Chem. Rev.* **2021**, *121*, 6654.
[165] M. Chen, J. Wu, T. Ye, J. Ye, C. Zhao, S. Bi, J. Yan, B. Mao, G. Feng, *Nat. Commun.* **2020**, *11*, 5809.
[166] J. Forero-Saboya, E. Hosseini-Bab-Anari, M. E. Abdelhamid, K. Moth-Poulsen, P. Johansson, *J. Phys. Chem. Lett.* **2019**, *10*, 4942.
[167] L. Suo, O. Borodin, T. Gao, M. Olguin, J. Ho, X. Fan, C. Luo, C. Wang, K. Xu, *Science* **2015**, *350*, 938.
[168] Y. Wang, X. Meng, J. Sun, Y. Liu, L. Hou, *Front. Chem.* **2020**, *8*, 595.
[169] H. I. Kim, E. Shin, S. H. Kim, K. M. Lee, J. Park, S. J. Kang, S. So, K. C. Roh, S. K. Kwak, S. Y. Lee, *Energy Storage Mater.* **2021**, *36*, 222.
[170] W. Sun, L. Suo, F. Wang, N. Eidson, C. Yang, F. Han, Z. Ma, T. Gao, M. Zhu, C. Wang, *Electrochem. Commun.* **2017**, *82*, 71.
[171] X. Hou, X. Ju, W. Zhao, J. Wang, X. He, L. Du, B. Yan, J. Li, E. Paillard, J. Sun, H. Lin, M. Winter, J. Li, *J. Power Sources* **2021**, *484*, 229255.
[172] H. G. Steinrück, C. Cao, M. R. Lukatskaya, C. J. Takacs, G. Wan, D. G. Mackanic, Y. Tsao, J. Zhao, B. A. Helms, K. Xu, O. Borodin, J. F. Wishart, M. F. Toney, *Angew. Chem., Int. Ed.* **2020**, *59*, 23180.
[173] Y. Shen, B. Liu, X. Liu, J. Liu, J. Ding, C. Zhong, W. Hu, *Energy Storage Mater.* **2021**, *34*, 461.
[174] F. Wang, L. Suo, Y. Liang, C. Yang, F. Han, T. Gao, W. Sun, C. Wang, *Adv. Energy Mater.* **2017**, *7*, 1600922.
[175] S. Ko, Y. Yamada, K. Miyazaki, T. Shimada, E. Watanabe, Y. Tateyama, T. Kamiya, T. Honda, J. Akikusa, A. Yamada, *Electrochem. Commun.* **2019**, *104*, 106488.
[176] P. Jaumaux, X. Yang, B. Zhang, J. Safaei, X. Tang, D. Zhou, C. Wang, G. Wang, *Angew. Chem., Int. Ed.* **2021**, *60*, 19965.
[177] M. R. Lukatskaya, J. I. Feldblyum, D. G. Mackanic, F. Lissel, D. L. Michels, Y. Cui, Z. Bao, *Energy Environ. Sci.* **2018**, *11*, 2876.
[178] X. He, B. Yan, X. Zhang, Z. Liu, D. Bresser, J. Wang, R. Wang, X. Cao, Y. Su, H. Jia, C. P. Grey, H. Frielinghaus, D. G. Truhlar, M. Winter, J. Li, E. Paillard, *Nat. Commun.* **2018**, *9*, 5320.
[179] J. Xie, Z. Liang, Y. C. Lu, *Nat. Mater.* **2020**, *19*, 1006.
[180] X. Gong, H. Xu, M. Zhang, X. Cheng, Y. Wu, H. Zhang, H. Yan, Y. Dai, J. C. Zheng, *J. Power Sources* **2021**, *505*, 230078.
[181] Y. Shang, N. Chen, Y. Li, S. Chen, J. Lai, Y. Huang, W. Qu, F. Wu, R. Chen, *Adv. Mater.* **2020**, *32*, 2004017.
[182] R.-S. Kühnel, D. Reber, C. Battaglia, *J. Electrochem. Soc.* **2020**, *167*, 070544.
[183] Z. Zhao, Y. Huang, F. Qiu, W. Ren, C. Zou, X. Li, M. Wang, Y. Lin, *J. Mater. Sci.* **2021**, *56*, 11027.
[184] J. Wu, X. Wang, Q. Liu, S. Wang, D. Zhou, F. Kang, D. Shanmukaraj, M. Armand, T. Rojo, B. Li, G. Wang, *Nat. Commun.* **2021**, *12*, 5746.
[185] D. Xu, B. Wang, Q. Wang, S. Gu, W. Li, J. Jin, C. Chen, Z. Wen, *ACS Appl. Mater. Interfaces* **2018**, *10*, 17809.
[186] W. Ren, C. Ding, X. Fu, Y. Huang, *Energy Storage Mater.* **2021**, *34*, 515.
[187] C. He, J. Liu, J. Cui, J. Li, X. Wu, *Solid State Ionics* **2018**, *315*, 102.
[188] Y. Huang, Y. Huang, B. Liu, H. Cao, L. Zhao, A. Song, Y. Lin, M. Wang, X. Li, Z. Zhang, *Electrochim. Acta* **2018**, *286*, 242.
[189] S. Wang, L. Zhou, M. K. Tufail, L. Yang, P. Zhai, R. Chen, W. Yang, *Chem. Eng. J.* **2021**, *415*, 128846.
[190] S. H. Wang, Y. Y. Lin, C. Y. Teng, Y. M. Chen, P. L. Kuo, Y. L. Lee, C. Te Hsieh, H. Teng, *ACS Appl. Mater. Interfaces* **2016**, *8*, 14776.
[191] X. Cheng, J. Pan, Y. Zhao, M. Liao, H. Peng, *Adv. Energy Mater.* **2018**, *8*, 1702184.
[192] S. Liang, W. Yan, X. Wu, Y. Zhang, Y. Zhu, H. Wang, Y. Wu, *Solid State Ionics* **2018**, *318*, 2.
[193] D. Xu, J. Jin, C. Chen, Z. Wen, *ACS Appl. Mater. Interfaces* **2018**, *10*, 38526.
[194] C. H. Tsao, Y. H. Hsiao, C. H. Hsu, P. L. Kuo, *ACS Appl. Mater. Interfaces* **2016**, *8*, 15216.
[195] R. Liu, Z. Wu, P. He, H. Fan, Z. Huang, L. Zhang, X. Chang, H. Liu, C. an Wang, Y. Li, *J. Mater.* **2019**, *5*, 185.
[196] S. Wang, L. Zhang, A. Wang, X. Liu, J. Chen, Z. Wang, Q. Zeng, H. H. Zhou, X. Jiang, L. Zhang, *ACS Sustainable Chem. Eng.* **2018**, *6*, 14460.
[197] A. J. Nagajothi, R. Kannan, S. Rajashabala, *Ionics* **2018**, *24*, 1407.
[198] A. Saminathan, S. Krishnasamy, G. Venkatachalam, *Ind. Eng. Chem. Res.* **2020**, *59*, 21028.
[199] Y. F. Liang, Y. Xia, S. Z. Zhang, X. L. Wang, X. H. Xia, C. D. Gu, J. B. Wu, J. P. Tu, *Electrochim. Acta* **2019**, *296*, 1064.
[200] J. Huang, Y. Liao, G. Li, N. Xu, M. Xu, W. Li, *Electrochim. Acta* **2019**, *299*, 45.
[201] X. Song, W. Qi, H. Zhang, G. Wang, *Solid State Ionics* **2020**, *347*, 115266.
[202] J. Guo, H. Hou, J. Cheng, C. Wang, Q. Wang, H. Sun, X. Chen, *J. Mater. Sci.: Mater. Electron.* **2021**, *32*, 81.
[203] B. Liu, Y. Huang, Y. Huang, X. Deng, A. Song, Y. Lin, M. Wang, X. Li, Y. Wu, H. Cao, *J. Appl. Electrochem.* **2019**, *49*, 1167.
[204] H. Huang, F. Ding, H. Zhong, H. Li, W. Zhang, X. Liu, Q. Xu, *J. Mater. Chem. A* **2018**, *6*, 9539.
[205] G. X. Dong, H. J. Li, Y. Wang, W. J. Jiang, Z. S. Ma, *Ionics* **2021**, *27*, 2955.
[206] W. Ren, Y. Huang, X. Xu, B. Liu, S. Li, C. Luo, X. Li, M. Wang, H. Cao, *J. Mater. Sci.* **2020**, *55*, 12249.
[207] B. Li, Y. Huang, P. Cheng, B. Liu, Z. Yin, Y. Lin, X. Li, M. Wang, H. Cao, Y. Wu, *Electrochim. Acta* **2019**, *320*, 134572.
[208] L. Zhao, Y. Huang, B. Liu, Y. Huang, A. Song, Y. Lin, M. Wang, X. Li, H. Cao, *Electrochim. Acta* **2018**, *278*, 1.

[209] A. Hosseinioun, E. Paillard, *J. Membr. Sci.* **2020**, *594*, 117456.
[210] J. Zhao, J. Zhang, P. Hu, J. Ma, X. Wang, L. Yue, G. Xu, B. Qin, Z. Liu, X. Zhou, G. Cui, *Electrochim. Acta* **2016**, *188*, 23.
[211] J. Wan, J. Zhang, J. Yu, J. Zhang, *ACS Appl. Mater. Interfaces* **2017**, *9*, 24591.
[212] L. Li, M. Yu, F. Wang, X. Zhang, Z. Shao, *Energy Technol.* **2019**, *7*, 1800768.
[213] C. Luo, Y. Huang, Z. Yin, H. Xu, X. Qin, X. Li, M. Wang, Y. Lin, *Mater. Chem. Phys.* **2020**, *250*, 123174.
[214] F. Qiu, Y. Huang, X. Hu, B. Li, X. Zhang, C. Luo, X. Li, M. Wang, Y. Wu, H. Cao, *ACS Appl. Energy Mater.* **2019**, *2*, 6031.
[215] J. Y. Han, Y. Huang, Y. Chen, A. M. Song, X. H. Deng, B. Liu, X. Li, M. S. Wang, *ChemElectroChem* **2020**, *7*, 1213.
[216] X. Deng, Y. Huang, A. Song, B. Liu, Z. Yin, Y. Wu, Y. Lin, M. Wang, X. Li, H. Cao, *Mater. Chem. Phys.* **2019**, *229*, 232.
[217] Z. Du, Y. Su, Y. Qu, L. Zhao, X. Jia, Y. Mo, F. Yu, J. Du, Y. Chen, *Electrochim. Acta* **2019**, *299*, 19.
[218] M. Yadav, M. Kumar, N. Srivastava, *Electrochim. Acta* **2018**, *283*, 1551.
[219] A. Song, Y. Huang, X. Zhong, H. Cao, B. Liu, Y. Lin, M. Wang, X. Li, *Electrochim. Acta* **2017**, *245*, 981.
[220] L. Li, Q. Zhang, H. Huo, J. Zhou, L. Li, *RSC Adv.* **2016**, *6*, 88820.
[221] D. Hellio, M. Djabourov, *Macromol. Symp.* **2006**, *241*, 23.
[222] F. Baskoro, H. Q. Wong, H. J. Yen, *ACS Appl. Energy Mater.* **2019**, *2*, 3937.
[223] A. Arya, A. L. Sharma, *Ionics* **2017**, *23*, 497.
[224] C. Dong, F. Xu, L. Chen, Z. Chen, Y. Cao, *Small Struct* **2021**, *2*, 2100001.
[225] S. A. Langevin, B. Tan, A. W. Freeman, J. C. Gagnon, C. M. Hoffman, M. W. Logan, J. P. Maranchi, K. Gerasopoulos, *Chem. Commun.* **2019**, *55*, 13085.
[226] A. Cresce, N. Eidson, M. Schroeder, L. Ma, Y. Howarth, C. Yang, J. Ho, R. Dillon, M. Ding, A. Bassett, J. Stanzione, R. Tom, T. Soundappan, C. Wang, K. Xu, *J. Power Sources* **2020**, *469*, 228378.
[227] M. Safa, A. Chamaani, N. Chawla, B. El-Zahab, *Electrochim. Acta* **2016**, *213*, 587.
[228] M. W. Logan, S. Langevin, B. Tan, A. W. Freeman, C. Hoffman, D. B. Trigg, K. Gerasopoulos, *J. Mater. Chem. A* **2020**, *8*, 8485.
[229] T. Guo, J. Song, Y. Jin, Z. Sun, L. Li, *Carbohydr. Polym.* **2019**, *206*, 801.
[230] C. M. Costa, Y. H. Lee, J. H. Kim, S. Y. Lee, S. Lanceros-Méndez, *Energy Storage Mater.* **2019**, *22*, 346.
[231] M. Waqas, S. Ali, C. Feng, D. Chen, J. Han, W. He, *Small* **2019**, *15*, 1901689.
[232] C. Shi, P. Zhang, S. Huang, X. He, P. Yang, D. Wu, D. Sun, J. Zhao, *J. Power Sources* **2015**, *298*, 158.
[233] L. F. Fang, J. L. Shi, B. K. Zhu, L. P. Zhu, *J. Membr. Sci.* **2013**, *448*, 143.
[234] Y. Pan, S. Chou, H. K. Liu, S. X. Dou, *Natl. Sci. Rev.* **2017**, *4*, 917.
[235] W. D. Hsu, P. W. Yang, H. Y. Chen, P. H. Wu, P. C. Wu, C. W. Hu, L. Saravanan, Y. F. Liao, Y. T. Su, D. Bhalothia, T. Y. Chen, C. C. Chang, *Sci. Rep.* **2021**, *11*, 1929.
[236] K. J. Kim, Y. H. Kim, J. H. Song, Y. N. Jo, J. S. Kim, Y. J. Kim, *J. Power Sources* **2010**, *195*, 6075.
[237] D. W. Ihm, J. G. Noh, J. Y. Kim, *J. Power Sources* **2002**, *109*, 388.
[238] Y. Yang, W. Wang, J. Zhang, *Mater. Today Energy* **2020**, *16*, 100420.
[239] Y. Yang, B. Li, L. Li, S. Seeger, J. Zhang, *iScience* **2019**, *16*, 420.
[240] X. Chen, W. Xu, J. Xiao, M. H. Engelhard, F. Ding, D. Mei, D. Hu, J. Zhang, J. G. Zhang, *J. Power Sources* **2012**, *213*, 160.
[241] W. Xiao, L. Zhao, Y. Gong, J. Liu, C. Yan, *J. Membr. Sci.* **2015**, *487*, 221.
[242] C. Karuppiah, Y. C. Hsieh, S. L. Beshahwured, X. W. Wu, S. H. Wu, R. Jose, S. J. Lue, C. C. Yang, *ACS Appl. Energy Mater.* **2020**, *3*, 8487.
[243] W. Xiao, J. Song, L. Huang, Z. Yang, Q. Qiao, *Ceram. Int.* **2020**, *46*, 29212.
[244] Y. Xie, Y. Pan, P. Cai, *Ind. Eng. Chem. Res.* **2020**, *59*, 15242.
[245] N. Delaporte, A. Perea, A. Paolella, J. Dubé, M. J. Vigeant, H. Demers, D. Clément, W. Zhu, V. Gariépy, K. Zaghib, *J. Power Sources* **2021**, *506*, 230189.
[246] A. M. Barbe, P. A. Hogan, R. A. Johnson, *J. Membr. Sci.* **2000**, *172*, 149.
[247] P. Pal, *Groundwater Arsenic Remediation*, Elsevier Science, Oxford **2015**, pp. 179–270.
[248] S. Prakash, W. E. Mustain, P. A. Kohl, *Micro Fuel Cells* **2009**, 1.
[249] D. Wang, J. Xiao, W. Xu, Z. Nie, C. Wang, G. Graff, J. G. Zhang, *J. Power Sources* **2011**, *196*, 2241.
[250] K. W. Leitner, H. Wolf, A. Garsuch, F. Chesneau, M. Schulz-Dobrick, *J. Power Sources* **2013**, *244*, 548.
[251] X. Zuo, J. Wu, X. Ma, X. Deng, J. Cai, Q. Chen, J. Liu, J. Nan, *J. Power Sources* **2018**, *407*, 44.
[252] S. Huang, T. Zhu, *J. Power Sources* **2011**, *196*, 3664.
[253] D. Fu, B. Luan, S. Argue, M. N. Bureau, I. J. Davidson, *J. Power Sources* **2012**, *206*, 325.
[254] D. Takemura, S. Aihara, K. Hamano, M. Kise, T. Nishimura, H. Urushibata, H. Yoshiyasu, *J. Power Sources* **2005**, *146*, 779.
[255] P. Kritzer, *J. Power Sources* **2006**, *161*, 1335.
[256] H. S. Jeong, E. S. Choi, S. Y. Lee, J. H. Kim, *J. Membr. Sci.* **2012**, *415–416*, 513.
[257] X. Luo, Y. Liao, Y. Zhu, M. Li, F. Chen, Q. Huang, W. Li, *J. Power Sources* **2017**, *348*, 229.
[258] M. Waqas, S. Ali, W. Lv, D. Chen, B. Boateng, W. He, *Adv. Mater. Interfaces* **2019**, *6*, 1801330.
[259] S. Caimi, H. Wu, M. Morbidelli, *ACS Appl. Energy Mater.* **2018**, *1*, 5224.
[260] S. Ali, C. Tan, M. Waqas, W. Lv, Z. Wei, S. Wu, B. Boateng, J. Liu, J. Ahmed, J. Xiong, J. B. Goodenough, W. He, *Adv. Mater. Interfaces* **2018**, *5*, 1701147.
[261] V. T. Bui, V. T. Nguyen, N. A. Nguyen, R. Umapathi, L. L. Larina, J. H. Kim, H. S. Kim, H. S. Choi, *Membranes* **2021**, *11*, 1.
[262] S. Ko, Y. Yamada, A. Yamada, *Batteries Supercaps* **2020**, *3*, 910.
[263] Z. Liu, Y. Jiang, Q. Hu, S. Guo, L. Yu, Q. Li, Q. Liu, X. Hu, *Energy Environ. Mater.* **2021**, *4*, 336.
[264] L. Ding, N. Yan, S. Zhang, R. Xu, T. Wu, F. Yang, Y. Cao, M. Xiang, *ACS Appl. Mater. Interfaces* **2022**, *14*, 6714.
[265] M. Baginska, B. J. Blaiszik, R. J. Merriman, N. R. Sottos, J. S. Moore, S. R. White, *Adv. Energy Mater.* **2012**, *2*, 583.
[266] D. Li, D. Shi, Z. Yuan, K. Feng, H. Zhang, X. Li, *J. Membr. Sci.* **2017**, *542*, 1.
[267] D. Wu, C. Shi, S. Huang, X. Qiu, H. Wang, Z. Zhan, P. Zhang, J. Zhao, D. Sun, L. Lin, *Electrochim. Acta* **2015**, *176*, 727.
[268] G. Sun, B. Liu, H. Niu, F. Hao, N. Chen, M. Zhang, G. Tian, S. Qi, D. Wu, *J. Membr. Sci.* **2020**, *595*, 117509.
[269] G. Sun, L. Kong, B. Liu, H. Niu, M. Zhang, G. Tian, S. Qi, D. Wu, *J. Membr. Sci.* **2019**, *582*, 132.
[270] Y. Zhai, K. Xiao, J. Yu, J. Yang, B. Ding, *J. Mater. Chem. A* **2015**, *3*, 10551.
[271] G. Sun, G. Dong, L. Kong, X. Yan, G. Tian, S. Qi, D. Wu, *Nanoscale* **2018**, *10*, 22439.
[272] J. J. Woo, S. H. Nam, S. J. Seo, S. H. Yun, W. B. Kim, T. Xu, S. H. Moon, *Electrochem. Commun.* **2013**, *35*, 68.
[273] K. Liu, W. Liu, Y. Qiu, B. Kong, Y. Sun, Z. Chen, D. Zhuo, D. Lin, Y. Cui, *Sci. Adv.* **2017**, *3*, 1601978.
[274] S. Kim, T. Han, J. Jeong, H. Lee, M. H. Ryou, Y. M. Lee, *Electrochim. Acta* **2017**, *241*, 553.
[275] S. Klein, J. M. Wrogemann, S. van Wickeren, P. Harte, P. Bärmann, B. Heidrich, J. Hesper, K. Borzutzki, S. Nowak, M. Börner, M. Winter, J. Kasnatscheew, T. Placke, *Adv. Energy Mater.* **2022**, *12*, 2102599.
[276] J. Müller, M. Abdollahifar, A. Vinograd, M. Nöske, C. Nowak, S. J. Chang, T. Placke, W. Haselrieder, M. Winter, A. Kwade, N. L. Wu, *Chem. Eng. J.* **2021**, *407*, 126603.

[277] A. Banerjee, Y. Shilina, B. Ziv, J. M. Ziegelbauer, S. Luski, D. Aurbach, I. C. Halalay, *J. Electrochem. Soc.* **2017**, *164*, A6315.
[278] W. Li, *J. Electrochem. Soc.* **2020**, *167*, 090514.
[279] H. Wang, Y. Huang, C. Huang, X. Wang, K. Wang, H. Chen, S. Liu, Y. Wu, K. Xu, W. Li, *Electrochim. Acta* **2019**, *313*, 423.
[280] Z. Chang, Y. Qiao, H. Deng, H. Yang, P. He, H. Zhou, *Energy Environ. Sci.* **2020**, *13*, 1197.
[281] J. Xu, X. Xiao, S. Zeng, M. Cai, M. W. Verbrugge, *ACS Appl. Energy Mater.* **2018**, *1*, 7237.
[282] H. Bin Son, M. Shin, W. J. Song, D. Y. Han, S. Choi, H. Cha, S. Nam, J. Cho, S. Choi, S. Yoo, S. Park, *Energy Storage Mater.* **2021**, *36*, 355.
[283] A. Manthiram, X. Yu, S. Wang, *Nat. Rev. Mater.* **2017**, *2*, 16103.
[284] Y. Sun, P. Guan, Y. Liu, H. Xu, S. Li, D. Chu, *Crit. Rev. Solid State Mater. Sci.* **2019**, *44*, 265.
[285] N. Kamaya, K. Homma, Y. Yamakawa, M. Hirayama, R. Kanno, M. Yonemura, T. Kamiyama, Y. Kato, S. Hama, K. Kawamoto, A. Mitsui, *Nat. Mater.* **2011**, *10*, 682.
[286] P. Molaiyan, R. Witter, *Mater. Des. Process. Commun.* **2019**, *1*, 44.
[287] J. Janek, W. G. Zeier, *Nat. Energy* **2016**, *1*, 16141.
[288] P. Molaiyan, R. Witter, *Mater. Des. Process. Commun.* **2021**, *3*, 226.
[289] E. J. Cheng, T. Kimura, M. Shoji, H. Ueda, H. Munakata, K. Kanamura, *ACS Appl. Mater. Interfaces* **2020**, *12*, 10382.
[290] M. Vijayakumar, Y. Inaguma, W. Mashiko, M. P. Crosnier-Lopez, C. Bohnke, *Chem. Mater.* **2004**, *16*, 2719.
[291] N. Zhao, W. Khokhar, Z. Bi, C. Shi, X. Guo, L. Z. Fan, C. W. Nan, *Joule* **2019**, *3*, 1190.
[292] A. J. Samson, K. Hofstetter, S. Bag, V. Thangadurai, *Energy Environ. Sci.* **2019**, *12*, 2957.
[293] S. Chen, D. Xie, G. Liu, J. P. Mwizerwa, Q. Zhang, Y. Zhao, X. Xu, X. Yao, *Energy Storage Mater.* **2018**, *14*, 58.
[294] C. Dietrich, D. A. Weber, S. J. Sedlmaier, S. Indris, S. P. Culver, D. Walter, J. Janek, W. G. Zeier, *J. Mater. Chem. A* **2017**, *5*, 18111.
[295] J. Lau, R. H. DeBlock, D. M. Butts, D. S. Ashby, C. S. Choi, B. S. Dunn, *Adv. Energy Mater.* **2018**, *8*, 1800933.
[296] X. Li, J. Liang, X. Yang, K. R. Adair, C. Wang, F. Zhao, X. Sun, *Energy Environ. Sci.* **2020**, *13*, 1429.
[297] J. Cuan, Y. Zhou, T. Zhou, S. Ling, K. Rui, Z. Guo, H. Liu, X. Yu, *Adv. Mater.* **2019**, *31*, 1803533.
[298] S. Kim, H. Oguchi, N. Toyama, T. Sato, S. Takagi, T. Otomo, D. Arunkumar, N. Kuwata, J. Kawamura, S. ichi Orimo, *Nat. Commun.* **2019**, *10*, 1081.
[299] K. Xu, *Chem. Rev.* **2014**, *114*, 11503.
[300] Y. Jin, K. Liu, J. Lang, D. Zhuo, Z. Huang, C. an Wang, H. Wu, Y. Cui, *Nat. Energy* **2018**, *3*, 732.
[301] X. Huang, C. Liu, Y. Lu, T. Xiu, J. Jin, M. E. Badding, Z. Wen, *J. Power Sources* **2018**, *382*, 190.
[302] K. Waetzig, A. Rost, C. Heubner, M. Coeler, K. Nikolowski, M. Wolter, J. Schilm, *J. Alloys Compd.* **2020**, *818*, 153237.
[303] U. Oteo, M. Martinez-Ibañez, I. Aldalur, E. Sanchez-Diez, J. Carrasco, M. Armand, H. Zhang, *ChemElectroChem* **2019**, *6*, 1019.
[304] Y. Seo, Y. C. Jung, M. S. Park, D. W. Kim, *J. Membr. Sci.* **2020**, *603*, 117995.
[305] P. López-Aranguren, X. Judez, M. Chakir, M. Armand, L. Buannic, *J. Electrochem. Soc.* **2020**, *167*, 020548.
[306] P. Yao, H. Yu, Z. Ding, Y. Liu, J. Lu, M. Lavorgna, J. Wu, X. Liu, *Front. Chem.* **2019**, *7*, 522.
[307] Y. Gu, F. Liu, G. Liu, *Int. J. Electrochem. Sci.* **2020**, *15*, 11986.
[308] K. Luo, L. Yi, X. Chen, L. Yang, C. Zou, X. Tao, H. Li, T. Wu, X. Wang, *J. Electroanal. Chem.* **2021**, *895*, 115462.
[309] Z. Chen, G. T. Kim, Z. Wang, D. Bresser, B. Qin, D. Geiger, U. Kaiser, X. Wang, Z. X. Shen, S. Passerini, *Nano Energy* **2019**, *64*, 103986.
[310] Y. Zheng, X. Li, W. R. Fullerton, Q. Qian, M. Shang, J. Niu, C. Y. Li, *ACS Appl. Energy Mater.* **2021**, *4*, 5639.
[311] J. Wen, Q. Zhao, X. Jiang, G. Ji, R. Wang, G. Lu, J. Long, N. Hu, C. Xu, *ACS Appl. Energy Mater.* **2021**, *4*, 3660.
[312] T. Asano, A. Sakai, S. Ouchi, M. Sakaida, A. Miyazaki, S. Hasegawa, *Adv. Mater.* **2018**, *30*, 1803075.
[313] S. K. Jung, H. Gwon, G. Yoon, L. J. Miara, V. Lacivita, J. S. Kim, *ACS Energy Lett.* **2021**, *6*, 2006.
[314] K. H. Park, K. Kaup, A. Assoud, Q. Zhang, X. Wu, L. F. Nazar, *ACS Energy Lett.* **2020**, 533.
[315] X. Li, J. Liang, J. Luo, M. Norouzi Banis, C. Wang, W. Li, S. Deng, C. Yu, F. Zhao, Y. Hu, T. K. Sham, L. Zhang, S. Zhao, S. Lu, H. Huang, R. Li, K. R. Adair, X. Sun, *Energy Environ. Sci.* **2019**, *12*, 2665.
[316] X. Li, J. Liang, N. Chen, J. Luo, K. R. Adair, C. Wang, M. N. Banis, T. K. Sham, L. Zhang, S. Zhao, S. Lu, H. Huang, R. Li, X. Sun, *Angew. Chem., Int. Ed.* **2019**, *58*, 16427.
[317] D. Park, H. Park, Y. Lee, S. O. Kim, H. G. Jung, K. Y. Chung, J. H. Shim, S. Yu, *ACS Appl. Mater. Interfaces* **2020**, *12*, 34806.
[318] L. Zhou, C. Y. Kwok, A. Shyamsunder, Q. Zhang, X. Wu, L. F. Nazar, *Energy Environ. Sci.* **2020**, *13*, 2056.
[319] J. Liang, X. Li, S. Wang, K. R. Adair, W. Li, Y. Zhao, C. Wang, Y. Hu, L. Zhang, S. Zhao, S. Lu, H. Huang, R. Li, Y. Mo, X. Sun, *J. Am. Chem. Soc.* **2020**, *142*, 7012.
[320] H. Kwak, D. Han, J. Lyoo, J. Park, S. H. Jung, Y. Han, G. Kwon, H. Kim, S. T. Hong, K. W. Nam, Y. S. Jung, *Adv. Energy Mater.* **2021**, *11*, 2003190.
[321] R. Schlem, A. Banik, S. Ohno, E. Suard, W. G. Zeier, *Chem. Mater.* **2021**, *33*, 327.
[322] X. Li, J. Liang, K. R. Adair, J. Li, W. Li, F. Zhao, Y. Hu, T. K. Sham, L. Zhang, S. Zhao, S. Lu, H. Huang, R. Li, N. Chen, X. Sun, *Nano Lett.* **2020**, *20*, 4384.
[323] K. Kim, D. Park, H. G. Jung, K. Y. Chung, J. H. Shim, B. C. Wood, S. Yu, *Chem. Mater.* **2021**, *33*, 3669.
[324] S. Y. Kim, K. Kaup, K. H. Park, A. Assoud, L. Zhou, J. Liu, X. Wu, L. F. Nazar, *ACS Mater. Lett.* **2021**, *3*, 930.
[325] S. Zhang, F. Zhao, S. Wang, J. Liang, J. Wang, C. Wang, H. Zhang, K. Adair, W. Li, M. Li, H. Duan, Y. Zhao, R. Yu, R. Li, H. Huang, L. Zhang, S. Zhao, S. Lu, T. K. Sham, Y. Mo, X. Sun, *Adv. Energy Mater.* **2021**, *11*, 2100836.
[326] A. Sakuda, A. Hayashi, M. Tatsumisago, *Sci. Rep.* **2013**, *3*, 2261.
[327] Y. Kato, S. Hori, T. Saito, K. Suzuki, M. Hirayama, A. Mitsui, M. Yonemura, H. Iba, R. Kanno, *Nat. Energy* **2016**, *1*, 16030.
[328] R. Schlem, C. F. Burmeister, P. Michalowski, S. Ohno, G. F. Dewald, A. Kwade, W. G. Zeier, *Adv. Energy Mater.* **2021**, *11*, 2101022.
[329] F. Zheng, M. Kotobuki, S. Song, M. O. Lai, L. Lu, *J. Power Sources* **2018**, *389*, 198.
[330] Y. Nikodimos, C.-J. Huang, B. W. Taklu, W.-N. Su, B. J. Hwang, *Energy Environ. Sci.* **2022**, *15*, 991.
[331] A. Kuhn, O. Gerbig, C. Zhu, F. Falkenberg, J. Maier, B. V. Lotsch, *Phys. Chem. Chem. Phys.* **2014**, *16*, 14669.
[332] S. Harm, A. K. Hatz, I. Moudrakovski, R. Eger, A. Kuhn, C. Hoch, B. V. Lotsch, *Chem. Mater.* **2019**, *31*, 1280.
[333] G. Sahu, Z. Lin, J. Li, Z. Liu, N. Dudney, C. Liang, *Energy Environ. Sci.* **2014**, *7*, 1053.
[334] J. Liang, N. Chen, X. Li, X. Li, K. R. Adair, J. Li, C. Wang, C. Yu, M. Norouzi Banis, L. Zhang, S. Zhao, S. Lu, H. Huang, R. Li, Y. Huang, X. Sun, *Chem. Mater.* **2020**, *32*, 2664.
[335] X. Sun, A. M. Stavola, D. Cao, A. M. Bruck, Y. Wang, Y. Zhang, P. Luan, J. W. Gallaway, H. Zhu, *Adv. Energy Mater.* **2021**, *11*, 2002861.
[336] D. H. S. Tan, E. A. Wu, H. Nguyen, Z. Chen, M. A. T. Marple, J. M. Doux, X. Wang, H. Yang, A. Banerjee, Y. S. Meng, *ACS Energy Lett.* **2019**, *4*, 2418.
[337] E. Zhao, L. He, Z. Zhang, J. M. Doux, D. H. S. Tan, E. A. Wu, G. Deysher, Y. T. Chen, J. Zhao, F. Wang, Y. S. Meng, *Chem. Commun.* **2021**, *57*, 10787.

[338] M. A. Kraft, S. Ohno, T. Zinkevich, R. Koerver, S. P. Culver, T. Fuchs, A. Senyshyn, S. Indris, B. J. Morgan, W. G. Zeier, *J. Am. Chem. Soc.* **2018**, *140*, 16330.
[339] A. Gautam, M. Sadowski, N. Prinz, H. Eickhoff, N. Minafra, M. Ghidiu, S. P. Culver, K. Albe, T. F. Fässler, M. Zobel, W. G. Zeier, *Chem. Mater.* **2019**, *31*, 10178.
[340] P. Wang, H. Liu, S. Patel, X. Feng, P. H. Chien, Y. Wang, Y. Y. Hu, *Chem. Mater.* **2020**, *32*, 3833.
[341] P. Adeli, J. D. Bazak, A. Huq, G. R. Goward, L. F. Nazar, *Chem. Mater.* **2021**, *33*, 146.
[342] P. Adeli, J. D. Bazak, K. H. Park, I. Kochetkov, A. Huq, G. R. Goward, L. F. Nazar, *Angew. Chem., Int. Ed.* **2019**, *58*, 8681.
[343] S. S. Shin, J. S. Kim, S. Choi, H. Il Ji, K. J. Yoon, J. H. Lee, K. Y. Chung, H. Kim, *Chem. Commun.* **2021**, *57*, 3453.
[344] W. D. Jung, J. S. Kim, S. Choi, S. Kim, M. Jeon, H. G. Jung, K. Y. Chung, J. H. Lee, B. K. Kim, J. H. Lee, H. Kim, *ACS Appl. Mater. Interfaces* **2020**, *20*, 2303.
[345] C. Wang, S. Hwang, M. Jiang, J. Liang, Y. Sun, K. Adair, M. Zheng, S. Mukherjee, X. Li, R. Li, H. Huang, S. Zhao, L. Zhang, S. Lu, J. Wang, C. V. Singh, D. Su, X. Sun, *Adv. Energy Mater.* **2021**, *11*, 2100210.
[346] L. Ye, X. Li, *Nature* **2021**, *593*, 218.
[347] Z. Zhang, Y. Shao, B. Lotsch, Y. S. Hu, H. Li, J. Janek, L. F. Nazar, C. W. Nan, J. Maier, M. Armand, L. Chen, *Energy Environ. Sci.* **2018**, *11*, 1945.
[348] S. Randau, D. A. Weber, O. Kötz, R. Koerver, P. Braun, A. Weber, E. Ivers-Tiffée, T. Adermann, J. Kulisch, W. G. Zeier, F. H. Richter, J. Janek, *Nat. Energy* **2020**, *5*, 259.
[349] A. Y. Kim, F. Strauss, T. Bartsch, J. H. Teo, J. Janek, T. Brezesinski, *Sci. Rep.* **2021**, *11*, 5367.
[350] A. Y. Kim, F. Strauss, T. Bartsch, J. H. Teo, T. Hatsukade, A. Mazilkin, J. Janek, P. Hartmann, T. Brezesinski, *Chem. Mater.* **2019**, *31*, 9664.
[351] Y. G. Lee, S. Fujiki, C. Jung, N. Suzuki, N. Yashiro, R. Omoda, D. S. Ko, T. Shiratsuchi, T. Sugimoto, S. Ryu, J. H. Ku, T. Watanabe, Y. Park, Y. Aihara, D. Im, I. T. Han, *Nat. Energy* **2020**, *5*, 299.
[352] B. Zahiri, A. Patra, C. Kiggins, A. X. Bin Yong, E. Ertekin, J. B. Cook, P. V. Braun, *Nat. Mater.* **2021**, *20*, 1392.
[353] S. Zhang, Z. Li, Y. Guo, L. Cai, P. Manikandan, K. Zhao, Y. Li, V. G. Pol, *Chem. Eng. J.* **2020**, *400*, 125996.
[354] Z. Zhang, L. Wu, D. Zhou, W. Weng, X. Yao, *Nano Lett.* **2021**, *21*, 5233.
[355] Y. Liu, Y. Zhao, W. Lu, L. Sun, L. Lin, M. Zheng, X. Sun, H. Xie, *Nano Energy* **2021**, *88*, 106205.
[356] J. Park, D. Han, H. Kwak, Y. Han, Y. J. Choi, K. W. Nam, Y. S. Jung, *Chem. Eng. J.* **2021**, *425*, 130630.
[357] A. M. Bates, Y. Preger, L. Torres-Castro, K. L. Harrison, S. J. Harris, J. Hewson, *Joule* **2022**, *6*, 1.
[358] W. Huang, X. Feng, X. Han, W. Zhang, F. Jiang, *Cell Rep. Phys. Sci.* **2021**, *2*, 100285.
[359] X. Feng, D. Ren, X. He, M. Ouyang, *Joule* **2020**, *4*, 743.
[360] J. Hou, L. Lu, L. Wang, A. Ohma, D. Ren, X. Feng, Y. Li, Y. Li, I. Ootani, X. Han, W. Ren, X. He, Y. Nitta, M. Ouyang, *Nat. Commun.* **2020**, *11*, 5100.
[361] X. Han, L. Lu, Y. Zheng, X. Feng, Z. Li, J. Li, M. Ouyang, *eTransportation* **2019**, *1*, 100005.
[362] D. Rettenwander, C. A. Geiger, M. Tribus, P. Tropper, R. Wagner, G. Tippelt, W. Lottermoser, G. Amthauer, *J. Solid State Chem.* **2015**, *230*, 266.

Heather Cavers completed her B.Sc. in Chemistry at the University of Manitoba, Winnipeg, Canada, after which she obtained her M.Sc. and her doctorate in materials science and engineering (2021) from Christian-Albrecht University of Kiel, Germany. Her thesis topic was regarding aspects of the chemistry of silicon/sulfur lithium-ion battery full-cells. She is currently working as a postdoc at the Institute of Particle Technology (iPAT), Technische Universität Braunschweig, Germany. Her research expertise includes materials science, electrochemistry, and novel lithium-ion battery materials.

Palanivel Molaiyan obtained his doctoral studies in applied physics (2020) from Tallinn University of Technology, Tallinn, Estonia. His thesis topic is entitled solid-state electrolytes for fluoride ion batteries. He worked as a research associate at the Institute of Particle Technology (iPAT), Technische Universität Braunschweig, Germany. Presently, He is working as a postdoc researcher (2021) at Sustainable Chemistry unit, University of Oulu, Finland. His research expertise is in materials science, advanced battery materials, and electrochemistry. His primary research work involves sulfide, halide, and fluoride materials-based solid-state electrolytes to develop all-solid-state batteries.

Mozaffar Abdollahifar received his doctorate in chemical engineering and energy storage materials from National Taiwan University (NTU) in 2018, focused on the supercapacitor electrodes and cathode materials of lithium-ion batteries (LIBs). After a postdoctoral stay at the NTU (two years), he is appointed as research scientist in the Institute for Particle Technology (iPAT), and the Battery LabFactory Braunschweig (BLB) of Technische Universität Braunschweig. His research interests include battery materials, such as anode and cathode materials for LIBs and lithium–sulfur batteries, and recycling end-of-life LIBs to recover valuable materials, particularly graphite anode materials.

Ulla Lassi completed her doctorate in chemistry (2003) at the University of Oulu, Finland. Since 2006, she is a Professor in Applied Chemistry and Process Chemistry at Faculty of Technology, University of Oulu, Finland. Currently, she is the Head of Research Unit of Sustainable Chemistry, University of Oulu, Finland. Her research areas involve inorganic material chemistry in industrial applications, such as heterogeneous catalysis in biomass conversion, wastewater treatment, and lithium-ion batteries. She is also an active member in several scientific and educational societies and committees and has several positions of trust.

Arno Kwade worked for nine years as a process engineer in the industry after finishing his doctorate in ultrafine milling in stirred media mills at Technische Universität Braunschweig in 1996. Since 2005 he has led as a professor at Technische Universität Braunschweig, Institute for Particle Technology, Germany. His research focusses on developing process–structure–property relationships for processes in which particles are mechanically stressed and formulated from milling and mechanochemical synthesis over mixing to production and calendaring of electrodes for lithium-ion and solid-state batteries. He is also Chairman of the Battery LabFactory Braunschweig (BLB) and the Centre of Pharmaceutical Engineering (PVZ).